Compartmentalization of Proximal G alpha q-Receptor Signaling in Adult Cardiac Myocytes

A DISSERTATION SUBMITTED TO THE FACULTY OF THE UNIVERSITY OF MINNESOTA BY

Erika Dahl

IN PARTIAL FULFILLMENT FOR THE REQUIREMENTS FOR THE DEGREE OF DOCTOR OF PHILOSOPHY

Advisor: Timothy D. O'Connell, PhD

March 2018

ACKNOWLEDGEMENTS

During my time at Augustana College, I was fortunate enough to have the guidance of my academic advisor Dr. Mark Larson. Dr. Larson was the person who inspired me to pursue scientific research. I will be forever grateful to him and to the South Dakota Biomedical Research Infrastructure Network for the undergraduate research experience I had in the O'Connell lab. Thank you, Dr. Larson, for your wisdom.

After circumstance brought the O'Connell lab to the University of Minnesota, I knew I would continue my research career with the lab. Your approach to science, your vision for projects, and your perseverance have guided me through the ups and downs of this project. You've mentored me to be a better, and more patient scientist and person. For that, I am forever in your debt. Thank you, Tim, for your endless patience, humor, and guidance.

I am extremely lucky to have had such amazing lab mates during my time at the University of Minnesota. To Steve, thank you for teaching me the art of cloning and fielding all of my questions that began with "Hey Steve". To Chastity, thank you for being a sounding board when I was struggling in life and in lab. Thank you for showing me how to organize my life effectively, and being the personification of work ethic. I have been forever shaped (in a good way) by sharing a lab bench with you both over these seven years.

I am also extremely grateful for the guidance and input provided by the members of my thesis committee: Dr. John Osborn, Dr. Kevin Wickman, Dr. Stan Thayer, and Dr. Tim O'Connell. Your constructive comments and advice during my thesis research were paramount in the final product enclosed in this thesis. Thank you all.

To all the Pharmacology graduate students, especially Erica Schnettler, Zahra Masoud, Lydia Kotecki, and Nicole Wydeven, thank you all for being present for me during the good times and the bad. To the IBP graduate students, thank you all for inviting me into the IBP family. To Amber Lockridge and Tanya Meyers, thank you for always being willing to share your time and expertise with me. CCRB would not be the same without

both of you in it. To Jake Petersburg and Cody Lensing, thank you for the help when I found myself within a chemistry project. Thank you both for always being there for me when I needed it for scientific conversations and life conversations. To Cody Lensing, here's to 14 years of schooling together. I could not be more fortunate to have a friend like you to share so many experiences with. You've all made lasting impressions on me and I look forward to what the future holds for us.

DEDICATIONS

I would like to dedicate this thesis to my family. To my parents, Bill and Patti Dahl, thank you for always pushing me to pursue my dreams. Whether it was college sports or graduate school, you've always been there for me one hundred percent. I could not have gone through this process without you both. I am forever in your debt. I love you both. To my siblings, Andrea and Jessie, while we might not always speak the same language, I value your insights and your life wisdom. Thank you for always blazing a trail for me, and for being fiercely loyal to me. Thank you for always forgiving me when I bit off more than I could chew and for understanding that my time was stretched thin. I love you both so much.

To my amazing friends, namely Stephanie Goos, Jessica Rasmussen, and Danielle Gilbert (Johnson). Thank you for always talking to me when I'm having a crisis, for knowing when we need more wine, when we need a good workout, and for always being present for me. I could not have gone through this process as seamlessly as I did without you. I love you all.

To Sean, the person who has been with me day in and day out. Thank you. Thank you for being my seventy percent, for your unconditional love, for your patience, and for all the other things that I cannot adequately put into words. We've grown so much during these last four years, and I look forward to continuing that process. Thank you for being by my side and going through the ups and downs, and thank you for loving me through all of it.

ABSTRACT

Gq-coupled GPCRs (Gq-receptors) produce distinct physiological responses despite common proximal signaling mechanisms, yet the mechanistic basis for this remains unclear. In the heart, Gq-receptors are thought to induce myocyte hypertrophy through a mechanism termed excitation-transcription coupling, which provides a mechanistic basis for compartmentalization of calcium required for contraction versus inositol-1,4,5-trisphosphate-dependent intranuclear calcium required for hypertrophy. Here, we identify subcellular compartmentalization of Gq-receptor signaling as a mechanistic basis for unique Gq-receptor-induced hypertrophic phenotypes in cardiac myocytes. We show that α1-adrenergic receptors (α1-ARs) co-localize with phospholipase-Cβ1 (PLCβ1) and phosphatidylinositol-4,5-bisphosphate (PIP_2) at the nuclear membrane. Further, nuclear α1-ARs induce intranuclear PLCβ1 activity leading to the activation of perinuclear and cytosolic ERK, histone deacetylase 5 (HDAC5) export, and a robust transcriptional response. Conversely, we found that angiotensin receptors localize to the sarcolemma and induce sarcolemmal PLCβ1 activity leading to the activation of cytosolic ERK, but fail to promote HDAC5 nuclear export, while producing a transcriptional response that is mostly a subset of α1-induced transcription. In summary, these results link Gq-receptor compartmentalization to unique patterns of PLCβ1 activation, ERK activation, and hypertrophic transcription and significantly revise our understanding of excitation-transcription coupling.

TABLE OF CONTENTS

ACKNOWLEDGEMENTS i

DEDICATIONS iii

ABSTRACT iv

LIST OF TABLES viii

LIST OF FIGURES ix

CHAPTER 1. INTRODUCTION 1

1.1 Cardiac G Protein Coupled Receptors 1
1.2 Cardiac Gαq Receptor Signaling 2
1.2.1 Phospholipase Cβ 3
1.2.2 Phosphotidyl-4,5-bisphosphate 3
1.2.3 Diacylglycerol and Protein Kinase C 4
1.2.4 Inositol-1,4,5-trisphosphate 5
1.2.5 Mitogen Activated Protein Kinase Cascade 6
1.2.6 Gq-Receptor Desensitization 6
1.3 Cardiac Nuclear G-Protein Coupled Receptors 7
1.4 Cardiac Nuclear Gαq Receptor Signaling 9
1.4.1. Overview of Nuclear Gq-receptor Signaling Partners 10
1.4.2 Calmodulin 10
1.4.3 Calmodulin Dependent Protein Kinase II 11
1.4.4 Protein Kinase D 11

1.4.5 Calcineurin 12

1.4.5 Regulation and Desensitization of Nuclear Gq-Receptors 12

1.5 Differential Signaling of Cardiac Gαq Receptors 14
1.6 Overarching Hypothesis and Aims 15
1.6.1 To define and compare the localization of endogenous α1-ARs and AT-Rs in adult cardiac myocytes. 16

1.6.2 To define proximal PLCβ1 signaling downstream of α1-ARs and AT-Rs 17

1.6.3 To define Gq-receptor activation of downstream ERK signaling 18

1.6.4 To define Gq-receptor activation of terminal hypertrophic gene activation.... 18

CHAPTER 2. α1-ARs and AT-Rs Localize to Different Subcellular Compartments in Adult Cardiac Myocytes 20

2.1 Summary 20
2.2 Introduction 20
2.3 Methods 21
2.4 Results 25
2.5 Discussion 33
2.6 Acknowledgements 33
CHAPTER 3. Differential Activation of PLCβ1 by Gαq-Receptors in Adult Cardiac Myocytes 34

3.1 Summary 34
3.2 Introduction 34
3.3 Methods 35
3.4 Results 40
Phospholipase Cβ1 (PLCβ1) and its substrate phosphatidylinositol-4,5-bisphosphate (PIP_2) localize to the nuclei in adult cardiac myocytes 40
3.5 Discussion 51

3.6 Acknowledgements 51
CHAPTER 4. Differential Activation of ERK by Gαq-Receptors in Adult Cardiac Myocytes 53
4.1 Summary 53
4.2 Introduction 53
4.3 Methods 54
4.4 Results 56
4.5 Discussion 63
4.6 Acknowledgements 63
CHAPTER 5. Differential Activation of Hypertrophic Transcriptomes by Gαq-Receptors in Adult Cardiac Myocytes 64
5.1 Summary 64
5.2 Introduction 64
5.3 Methods 65
5.4 Results 68
5.5 Discussion 81
5.6 Acknowledgements 81
CHAPTER 6. CONCLUSIONS AND FUTURE DIRECTIONS 82
6.1 Conclusions 83
6.2 Future Directions 89
Bibliography 92

LIST OF TABLES

Table 5.1. Molecular function of Hypertrophic Genes induced by α1ARs, ATRs, or in common..... 75

Table 5.2. Molecular function of Survival Signaling Genes induced by α1ARs, ... 77

ATRs, or in common..... 77

Table 5.3. Molecular function of Inotropy Genes induced by α1ARs, AT-Rs, or in..... 78

common..... 78

Table 5.4. Molecular function of Fibrosis Genes induced by α1ARs, AT-Rs, or in common.

..... 79

LIST OF FIGURES

Figure 2.1. α1-ARs localize to the nuclei and AT-Rs localize to the sarcolemma in adult cardiac myocytes..... 28

Figure 2.2. Synthesis and validation of α1-AR Qdot-565. 30

Figure 2.3. NCX1 localizes to the sarcolemma and not the center of adult cardiac myocytes. 32

Figure 3.1. Validation of PLCβ1 antibody in N38 cells. 44

Figure 3.2. PLCβ1 and PIP_2 localize to the nuclear membrane in adult cardiac myocytes 45

Figure 3.3. AT-Rs, but not α1-ARS, activate PLCβ1 at the sarcolemma in adult cardiac myocytes 47

Figure 3.4. α1-ARs and, to a lesser extent, AT-Rs activate PLCβ1 at the nuclear membrane in adult cardiac myocytes..... 49

Figure 4.1. α1-ARs activate ERK in the cytosol and at the nucleus in two-thirds of adult cardiac myocytes..... 58

Figure 4.2. AT-Rs activate ERK in the cytosol in one-third of adult cardiac myocytes. . 60

Figure 4.3. Compilation of ERK1/2 activation downstream of α1-ARs and AT-Rs in cardiac myocytes..... 61

Figure 4.4. α1-ARs, but not AT-Rs, promote mitochondrial membrane stabilization and cardiac myocyte cell survival..... 62

Figure 5.1. α1-ARS induce HDAC5 export, whereas AT-Rs do not. 71

Figure 5.2. α1-ARs robustly activate transcriptional responses in adult cardiac myocytes whereas AT-ARs do not..... 73

Figure 6.1. Novel model of excitation-transcription coupling in adult cardiac myocytes.87

CHAPTER 1. INTRODUCTION

1.1 Cardiac G Protein Coupled Receptors

G-protein coupled receptors (GPCRs) are the largest family of membrane proteins in the human genome and mediate most cellular responses to hormones and neurotransmitters (1, 2). GPCRs share common structural morphology which includes seven hydrophobic transmembrane domains separated by alternating intracellular and extracellular loops with an extracellular amino terminus and an intracellular carboxy terminus (2). Vertebrate GPCRs can be divided into 5 families: rhodopsin (701 receptors), secretin (15 receptors), glutamate (15 receptors), adhesion (24 receptors), and Frizzled/Taste (24 receptors) (3). In the heart, receptors from each of the GPCR families have been identified. Examples of rhodopsin family members expressed in the heart include α1-adrenergic receptors (α1-ARs), β-adrenergic receptors (β-ARs), angiotensin receptors (AT-Rs), and endothelin receptors (ET-Rs) (4). Examples of secretin family members expressed in the heart include glucagon-like peptide-1 receptor (5) and the glucagon receptor (6). Examples of glutamate family members expressed in the heart include the gamma-aminobutyric acid type B receptor 1 and 2 (7). Examples of adhesion family members expressed in the heart include ETL (8) and the brain-specific angiogenesis inhibitor 1 and 2 receptors (9). Examples of frizzled/taste members expressed in the heart include the taste receptor type 1 and taste receptor type 2 (10).

In order for GPCRs to mediate cellular events secondary to ligand binding, G-proteins, also known as guanine nucleotide-binding proteins, couple to GPCRs to illicit signaling events within the cell. G-proteins fall under two categories: heterotrimeric G-proteins and small G-proteins belonging to the Ras superfamily. While the Ras superfamily of G-proteins is paramount to cellular signaling, this chapter will focus on the heterotrimeric G-proteins which consist of the α, β, and γ subunits. Currently, there are 20 known Gα subunits, 6 Gβ subunits, and 11 Gγ subunits (11). In the basal state, the α, β, and γ subunits are tightly bound to the GPCR with the α-subunit bound to guanosine diphosphate (GDP). Upon ligand binding, the GPCR undergoes a conformational change which allows the GPCR to act as a guanine nucleotide exchange factor, exchanging the α-subunit GDP for guanosine triphosphate (GTP). The GDP to GTP exchange causes the α-subunit to dissociate from the $\beta\gamma$ subunit and ultimately confer

downstream signaling events. The heterotrimeric α-subunits consist of many classes, but the five main classes are stimulatory Gαs, inhibitory Gαi, Gαq, Gαolf, and Gα12/13. Canonically, Gαs activates adenylyl cyclase, Gαi inhibits adenylyl cyclase, Gαq activates phospholipase C, Gαolf belongs to the Gαs subfamily and thus activates adenylyl cyclase, and Gα12/13 regulates the Rho guanine nucleotide exchange factor. Examples of receptors that primarily couple to these G protein subunits in cardiac myocytes include: 1) Gαs coupled β-adrenergic type 1 receptors which increase heart rate, cardiac contractility, cardiac action potential conduction velocity, and relaxation (12). 2) Gαi coupled adenosine receptors which have a negative chronotropic effect by suppressing the automaticity of cardiac pacemakers, and a negative dromotropic effect through inhibition of AV-nodal conduction (13). 3) Gαq coupled α1-adrenergic receptors which mediate positive inotropy, cardiac myocyte cell survival, and physiologic hypertrophy (14). 4) Gαolf receptors are only present in the olfactory system. 5) Finally, many receptors have been found to couple to multiple G-proteins such as AT-Rs and ET-Rs which have also been found to couple to both Gαq and Gα12/13 (15). Yet, receptors that uniquely couple to Gα12/13 may have been overlooked due to insufficient techniques used to identify G-protein binding (15). Activation of Gα12/13 mediates translocation of RhoGEF from the cytosol to the plasma membrane, and stimulate the guanine nucleotide exchange factor activity of RhoGEF (15).

1.2 Cardiac Gαq Receptor Signaling

Of interest to this body of work are the GPCRs that primarily signal through Gαq/11 in the heart. These receptors include α1-ARs, ET-Rs, and AT-Rs. Classically, when ligand binds the Gαq coupled GPCR (Gq-receptor), GDP is exchanged for GTP and the α-subunit dissociates from the βγ subunits. The α-subunit activates phospholipase Cβ (PLCβ) at the cell membrane. PLCβ cleaves membrane bound phosphatidylinositol-4,5-bisphosphate (PIP_2) to form diacylglycerol (DAG) and inositol 1,4,5-trisphosphate (IP_3). DAG remains associated with the cell membrane and goes on to recruit and activate protein kinase C (PKC) family members, ultimately leading to phosphorylation of proteins that regulate calcium homeostasis and direct phosphorylation of contractile proteins in the heart (16). IP_3 is freely diffusible within the

cell and goes on to bind its receptor, the inositol trisphosphate receptor (IP3R), to release calcium from intracellular stores. Each of these main signaling molecules will be discussed in detail below.

1.2.1 Phospholipase Cβ

In canonical Gq-receptor signaling, ligand binds to the receptor causing dissociation of the G-protein and subsequent activation of PLCβ. The PLC isozyme family consists of six subfamilies: PLC β, γ, δ, ε, ζ, and η (17-19). In the heart, the main isoforms of PLC expressed are PLCβ, γ, δ, and ε (20-22). Cardiac Gq-coupled receptors primarily signal through PLCβ, and three isoforms of PLCβ have been identified in the heart: PLCβ1, PLCβ3, PLCβ4 (23). Sensitivity of activation by Gαq is greatest with PLCβ1 and PLCβ3 (24). In the heart, PLCβ1 is the major isoform expressed and exists as two splice variants PLCβ1a and PLCβ1b (25). Current literature indicates that PLCβ1b, but not PLCβ1a, localizes to the sarcolemma through interaction of the PLCβ1b proline rich domain with the scaffolding protein Shank3 (26). Therefore, PLCβ1a is thought to not be active in cardiac myocytes due to its inability to target the membrane and interact with its substrate PIP_2 (27). Further, overexpression of the PLCβ1b isoform, but not the PLCβ1a isoform, induced cardiac contractile dysfunction *in vivo* (27). Yet, these results are based on overexpression models and sufficient modalities to study the endogenous PLCβ1 protein still need to be developed in order to fully understand the intricacies of PLCβ1 activation in adult cardiac myocytes. New insights on PLCβ1 localization from our lab indicate PLCβ1 localizes to the nuclear membrane in adult cardiac myocytes (28). While no specific isoform of PLCβ1 was identified, this result gives evidence to the idea that Gq-receptor signaling through PLCβ1 is possible at the nucleus in adult cardiac myocytes.

1.2.2 Phosphotidyl-4,5-bisphosphate

PIP_2, the substrate of PLCβ1, is generated from the phosphorylation of phosphotidylinositol at the 4' position by phosphotidylinositol 4-kinase and subsequent

phosphorylation at the 5' position by phosphatidylinositol 4-phosphate 5-kinase (29). PIP_2 represents less than 1% of total membrane phospholipids, but controls crucial signaling cascades in cardiac myocytes (30). Intact PIP_2 has been implicated in a variety of cell processes including membrane trafficking, membrane-cytoskeletal linkages, ion channel gating, and cell signaling (30). Upon Gq-receptor activation, PLCβ1 hydrolyzes PIP_2 into IP_3 and DAG, effectively depleting PIP_2 at the membrane. Hydrolysis of PIP_2 downstream of Gq-receptor mediated PLCβ1 activation can be visualized using the pleckstrin homology domain of PLCδ fused to GFP (GFP-PHD) (31). The pleckstrin homology domain of PLCδ selectively binds PIP_2 with high affinity at the sarcolemma in the basal state in adult cardiac myocytes (32). Our recent work using a nuclear localized GFP-PHD and mass spectrometry localize PIP_2 to cardiac nuclear membranes which supports the idea of nuclear Gq-receptor signaling in cardiac myocytes. Furthermore, due to the low mobility of PIP_2 in cardiac membranes, hydrolysis of PIP_2 occurs in close proximity to the stimulated Gq-receptor indicating a tightly regulated role for PIP_2 in Gq-receptor mediated signal transduction (33).

1.2.3 Diacylglycerol and Protein Kinase C

One of the products of PLCβ1 mediate cleavage of PIP_2 is DAG. DAG consists of a glycerol molecule linked through ester bonds to two fatty acids at positions one and two (34). DAG is a hydrophobic molecule and thus stays bound within the membrane complex and does not diffuse throughout the cell. Like PIP_2, DAG is not uniformly produced throughout the cell upon Gq-receptor stimulation but in discrete pools (34). DAG signaling is negatively regulated by diacylglycerol kinases which convert DAG to phosphatidic acid. In cardiac myocytes, diacylglycerol kinase α, ε, and ζ are expressed with diacylglyercol kinase ζ being the predominant isoform (35). The main effectors of DAG are members of the protein kinase C (PKC) family which interact with DAG at the membrane through their conserved C1 domains. Other effectors of DAG include chimaerin, protein kinase D, mammalian unc13 (Munc13), Ras guanine-releasing protein and myotonic dystrophy kinase-related Cdc42-binding kinase families (36). The PKC isozymes that are expressed in cardiac myocytes include the conventional PKCs α and β which are activated by DAG and calcium, the novel PKCs δ and ε which are activated

by DAG alone, and the atypical PKCζ which is activated by neither DAG nor calcium (37). PKC isozymes target a plethora of proteins and thus have influence on many signaling cascades in cardiac myocytes. Of note, PKC isozymes modulate cardiac contractility through interactions with various cardiac contractile proteins, calcium dynamics through interaction with calcium channels, and activation of the p38 mitogen activated protein kinase cascade (MAPK) among others (38).

1.2.4 Inositol-1,4,5-trisphosphate

The other product of PLCβ1 mediate cleavage of PIP_2 is IP_3. Upon Gq-receptor stimulation, intracellular IP_3 and inositol species in general increases by a factor of >12 (39). IP_3 is freely soluble in the cytosol and goes on to bind to the IP3R in order to release calcium from intracellular stores. In the heart, the most abundant IP3R is the IP3R2 which localizes to the Z-lines, perinuclear region, and inner nuclear membrane in both atrial and ventricular cardiac myocytes (40). Differential roles for the IP3R2 in atrial and ventricular myocytes have been suggested, with atrial IP3R2s potentially contributing to arrhythmogenesis and ventricular IP3R2s contributing to excitation-transcription coupling (41-43). In ventricular myocytes, IP_3 binding to the IP3R2 at the inner nuclear membrane induces a localized calcium release from the nuclear envelope (43). Nuclear envelope calcium release activates calcium/calmodulin-dependent protein kinase II (CaMKII) and CaMKII phosphorylates histone deacytlase 5 (HDAC5) causing HDAC5 nuclear export and derepression of transcription (43). This IP_3-calcium-transcriptional response has been coined excitation-transcription coupling and will be discussed in more detail later in this chapter. Apart from the role that calcium acts in excitation-transcription coupling, calcium also play a critical role in excitation-contraction coupling. During excitation-contraction coupling the depolarization of the cardiac sarcolemma causes activation of L-type calcium channels which allows calcium to flow into the cardiac myocyte. This influx of calcium triggers calcium induced calcium release from the sarcoplasmic reticulum through the ryanodine receptors, ultimately causing cardiac myocyte contraction through calcium binding to the troponin-tropomyosin complex (44). It is important to note that the calcium mobilized downstream of IP3R2 stimulation is a separate pool of calcium than that which is mobilized during excitation-contraction coupling.

1.2.5 Mitogen Activated Protein Kinase Cascade

Another cascade initiated by stimulation of Gq-receptors is the mitogen activated protein kinase (MAPK) cascade. The MAPKs consist of p38 kinases, c-Jun N-terminal kinases (JNKs), and the functionally redundant extracellular regulated kinases 1 and 2 (ERK). Gq-receptors, including α1-ARs and ET-Rs, activate all three families of MAPKs in cardiac myocytes, with activation of the ERK cascade being the most robust (45-49). In adult cardiac myocytes, activation of the JNK downstream of Ras and activation p38 downstream of PKCs are associated with cellular responses to stress whereas ERK activation is generally thought to be associated with hypertrophy and growth (50, 51). Activation of Gq-receptors leads to activation of the low molecular weight GTP-binding Ras and subsequent translocation and activation of Raf to the membrane. Raf proceeds to phosphorylate and activate the MAP3Ks, which in turn phosphorylate and activate the MAP2Ks, which then go on to phosphorylate and activate the MAPKs of which ERK is a family member. ERK has been implicated in transducing signals of cardiac hypertrophy (52-54) through direct phosphorylation of transcription factors such as Elk-1, c-Fos, p53, and GATA4 (55). ERK activation has also been linked to increased survival in cardiac myocytes exposed to pro-death agonists (56).

1.2.6 Gq-Receptor Desensitization

While Gq-receptor activation is important to the physiologic function of cardiac myocytes, receptor desensitization is just as important. After Gq-receptor cell signaling has been initiated, a host of molecules work to attenuate the signaling cascade. The first proteins that were identified in the regulation of GPCR signaling were G-protein coupled receptor kinases (GRKs) and β-arrestins (57). Generally, GRKs act to desensitize GPCRs through phosphorylation of serine and threonine residues within the third intracellular loop and carboxyl-terminal tail domains of agonist activated receptors (58). In the heart, GRK2, 3 and 5 are expressed with GRKs 2 and 5 being the most abundant (58). Further, GRK subtypes 2 and 3 are also able to directly interact with the G$\beta\gamma$ subunits and PIP_2 in order to enhance GPCR phosphorylation and desensitization (59, 60). For multiple GPCRs, phosphorylation by GRKs is not sufficient to induce receptor desensitization and only upon the recruitment and binding of β-arrestins is the signal

attenuated through physical uncoupling of the heterotrimeric G proteins from the receptor (58). β-arrestin binding triggers the formation of clathrin-coated pits to traffic the receptor for proteasomal degradation or recycling (61). Finally, activation of GTPases causes heterotrimeric G proteins to reassemble, and repriming of the receptor for stimulation (61). Based upon studies of the α1B-AR subtype, α1-ARs are likely phosphorylated and desensitized by GRK2 and/or 3, and can be phosphorylated but not desensitized by GRK5 (62). Furthermore, α1B-ARs are readily endocytosed through interaction with β-arrestins and clathrin, whereas α1A-ARs are not (63). Based upon studies of the ET-R subtype A, ET-R desensitization and internalization likely occurs through GRK2 phosphorylation (64). AT-R desensitization occurs through phosphorylation by GRK2 and subsequent recruitment and formation of a β-arrestin/Src/AP-2 complex to promote internalization of the receptor through further interaction of ADP-ribosylation factor and clathrin (65, 66). Interestingly, AT-Rs are currently the only know Gq-receptor in cardiac myocytes to signal through the β-arrestin complex. Activation of AT-Rs using a biased ligand for β-arrestin signaling induces vasodilation, no cardiac hypertrophy but still increases cardiac contractility via β-arrestin mediated phosphorylation of tropomyosin and other contractile proteins (67).

1.3 Cardiac Nuclear G-Protein Coupled Receptors

Conventionally, GPCRs were thought to solely localize to the plasma membrane. Logically, this paradigm is most rational since activation of the receptors would occur through circulating ligand binding to the surface receptor, without further trafficking of the ligand to intracellular compartments. While many GPCRs localize to the plasma membrane of cells and modulate activity of membrane enzymes, ion channels, and second messengers, many GPCRs have also been localized to the nuclear membrane in various cell types. These receptors include: AT1R and AT2R; bradykinin B2; α1A-AR and α1B-AR; β1, β2, and minimally β3-adrenergic receptors (β1-, β2, β3-AR); endothelin subtype A and B receptors (ETRA, ETRB); c-erbB-4; fibroblast growth factor; insulin; interferon β; muscarinic cholinergic; nerve growth factor; neuropeptide Y; prostaglandin E2; lysophosphatidic acid type 1; urotensin II; and opioid receptors (68). In adult cardiac myocytes, functional AT1R, AT2R, ETRB, β1-AR, β3-AR, α1A-AR, and α1B-AR have all been localized to the nuclear compartment (56, 69-72). Cardiac nuclear Gαq receptors

include α1A-AR, α1B-AR, AT1R, and ETR-B. While there is still much to be defined about how each receptor is processed, trafficked, and inserted into the nuclear membrane in adult cardiac myocytes, each nuclear Gαq receptor mentioned above has a nuclear localization sequence (NLS) that is required to traffic the receptors to the nuclear membrane (73).

Transport of molecules into and out of the nucleus requires passage through nuclear pore complexes (NPC). NPCs allow passive diffusion of ions and small proteins (<40kDa), but larger molecules must contain the appropriate targeting signal such as an NLS or nuclear export signal (NES) (74). The shuttling of macromolecules between the cytoplasm and the nucleus is facilitated by carrier proteins that are collectively referred to as karyopherins, the largest class of which is the β-karyopherins (75). The first step of cytoplasmic to nuclear shuttling is identification of the cargo's NLS by the β-karyopherins, importin α and β. The NLS consists of either monopartite or bipartite stretches of basic amino acid residues. The monopartite NLS was first described in the SV40 large T antigen (PKKKRRV, basic amino acids underlined) (76). The bipartite NLS was first described in nucleoplasmin (KRPAATKKAGQAKKKK, basic amino acids underlined) (77). Importin α binds the NLS of the cargo protein and facilities binding of the cargo protein to importin β forming a complex of importin α and β bound to the cargo protein. The cargo is then shuttled to the NPC where importin β facilitates interactions with the NPC proteins in order to deliver the cargo protein to the nucleus. Once imported into the nucleus, proteins such as Nup2 and Cse1 act as release factors to dissociate importin α and β from the cargo (78). The importins are then shuttled out of the nucleus and into the cytoplasm by Cse1, and the process of nuclear transport can begin again (74). This NLS mediated nuclear import process is thought to be the way in which GPCRs are shuttled from the endoplasmic reticulum and inserted into the nuclear membrane (79). Other mechanisms associated with GPCR nuclear trafficking include lateral diffusion through peripheral channels between the NPC and the nuclear membrane and movement through the NPC using linkers (80).

The α1A-AR bipartite NLS (KKAFQNVLRIQCLCRK) and the α1B-AR monopartite NLS (RGRGRRRRRRR) both lie in the carboxy-tail region of their respective receptors (81). Mutation of either the α1A-AR or α1B-AR NLS results in mislocalization of either receptor, and inability of either receptor to activate downstream

signaling in adult cardiac myocytes (81). The AT1R NLS (KKFKKY) was identified in the carboxy-tail region of the receptor using mutants in HEK293 cells (82). The ETRB NLS has not been identified using rigorous experimental testing, but the NLS mapper (83) predicts a bipartite NLS (RFKNCFKSCLCCWCQTFEEKQSLEEKQSCLKF) at the carboxy-tail region of the receptor. Further, functional ETRBs have been identified on the nuclei of adult ventricular cardiac myocytes (71).

1.4 Cardiac Nuclear Gαq Receptor Signaling

Activating nuclear receptors requires ligands to either 1) enter the cell from the extracellular space through a channel at the cell surface, like α1-ARs or 2) be produced within the cell and go on to activate intracellular receptors like AT-Rs and ET-Rs. α1-ARs are activated by the endogenous cathecholamines epinephrine and norepinephrine. In adult cardiac myocytes, catecholamines entry into the cell is facilitated by extraneuronal monamine transporter/organic cation transporter 3 (EMT/OCT3) (28). OCT3 is present in adult cardiac myocytes and inhibition of OCT3 by corticosterone prevents α1-AR activation of downstream signaling partners (28). Further, the latency for contractile responses to α1-AR agonism is minutes versus seconds that would be expected for a receptor at the cell surface, consistent with translocation of the catecholamine from the outside to the inside of the cell (14). Angiotensin II (AngII), the ligand for both AT1R and AT2R, can be synthesized in cardiac myocytes (84). AngII is formed from the pro-peptides angiotensinogen and angiotensin I. Angiotensinogen is cleaved by the protease renin to form the protein angiotensin I. Angiotensin I is cleaved by angiotensin converting enzyme (ACE) to form AngII. The basal rate of intracellular AngII synthesis in cardiac myocytes is low, but upon stimulation with the β-AR agonist isoproterenol or high glucose, intracellular AngII synthesis increases (84). Further, cardiac myocytes expressed angiotensinogen, renin, and ACE indicating that the machinery is present in order to produce intracellular AngII (84). Endothelin-1 (ET-1) is the ligand for both the ETR-A and ETR-B in adult cardiac myocytes (85). ET-1, like AngII, is formed from a pro-peptide. Prepro-ET-1 is a 212 amino acid that is formed from the transcription of the endothelin gene, Edn1 (86). A 17-aa leader sequence targets preproET-1 to the endoplasmic reticulum where it enters the secretory pathway (87). Prior to exocytosis, furin-like proteases cleave preproET-1 to a 38-aa protein called big

ET-1 (88). The final cleavage step is mediated by endothelin-converting enzymes that cleave big ET-1 into active ET-1 (89, 90). Adult cardiac myocytes produce ET-1 at a low level in a resting state, but upon electrical stimulation cardiac myocytes increase ET-1 production at a variable rate (91).

1.4.1. Overview of Nuclear Gq-receptor Signaling Partners

The Gq-receptor signaling partners Gαq, PLCβ1, IP_3, and various PKCs have been identified in the nucleus of multiple cell types. Gαq has been identified in the nuclear membrane of HEK293 cells, primary neural cell cultures, and adult cardiac myocytes (92). PLCβ1 has been identified in the nucleus of Swiss 3T3 cells (93), rat liver cells (94), PC12 pheochromocytoma cells (95), and adult cardiac myocytes (28). IP_3 acting at the inner nuclear membrane through the IP3R2 has been demonstrated to be physiologically relevant. In neonatal rat ventricular myocytes, IP_3 acting at the nucleus is necessary to induce hypertrophy downstream of endothelin 1 (ET-1) acting on the ETRs (96). α1-ARs increase calcium spark frequency and induce “calcium waves” in the nuclear compartment which do not spread to the cytosol in neonatal rat ventricular myocytes (97). In adult cardiac myocytes, activation of the IP3R2 at the inner nuclear membrane activates calcium dependent excitation-transcription coupling. Upon IP_3 binding to the IP3R2, calcium is released from the nucleoplasm, the compartment separated from the cytoplasm by the nuclear envelope. Experiments on isolated nuclei, permeabilized, and intact cardiac myocytes show the activation of the IP3R2 increases nuclear calcium (97, 98). This increase in nuclear calcium leads to activation of multiple calcium-dependent proteins that modulate gene expression in adult cardiac myocytes including calmodulin, CaMKII, protein kinase D (PKD) and calciuneurin.

1.4.2 Calmodulin

Calmodulin is a highly-conserved calcium binding protein that is ubiquitously expressed in mammals, and is considered a major transducer of calcium signals in mammalian cells (44). Calmodulin acts as a calcium sensor for other proteins. When intracellular calcium concentrations rise, calmodulin binds calcium and undergoes a conformational change. This conformational change allows calmodulin to bind effector

proteins and thus propagate downstream signaling events (99). The most well studied of these calmodulin effector proteins in CaMKII.

1.4.3 Calmodulin Dependent Protein Kinase II

CaMKII is a serine-threonine kinase that exists as a dodecameric structure (100). CaMKII functions to coordinate calcium signals into downstream effects such as sarcoplasmic reticulum calcium uptake and release, chronotropic control, excitation-contraction coupling, and excitation-transcription coupling in adult cardiac myocytes (101). CaMKII exists in four isoforms (α, β, γ, and δ) with the δ isoform being the most abundant in the heart (102). The two dominant subtypes of CaMKIIδ expressed in the heart are CaMKIIδ_B and CamKIIδ_C, and different stoichiometries of these two subtypes are what comprise of the final multimeric CaMKIIδ enzyme (103). CaMKII nuclear localization is facilitated through the NLS present on in the CaMKIIδ_B variable domain (104). In the nucleus, activation of CaMKII downsteam of Gq-receptors promotes CaMKII mediated phosphorylation of HDAC4 and HDAC5 (105). Phosphorylation of HDAC4 and HDAC5 derepresses transcription and promotes re-expression of the fetal gene program, a hypertrophic hallmark, including atrial naturetic peptide, brain naturetic peptide, myosin light chain-2, and α- and β-myosin heavy chain (106-108).

1.4.4 Protein Kinase D

PKD belongs to the calcium/calmodulin-dependent protein kinase group of serine/threonine kinases. PKD consists of 3 isoforms: PKD1, PKD2, and PKD3 (109, 110). PKD is a 918-aa serine/threonine kinase that consists of an N-terminal regulatory domain,containing 2 cysteine-rich, zinc finger–like motifs and a pleckstrin homology domain, and a C-terminal catalytic domain (109, 111). All three PKD isoforms are expressed in the neonatal and adult heart with PKD1 being the primary isoform expressed (110, 112, 113). Activation of PKD downstream of Gq-receptors, including α1-ARs, ET-Rs, and AT-Rs, induces 1) phosphorylation of cardiac troponin I at serines 22 and 23 leading to reduced myofilament calcium sensitivity (114) and 2) phosphorylation of HDAC5 through direct interaction which facilitates the binding of 14-3-3 proteins and

induces the nuclear export and/or cytosolic retention of HDAC5 in neonatal rat ventricular myocytes (115).

1.4.5 Calcineurin

Calcineurin is a serine/threonine phosphatase, which, like CaMKII, is activated by binding of CaM (116). Under basal conditions, calcineurin exists in the cytosol of adult cardiac myocytes, but upon sustained, elevated calcium levels or disease states such as pressure overload calcineurin undergoes cytosolic to nuclear translocation (117). A putitive NLS sequence has been defined from amino acids 171-190 in calcineurin, the deletion of which prevents calcineurin cytosolic to nuclear translocation in cardiac myocytes (117). In the setting of hypertrophy, activated cytosolic calcineurin dephosphorylates the nuclear factor of activated T-cells (NFAT), promoting NFAT and calcineurin cytosolic to nuclear translocation (117, 118). Once in the nucleus, calcineurin and NFAT act to activate pathologic, but not physiologic, hypertrophic transcriptional responses (119, 120). These lines of evidence indicate that all the canonical excitation-transcription coupling Gq-receptor signaling partners: $G\alpha q$, $PLC\beta 1$, IP_3, calmodulin, CaMKII, PKD, and calcineurin are present within the nuclei of adult cardiac myocytes.

1.4.5 Regulation and Desensitization of Nuclear Gq-Receptors

With the discovery of Gq-receptor activation occurring at the nuclei in adult cardiac myocytes, much work has been done to identify regulators of nuclear Gq-signaling. The $G\alpha q$ coupled GPCR signaling regulators include GRKs and β-Arrestins. GRKs are separated into three subfamilies: rhodopsin kinases (GRKs 1 and 7), β-AR kinases (GRKs 2 and 3), and the GRK4 subfamily (GRKs 4, 5, and 6). Rhodopsin kinases and GRK4 are generally restricted to retina and testes, respectively (121). Only GRKs 2, 3, and 5 are appreciably expressed in the human heart, with GRKs 2 and 5 the most abundant in the myocardium (122-124). $\alpha 1$-ARs are a preferred substrate of GRK3 with an IC50 of 7 ± 0.4 pmol/mg of protein (125). ATR endocytosis in HEK293 cells is regulated by GRK2/3 (126). Endothelin receptors are also a preferred substrate of GRK3 with an IC50 of 5 ± 0.7 pmol/mg of protein (125). Yet, nuclear localization of GRK3 in cardiac myocytes has not been reported and GRK2 has been demonstrated to

be excluded from the nuclei in adult cardiac myocytes (127, 128). GRK5, on the other hand, includes a nuclear localization sequence and has been demonstrated to act as a histone deacetylase kinase (129, 130). Enhanced nuclear GRK5 activity increases transcription of genes associated with cardiac hypertrophy, through derepression of critical transcription factors (131). In adult rabbit myocytes, stimulation with AngII or phenylephrine (PE), an α1-AR agonist, but not ET-1 caused nuclear translocation of GRK5 as detected by immunostaining (132). These lines of evidence indicate that GRK5 may be the GRK regulating α1-AR signaling in intact adult cardiac myocytes due to the fact that the discovery of GRK3 regulated α1-AR signaling was done in an artificial system (125).

Canonically, after GRK phosphorylation of the active GPCR, β-Arrestins physically uncouple the G-protein from the receptor, terminating signaling which is the process known as desensitization (133). The two isoforms of β-arrestin are β-Arrestin 1 and β-arrestin-2 (134). Along with their role in the physical uncoupling of the G-protein from its receptor, β-arrestins have also been shown to promote degradation of second messenger molecules via recruitment of phosphodiesterases and kinases (135{Perry, 2002 #5912, 136). Apart from receptor desensitization, β-Arrestins can also initiate signaling cascades. Of note, AT1Rs, specifically the AT1A-R can initiate extracellular regulated kinase (ERK) signaling downstream of both Gαq and β-arrestin (137). There is currently no evidence to suggest that α1-ARs participate in biased signaling through β-arrestins. Further, β-arrestin 1 and 2 both contain a nuclear localization sequence in their N-domains, and a functional nuclear export signal is only present in the C-domain of β-arrestin 2 (138). Functionally, nuclear translocation of β-arrestin 1 is able to directly induce transcription, which was demonstrated in HEK293 cells transfected with the δ-opoid receptor (139). In neonatal rat myocytes, β-arrestin 2 mediates the nuclear to cytoplasmic translocation of HDAC4 downstream of β-adrenergic receptors (140). Taken together, both regulators of GPCR signaling, GRKs and β-arrestins, are able to access and interact with GPCRs at the cell surface and at the nuclear membrane indicating the potential for compartmentalized signaling in adult cardiac myocytes.

1.5 Differential Signaling of Cardiac Gαq Receptors

As stated previously, GPCRs in adult cardiac myocytes are found both on the sarcolemma and at the nuclear membrane. For Gq-receptors, functional AT-Rs and ET-Rs exist at both membranes, and α1-ARs exist primarily at the nuclear membrane (28, 71{Tadevosyan, 2010 #2920). For AT-Rs and ET-Rs, which localize to both membranes, differences in sarcolemmal versus nuclear signaling have been reported (141).

In fractionated adult cardiac myocytes, endogenous ATRs are detected by Western blot at the plasma and nuclear membranes, with the majority at the plasma membrane (69). Sarcolemmal, not nuclear, AT-Rs are thought to induce the detrimental effects of AT-Rs in cardiac myocytes since angiotensin receptor blockers improve outcomes in heart failure and do not readily to cross the sarcolemma (142). Cardiac myocyte cellular responses to sarcolemmal AT-R stimulation include negative inotropy, cardiac myocyte cell death, and induction of pathologic hypertrophy (143). Mice lacking cardiac AT-Rs are protected from detrimental cardiac remodeling after myocardial infarction as compared to their wild type counter parts (144). Nuclear AT-Rs may also lead to the development of cardiac hypertrophy and disease through activation by intracellular AngII (145). In neonatal rat ventricular myocytes, expression of adenoviral AngII resulted in cellular hypertrophy (146). In mice injected with a cardiac myocyte specific AngII plasmid which was retained in the myocytes developed cardiac hypertrophy, but transgenic mice whose cardiac myocytes chronically secreted AngII failed to develop hypertrophy (146, 147{Baker, 2004 #5941). Taken together, these data indicate that both sarcolemmal and nuclear AT-R signaling promotes pathologic cardiac myocyte hypertrophy.

Radioligand-binding on fractionated adult cardiac myocytes indicates that ETR levels are half that of α1-ARs, and identifies 95% of endogenous ETRs at the plasma membrane, with 5% of endogenous ETRs in the nuclear fraction (71, 81{Boivin, 2003 #2613). Sarcolemmal ET-Rs, primarily the A subtype, have been localized to the t-tubules in adult cardiac myocytes, specifically to the bottom of the t-tubules {Robu, 2003 #2977}. In cultured adult cardiac myocytes, activation of sarcolemmal ET-Rs by endothelin-1 promotes cardiac myocyte cell survival and positive inotropy (85). Yet, overexpression of endothelin-1 induces heart failure in mice, whereas ET-R knockout mice show less consistent results with global KO inducing embryonic lethality, and

cardiac-specific KO suggesting direct and indirect effects to induce heart failure. (148-150). Nuclear ET-Rs, primarily the B subtype, regulate nuclear calcium levels independent of sarcolemmal ET-Rs and gene expression in adult cardiac myocytes through excitation transcription coupling (151). While more work needs to be done to further understand the role of nuclear ET-Rs, the current evidence suggests that nuclear ET-Rs may be protective whereas sarcolemmal ET-Rs may be detrimental in the heart. This conclusion can be based on the evidence that mice that overexpress ET-1 exhibit cardiac hypertrophy and heart failure, and that extracellular ET-1 is unlikely to readily cross the sarcolemma and activate nuclear ET-Rs.

Early work with α1-AR antibodies localized the α1-AR to caveolae in adult cardiac myocytes (152), but these antibodies were not validated at the time of publication and have since been demonstrated to be non-specific for α1-ARs (153). Using validated approaches such as adenoviral expression, binding assays on fractionated myocytes, and fluorescently labeled ligands, α1-ARs have primarily been localized to the nuclear membrane in adult cardiac myocytes (14). Radioligand-binding on fractionated adult cardiac myocytes identifies 80% of endogenous α1-ARs in the nuclear fraction (28). Further, signaling through α1-ARs has been localized to the nuclear compartment including activation of intranuclear PKC species and initiation of ERK activation (28, 154). Taken together, these lines of evidence indicate that nuclear Gq-signaling through ET-Rs and α1-ARs may promote cardioprotective signaling whereas sarcolemmal and nuclear Gq-signaling through AT-Rs is detrimental.

1.6 Overarching Hypothesis and Aims

Due to the growing body of evidence that indicates that GPCRs do not solely localize to the cell surface in many different cell types including cardiac myocytes (68), we are seeking to *advance the paradigm that receptor subcellular localization dictates the function of the receptor*. Specifically, this thesis will focus on the functional implication of differential subcellular localization and signaling compartmentalization in the context of cardiac myocyte hypertrophic signaling of two Gq-coupled receptors: α1-ARs and AT-Rs. Convention holds that all Gq-receptors localize to and initiate pathologic remodeling from the sarcolemma in cardiac myocytes (155), yet further work with α1-ARs in adult mouse and human cardiac myocytes indicate that α1-ARs are unique Gq-

receptors based on function and localization (14). Unlike other Gq-receptors, α1-ARs localize to the nucleus and mediate physiologic hypertrophy, positive inotropy, and cardiac myocyte cell survival (14). In contrast, AT-Rs behave as prototypical Gq-receptors and localize to the sarcolemma and mediate pathologic hypertrophy, negative inotropy, and cardiac myocyte cell death (143). To test the *hypothesis that the differential effect of α1-ARs and AT-Rs on myocyte hypertrophic signaling is based on subcellular compartmentalization,* we addressed four different aspects of α1-ARs versus AT-Rs: 1) localization, 2) immediate proximal signaling through PLCβ1, 3) downstream signaling through ERK, and 4) terminal signaling through hypertrophic gene activation.

1.6.1 To define and compare the localization of endogenous α1-ARs and AT-Rs in adult cardiac myocytes.

Here we sought to identify the localization of α1-ARs and AT-Rs in intact adult cardiac myocytes. While much has been done to localize both α1-ARs and AT-Rs, the methods used thus far have been less than ideal. For α1-ARs, previous methods to localize the endogenous receptors have included binding assays using fractionated adult cardiac myocytes, and treatment with a tagged α1-AR ligand expression (28). Another method to determine α1-AR localization has been expression of exogenous α1-ARs tagged with a fluorescent moiety in an α1-null background (28). Drawbacks of these techniques include: 1) binding assays lack sensitivity, 2) tagged ligand had undesirable kinetics and is no longer available, and 3) exogenously expressed, fluorescently tagged α1-ARs do not allow for the detection of endogenous receptors. To address these short comings, we developed a novel α1-AR ligand that has improved kinetics and has the potential to be used in live-cell assays. For AT-Rs, previously used methods to localize the receptors have been based on antibody staining in intact adult cardiac myocytes and use of fractionated adult cardiac myocytes in Western blotting (69). These antibodies have not been validated, and there have been reports that GPCR antibodies overall do not detect a specific band (156). To address this short coming, we employed a fluorescently tagged Angiotensin II, the ligand for AT-Rs. This is the first time that endogenous AT-Rs have been localized in intact adult cardiac myocytes using a validated ligand.

1.6.2 To define proximal PLCβ1 signaling downstream of α1-ARs and AT-Rs

Here we sought to test the hypothesis that α1-ARs and AT-Rs activate PLCβ1 in different subcellular compartments corresponding to their localization, with α1-ARs activating PLCβ1 at the nucleus and AT-Rs activation PLCβ1 at the sarcolemma. Previous work has indicated that PLCβ1 only localizes to and is activated at the sarcolemma in adult cardiac myocytes based on the idea that nuclear localized PLCβ1 activity appears most often in undifferentiated cells, and thus is unlikely to occur in adult cardiac myocytes which are terminally differentiated (157). The sarcolemmal localization and activation of PLCβ1 has also been implicated in the development of cardiac arrhythmias and pathologic hypertrophy (27). AT-Rs localize to the sarcolemma and so we hypothesized that AT-Rs would activate PLCβ1 at the sarcolemma, but it was unclear if α1-ARs would activate PLCβ1 at the sarcolemma since α1-ARs localize to the nucleus in adult cardiac myocytes. Thus, we sought to challenge previous knowledge and investigate whether PLCβ1 and its substrate PIP_2 was present at the nucleus and whether it was activated downstream of α1-ARs or AT-Rs. In order to study sarcolemmal PLCβ1 activation downstream of α1-ARs and AT-Rs, we employed a fluorescent PLCβ1 biosensor. Using this biosensor we found that AT-Rs, but not α1-ARs, activate PLCβ1 at the sarcolemma. In order to study nuclear PLCβ1 activation downstream of α1-ARs and AT-Rs, we first sought to identify whether or not PLCβ1 and PIP_2 were present in the nuclear membrane of adult cardiac myocytes. Using immunocytochemistry we identified PLCβ1 at the nuclear envelope, and using a novel mass-spectrometry approach we identified PIP_2 in the nuclear fraction of adult cardiac myocytes. Further, we used the same PLCβ1 biosensor and tagged it with a NLS in order to study the activation of nuclear PLCβ1. We found that α1-ARs, and minimally AT-Rs, activate nuclear PLCβ1 in adult cardiac myocytes. Thus, our data support the hypothesis that α1-ARs and AT-Rs activate proximal signaling through PLCβ1 in different subcellular compartments in adult cardiac myocytes, with α1-ARs activating PLCβ1 primarily at the nucleus and AT-Rs activating PLCβ1 primarily at the sarcolemma. This is the first report of differential PLCβ1 localization and activation and PIP_2 localization in adult cardiac myocyte nuclear membranes.

1.6.3 To define Gq-receptor activation of downstream ERK signaling

Here we sought to test the hypothesis that α1-ARs and AT-Rs differentially activate ERK both in degree and intracellular location, and this differential activation might explain the differences between α1-ARs and AT-Rs on myocyte survival. In cardiac myocytes, convention indicates that Gq-receptor signaling promotes cell death. While true for angiotensin receptors (AT-Rs), we previously identified an α1A-adrenergic receptor (α1A-AR) ERK survival signaling pathway (56). We previously demonstrated that α1-ARs localize to and induce intranuclear signaling in adult cardiac myocytes, whereas AT-Rs primarily localize to and signal at the sarcolemma (69, 154). To test this hypothesis, we used an ERK activity biosensor to investigate α1-AR and AT-R mediated ERK activation with fluorescence lifetime imaging microscopy (FLIM) in adult cardiac myocytes. Our results indicate α1-ARs activate ERK more efficaciously with a different subcellular localization than AT-Rs, providing mechanistic insight into the differential effects on cell survival of these receptors. This is the first report of differential localization of ERK activity in adult cardiac myocytes, and it is the first report of FLIM being employed to study kinase activation and localization in adult cardiac myocytes.

1.6.4 To define Gq-receptor activation of terminal hypertrophic gene activation

Here, we hypothesized that α1-ARs, due to their close proximity to transcriptional machinery at the nucleus, would induce a more robust, cardioprotective transcriptome, and that AT-Rs, due to their distance from the nucleus, would induce a more moderate, pathologic transcriptome in adult cardiac myocytes. Convention indicates that Gq-receptors promote pathologic hypertrophy that ultimately leads to heart failure (155). In neonatal rat ventricular myocytes, Gq agonists such as AngII and phenylephrine cause an increase in cell size, reorganization of sarcomeric proteins, and re-expression of the fetal gene program (155). These responses in neonatal rat ventricular myocytes, a model of pathologic cardiac hypertrophy, mimic what is observed in animal models that over-express Gq (158, 159). While the conclusion of toxic Gq-receptor signaling is based

on these models, the models themselves may not represent physiologically relevant responses to Gq-stimulation. For example, neonatal rat ventricular myocytes express α1-ARs roughly 10-fold more than humans or mouse, which may result in an exaggerated hypertrophic response of neonatal rat ventricular myocytes to α1-AR stimulation by phenylephrine (14). Further, much of the animal data that implicated Gq-receptors in pathologic hypertrophic signaling was based on mice that overexpressed Gαq 8-fold, which markedly exceeds the 2-fold overexpression of Gαq seen in human heart failure (14). Finally, previous work from our lab indicates that α1-ARs activate physiologic hypertrophy (160). Physiologic hypertrophy is defined as an increase in heart size with either no change or an increase in fuction, this is in direct contrast for pathologic hypertrophy which is defined as an increase in heart size with a decrease in function. Together, these lines of evidence point to a more dual role for Gq-receptors in adult cardiac myocytes with some Gq-receptors such as AT-Rs activating pathologic hypertrophy and some Gq-receptors such as α1-ARs activating physiologic hypertrophy. Thus, we sought to understand the differences in AT-R and α1-AR mediated hypertrophic transcriptional activation in adult mice which express α1-ARs at similar levels to humans. To test this hypothesis, we used cardiac myocytes isolated from adult mice treated with either the α1-AR agonist phenylephrine or the AT-R agonist AngII and RNA-sequencing. We are the first to report differences in Gq-receptor mediated activation of transcription at the gene level in the adult mouse heart.

CHAPTER 2. α1-ARs and AT-Rs Localize to Different Subcellular Compartments in Adult Cardiac Myocytes

Erika F. Dahl[1], Chastity L. Healy[2], Timothy D. O'Connell, PhD[2]

[1] Department of Pharmacology, University of Minnesota, Minneapolis, MN 55455
[2] Department of Integrative Biology and Physiology, University of Minnesota, Minneapolis, MN 55455

2.1 Summary

Conventional models of GPCR signaling indicate that all GPCRs localize to and signal at the plasma membrane. Previous work from multiple groups indicates that this convention does not hold in all cell types. In adult cardiac myocytes, Gαq (Gq) coupled α1-adrenergic receptors (α1-ARs) localize primarily to the nuclear membrane, whereas other Gq receptors have been hypothesized to primarily localize to the sarcolemma. Previous modalities to study Gq-receptor localization in adult cardiac myocytes have lacked sensitivity and have not been rigorously validated. Here we developed and verified a novel tool to study α1-AR nuclear localization and identified α1-ARs primarily at the nuclear membrane, consistent with previous reports. Further, we verified a commercially available fluorescently labeled ligand to study the localization of angiotensin receptors (AT-R) and localized AT-Rs primarily to the sarcolemma in adult cardiac myocytes. These results indicate that α1-ARs and AT-Rs localize to different compartments in adult cardiac myocytes and that this difference in localization may explain the difference in physiologic function of these two Gq-receptors.

2.2 Introduction

Conventional models of G-protein coupled receptor (GPCR) signaling describe ligand binding to plasma membrane GPCRs, which then intitiate downstream signaling within the cell. This "outside-in" signaling model suggests that all GPCRs localize to and signal at the plasma membrane in all cells. Yet, further work has been done by multiple groups using a variety of cell types that indicates that not all GPCRs localize to the plasma membrane, and that there are functional GPCRs present on intracellular organelles including the nucleus (4, 141). In adult cardiac myocytes, both the α1A- and

α1B-AR primarily localize to the nuclear membrane (81). Further, functional studies indicate that both α1-AR subtypes are functional at the nuclear membrane and that mislocalization of either receptor through mutation of either nuclear localization sequence (NLS) prohibits functional signaling (81). Conversely, AT-Rs, specifically the type 1 receptor, has been primarily localized to the sarcolemma through studies using angiotensin receptor blockers which do not readily cross the sarcolemma and unvalidated antibodies (69, 143). Based on these findings, we hypothesized that these two Gq-receptors, α1-ARs and AT-Rs, localized to different subcellular compartments in adult cardiac myocytes and that this difference in subcellular localization may explain the different physiologic outcomes induced by these receptors.

2.3 Methods

Mouse Lines

In this study, male and female C57BL/6J mice (10-15 weeks of age) were used as the source of primary adult cardiac myocytes. Male and female C57BL/6J mice were included due to no historical evidence indicating differences in receptor (α1-AR and AT-R) density. All animals were treatment naïve and housed under 12-hour light/dark cycle and fed standard chow. The use of all animals in this study conformed to the PHS Guide for Care and Use of Laboratory Animals and was approved by the University of Minnesota Institutional Animal Care and Use Committee. The University of Minnesota provides AAALAC-accredited services and resources for using animals in research, including animal ordering, care, facilities, housing, and training for researchers and lab personnel.

Cell Lines

The cell line used in this study are HEK293 cells used for adenoviral amplification. HEK293 cells were cultured in Dulbecco's Modified Eagle's Medium (DMEM) supplemented with 10% fetal bovine serum and 1% penicillin/streptomycin. Cells were incubated at 5% CO_2 and 37°C. No information on sex or cell authentication information is available for this cell line.

Isolation and Culture of AMVM

As we have described previously (161), adult mouse ventricular myocytes were isolated from wild-type male and female C57BL/6J mice between 10 and 15 weeks of age. Briefly, mice were anesthetized with isoflurane (3% for induction, 1.5% for maintenance), injected with heparin (100 IU/mL), the pleural cavity was opened and the heart removed, cannulated on a retrograde perfusion apparatus, and perfused with collagenase type II to dissociate ventricular myocytes. Isolated cardiac myocytes were plated at a density of 50 rod-shaped myocytes per square millimeter on laminin-coated culture dishes. Myocytes were cultured in MEM with Hank's Balanced Salt Solution, 1 mg/ml bovine serum albumin, 10 mM 2,3-butanedione monoxime, and 100 U/ml Penicillin in a 2% CO_2 incubator at 37°C. All reagents were purchased from Sigma Aldrich unless otherwise specified. Full details of the buffers, enzymes, cell culture medium, all procedures for isolation and culturing of AMVM and a detailed diagram of the perfusion apparatus were described in detail previously (161). Following plating, myocytes were counted at a magnification of 20X to determine cell viability. Adenovirus was added based on previously determined multiplicity of infections. Infected myocytes were incubated in a 2% CO_2 incubator at 37°C for 40 hours. If myocytes were left uninfected (α1-AR QDot 565 and AngII-TAMRA) myocytes were incubated at in a 2% CO_2 incubator at 37°C for 24 hours before beginning experiments.

Isolation of Nuclei from AMVM

Immediately following isolation, myocytes were allowed to settle by gravity before aspiration of supernatant. Myocytes were washed in Buffer A (10 mM K-HEPES, 1.5 mM $MgCl_2$, 10 mM KCl, 0.2 mM activated Na_3VO_4, 1 mM DTT, 50 U/mL DNase, 10 μL/mL protease inhibitor cocktail) and centrifuged at 25 x *g* for 2 minutes. Supernatant was aspirated and the myocytes were resuspended in Buffer A. Myocytes were incubated on ice for 15 minutes to allow for swelling, and subsequently homogenized for 20 strokes using a dounce homogenizer. The homogenate was centrifuged for 2 minutes at 25 x *g*. The supernatant was collected and the pellet was resuspended in Buffer A. The homogenization and centrifugation steps were repeated, and the pellet was resuspended in Buffer A. The resuspended pellet was then sonicated and the homogenate was centrifuged at 2,000 x *g* for 15 minutes to collect nuclei. 1.95M sucrose was added to the pellet and layered on top of 1.95M sucrose in an Ultra-Clear Beckman Coulter 14 x 89 mm centrifuge tube. The supernatant containing the myocyte

sarcolemmal fraction and cytosolic fractions was added to a separate Ultra-Clear Beckman Coulter 14 x 89 mm centrifuge tube. The nuclei (tube 1) and myocyte sarcolemmal/cytosolic fractions (tube 2) were centrifuged at 100,000 x *g* for 90 minutes at 4°C. The nuclear pellet from tube 1 was resuspended in Buffer C (20 mM Na-HEPES, 1.5 mM $MgCl_2$, 0.2 mM EDTA, 0.2 mM EGTA, 25% Glycerol, 0.5 mM DTT, 0.5 mM PMSF, 10 μL/mL protease inhibitor cocktail). The supernatant from tube 2 was collected as the cytosolic fraction and the pellet from the tube 2 was resuspended in Buffer C for the myocyte sarcolemmal membrane fraction.

Adenoviral Production

α1A-GFP: As previously described (56), the α1A-GFP fusion protein was constructed with GFP fused to the C-terminus of the human α1A-AR (NM000680) cDNA. The α1A-AR cDNA was amplified with primers designed to remove the stop codon and insert Bgl II and Mlu I restriction sites 5' and 3', respectively. The resulting PCR product was cloned into pCR2.1-TOPO (Invitrogen), then subcloned into the Bgl II-Mlu I restriction sites in the multi-cloning site of the humanized $pGFP^2$-N3 vector with GFP at the C-terminus. To generate adenovirus, the α1A-GFP was amplified by PCR with primers designed to insert Pme I and Xba I restriction sites at the 5' and 3' ends, respectively. The resulting PCR product was cloned into the pCR2.1-TOPO vector (Invitrogen), then subcloned into the Pme I-Xba I restriction sites in the Ad5CMV K-NpA vector under control of the CMV promoter.

Viral amplification and purification: Viral amplification and purification was peformed by ViraQuest, Inc. For experiments, culture AMVM were counted at 20X and infected at the following multiplicity of infection for α1A-GFP: 1000 (titer: 5.9×10^{10}).

Synthesis of α1-QDot-565

The synthesis of α1-QDot-565 is a two-step process in which the pharmacophore of piperazinyl α1AR antagonists is first attached to biotinylated PEG, and the resulting α1-PEG-biotin product is then joined to a streptavidin coated QDot to create a novel fluorescent α1AR antagonist. First, 2-Piperazinyl-4-amino-6,7-dimethoxyquinazoline (MW = 289.33) was combined with Poly(ethylene glycol) (N-hydroxysuccinimide 5-pentanoate) ether 2-(biotinylamino)ethane (average M_n 3,800) at a molecular weight ratio of 1:2 in an excess of anhydrous dimethyl sulfoxide in a round bottom flask under a

blanket of argon. The mixture was constantly stirred and heated at 40°C for 40 hours. The reaction mixture was then added to an excess of HPLC grade diethyl ether, filtered, and speed vacuumed overnight. The dried precipitate was resuspended in water and subsequently lyophilized for 48 hours. The final product, 2-Piperazinyl-4-amino-6,7-dimethoxyquinazoline-Poly(ethylene glycol)-biotin, was then stored under a blanket of argon at -20°C. Second, 2-Piperazinyl-4-amino-6,7-dimethoxyquinazoline-Poly(ethylene glycol)-biotin was resuspended in water and added to streptavidin conjugated QDot 565 at a ratio of 20:1. The mixture was rocked at 4°C for 30 minutes in a dark tube to make the final product, α1-QDot 565.

Localization of α1-ARs in AMVM

To define the localization of α1-ARs in adult cardiac myocytes, cultured AMVM plated on coverslips were incubated with 25 nM α1-QDot 565 for 30 minutes at 37°C in the presence and absence of 5 μM prazosin. Myocytes were fixed in 4% paraformaldehyde and mounted in Fluoromount G. Confocal images were captured on an Olympus FluoView FV1000 IX2 Inverted Confocal Microscope at 60X magnification (oil immersion). To detect α1-ARs in the nuclear membrane, myocyte nuclei were isolated, and resuspended in buffer N (120.4 mM NaCl, 14.7 mM KCl, 0.6 mM KH_2PO_4, 0.6 mM Na_2HPO_4, 1.2 mM $MgSO_4$-$7H_2O$, 10 mM Na-HEPES, 4.6 mM $NaHCO_3$, 30 mM Taurine, 10 mM 2, 3-Butanedione monoxime, 5.5 mM Glucose) (161). Nuclei were subsequently incubated with 25 nM α1-QDot 565 for 15 minutes at 37°C. Nuclei were mounted in Fluoromount G and imaged with confocal microscopy as above.

Localization of AT-Rs in AMVM

To define the localization of AT-Rs in adult cardiac myocytes, cultured AMVM plated on coverslips were incubated with 1 μM Angiotensin II-TAMRA (AngII-TAMRA) in the presence and absence of 5 μM unlabeled AngII for 5 minutes at 37°C. Slides were prepared exactly as described for α1-QDot 565. Confocal images were captured on an Olympus FluoView FV1000 IX2 Inverted Confocal Microscope at 60X magnification (oil immersion). Images were deconvolved for 10 cycles using AutoQuant X3. 3D surface plots were created in FIJI using the 3D surface plot plugin. 3D images were created in FIJI using the volume viewer plugin.

Localization of NCX1 in AMVM

To define the localization of NCX1 in adult cardiac myocytes, cultured AMVM plated on coverslips were fixed and stained with anti NCX1 (1:200 dilution) followed by the appropriate AlexaFluor 488 secondary antibody (1:500 dilution). Cells were imaged by confocal microscopy.

Statistical Analysis

All data plotting and statistical analysis was performed using Prism 6 software. All information on statistical parameters can be found in figure legends. Images of α1-QDot 565 (α1-QDot 565, α1-QDot 565 + prazosin, QDot 565 alone (not shown)) were quantified using FIJI analyze particle plug-in. Data were analyzed by One-Way ANOVA and $P<0.05$ was considered significant.

2.4 Results

α1-ARs localize to the nuclei and AT-Rs localize to the sarcolemma in adult cardiac myocytes.

Here, we sought to define the subcellular localization of α1-ARs and AT-Rs in adult cardiac myocytes (**Figure 2.1**). Previously, we demonstrated that endogenous α1-ARs localize to the nucleus in adult mouse ventricular myocytes (AMVM)) (28, 81, 154). However, reagents typically employed to localize receptors are generally unreliable, especially α1-AR subtype-specific antibodies, which lack specificity (153), or fluorescent ligands, which are no longer commercially available, but nonetheless had suboptimal binding kinetics (28). To overcome these shortcomings, we developed a novel α1-AR ligand comprised of 2-piperazinyl-4-amino-6,7-dimethoxyquinazoline, the common pharmacophore of α1-AR antagonists such as terazosin and doxazosin, attached to a polyethylene glycol linker with a terminal biotin moiety fused to a streptavidin coated fluorescent quantum dot (QDot) with an emission wavelength of 565 nm (**Figure 2.2A**) (162). We validated the α1-QDot-565 by infecting wild-type (WT) AMVM with a green fluorescent protein labeled α1A-AR (α1A-GFP), incubating infected myocytes with the α1-QDot, and co-localizing the GFP and QDot fluorescent signals as an indication of receptor binding (**Figure 2.2B**). In AMVM expressing α1A-GFP, the α1-QDot-565 fluorescent signal co-localized with the GFP fluorescent signal at the nucleus, and

pretreatment with the α1-AR antagonist prazosin diminished QDot fluorescence to nearly undetectable levels, demonstrating specificity (**Figure 2.2C**). We employed the same method as above in uninfected WT AMVM, and the α1-QDot-565 bound to endogenous α1-ARs at the nuclei in WT AMVM in the absence of prazosin replicating our previous findings (28, 81, 154) (**Figures 2.1A** and **2.2C**, quantified in **2.1B**). Further, the α1-QDot-565 bound endogenous α1-ARs in nuclei isolated from WT AMVM, indicating the presence of α1-ARs at the nuclear membrane, again replicating our previous findings (28, 81, 154) (**Figure 2.1C**). Therefore, the α1-QDot-565 fluorescent ligand identified endogenous α1-ARs at the nucleus in AMVM, and outperformed prior fluorescent α1-ligands by improving kinetics (30 minutes) at lower concentrations (25 nM) (28)

Similar to α1-ARs, the lack of validated antibodies for AT-Rs led us to employ another fluorescent ligand to define the localization of endogenous AT-Rs in AMVM. In this case, we used angiotensin II (AngII), the endogenous ligand of AT-Rs, labeled with the red fluorophore tetramethylrhodamine (TAMRA). We incubated AMVM with AngII-TAMRA in the absence or presence of unlabeled AngII to demonstrate the specificity of AngII-TAMRA (**Figures 2.1D**, **2.1E** and **2.1F**). In AMVM, AngII-TAMRA produced a distinct localization in confocal sections from the myocyte surface (**Figure 2.1E, left panel**), whereas AngII-TAMRA showed much less specific binding in confocal sections from the middle of the myocyte (**Figure 2.1D, left panel**). Pretreatment with unlabeled AngII abolished the AngII-TAMRA signal indicating specificity (**Figure 2.1F**). To clarify receptor localization, slices from the top and middle of the cell were deconvolved, and 3D surface plots were created that identified AngII-TAMRA signal predominantly at the myocyte surface (**Figure 2.1D versus 2.1E, center and right panels**, arrows indicate localization). Finally, a volume rendering was created from a confocal stack of a myocyte labeled with AngII-TAMRA demonstrating that the majority of the AngII-TAMRA signal localized to the myocyte surface (**Figure 2.1G**). We attempted to co-stain AngII-TAMRA labeled cells with an antibody to the Na/Ca exchanger (NCX) to define sarcolemmal localization. However, this was unsuccessful because the antibody staining protocol, which included a detergent permeablization step, resulted in loss of AngII-TAMRA labeling (163). Alternatively, cardiac myocytes stained with NCX antibody alone show a similar staining pattern to AngII-TAMRA (**Figure 2.3**). Previously, a small population of AT-Rs was identified at the nucleus in AMVM based on immunochemical detection and

functional assays, although the overall physiologic significance of this population of AT-Rs is still unclear (69). Further, this population of nuclear AT-Rs, which is activated by intracrine AngII, represents only a fraction of total AT-Rs (69). Our results with AngII-TAMRA indicate that the majority of ligand-accessible AT-Rs exist at the sarcolemma, and failure to detect nuclear AT-Rs here is likely due to the fact that neither AngII nor AT-R antagonists readily cross the sarcolemma (142). In summary, AngII-TAMRA identified endogenous AT-Rs on the sarcolemma, and combined with results from α1-QDot-565 identification of endogenous α1-ARs at the nucleus, the data indicate that endogenous α1-ARs and AT-Rs localize to different subcellular compartments in adult cardiac myocytes.

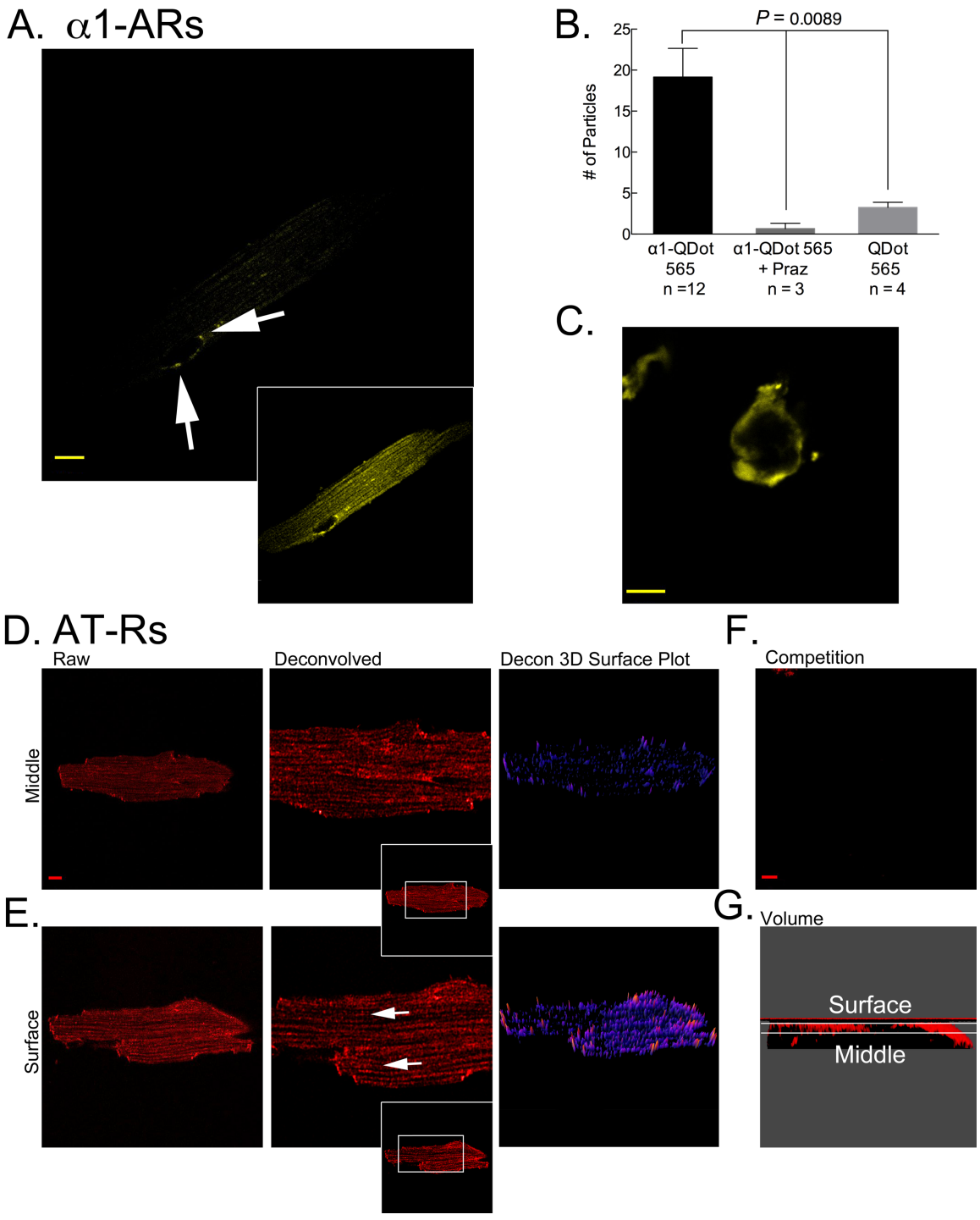

Figure 2.1. α1-ARs localize to the nuclei and AT-Rs localize to the sarcolemma in adult cardiac myocytes

A. *α1-ARs localize to the nuclei in AMVM.* α1-QDot-565 was added to cultured WT AMVM (25 nM, 30 min, 37°C). Myocytes were fixed and imaged by confocal microscopy (60X oil immersion). A representative myocyte is shown, arrows indicate nuclei. Inset is intentionally overexposed for visualization of whole cell. Scale bar = 10 μm. **B.** *Quantification of α1-QDot-565 localization.* The QDot fluorescent intensity from all cardiac myocytes was quantified using FIJI (number of cardiac myocytes, n, indicated in figure, see also **Figure 2.2**). QDot-565 alone images not shown. Data are presented as mean ± SEM. Data were analyzed by one-way ANOVA, and $P<0.05$ was considered significant. α1-QDot 565 (n=12 myocytes from 4 hearts); α1-QDot 565 + praz (n=3 myocytes from 2 hearts); QDot 565 alone (n=4 myocytes from 1 heart). Scale bar = 10 μm. **C.** *α1-QDot-565 labels nuclei isolated from AMVM*. Nuclei were isolated from WT AMVM and incubated with α1-AR-QDot-565 (25 nM, 15 min, 37°C). Nuclei were fixed and imaged as in **A**. One representative nuclei is shown. **D and E.** *AT-Rs localize to the sarcolemma in AMVM.* AngII-TAMRA (1 μM, 5 min, 37°C) was added to WT AMVM. Raw optical sections of the middle (top, left) and top (bottom, left) of the myocytes were captured by confocal microscopy (60X oil immersion). Deconvolution of optical sections from the middle (top, center) and surface (bottom, center) was achieved using AutoQuant X3. Arrows indicate AT-R localization at the sarcolemma. 3D surface images of deconvolved images middle (top, right) and surface (bottom, right) were created using FIJI to demonstrate receptor density. Scale bar = 10 μm. **F**. *AngII-TAMRA is specific for AT-Rs in AMVM*. WT AMVM were pretreated with an excess of unlabeled AngII (50 μM, 2 min, 37°C) then incubated with AngII-TAMRA (1 μM, 5 min, 37°C). Signal was undetectable indicating specificity. Scale bar = 10 μm. **G.** *Volume plot of AngII-TAMRA treated AMVM showing surface localization*. 3D volume plot was created using FIJI.

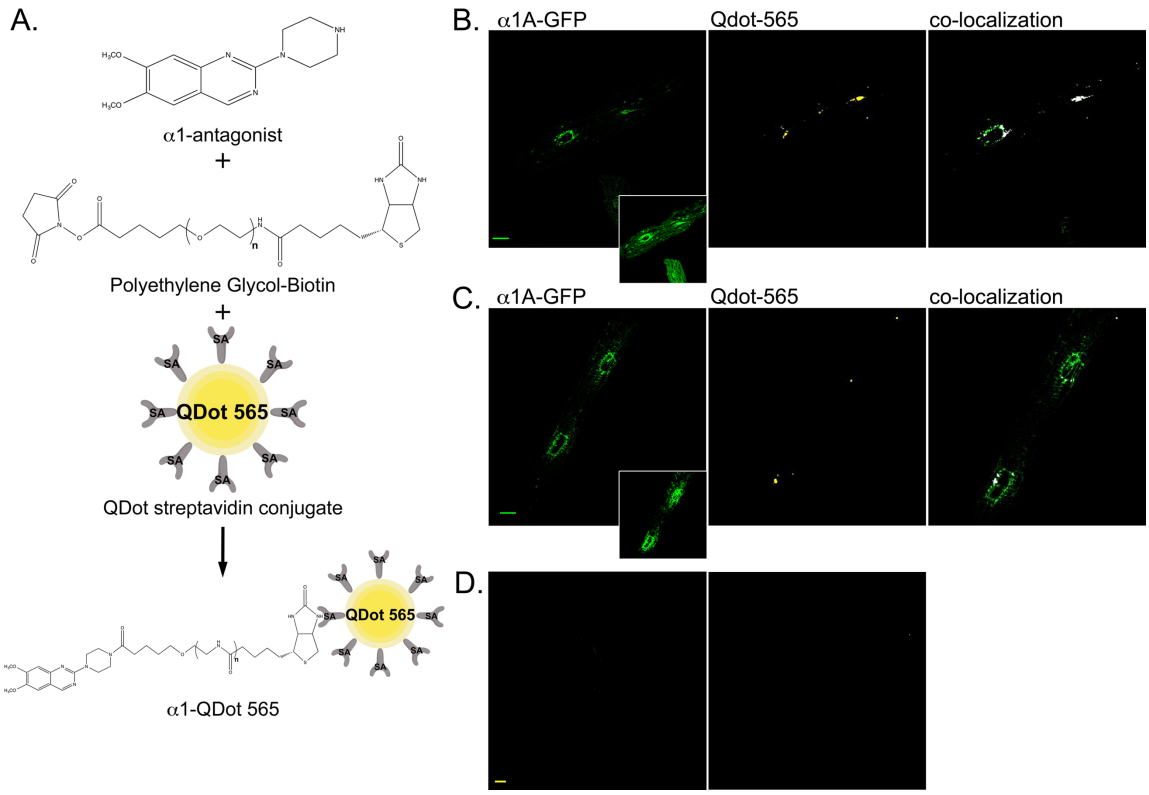

Figure 2.2. Synthesis and validation of α1-AR Qdot-565.

A. *Synthesis of α1-AR-QDot-565.* The structural backbone of the piperazole class of α1-AR antagonists, 2-Piperazinyl-4-amino-6,7-dimethoxyquinazoline, was attached to biotinylated PEG (Poly(ethylene glycol) (N-hydroxysuccinimide 5-pentanoate) ether 2-(biotinylamino)ethane). The resulting α1-antagonist-PEG-biotinylated molecule was then coupled to streptavidin conjugated QDot-565 to make α1-QDot-565. **B.** *Validation of α1-QDot-565.* To define the specificity of the α1-QDot-565, WT AMVM were infected with an adenovirus expressing α1A-GFP and then treated with 25 nM α1AR-QDot-565. Cells were fixed and imaged by confocal microscopy. α1A-GFP signal (green), QDot-565 signal (yellow), and co-localization determined in post-processing (white). Scale bar = 10 μm. **C.** S*pecificity of α1-QDot-565.* Myocytes expressing α1A-GFP were pretreated with an excess of unlabeled praz (5 μM) then treated with 25 nM α1-AR-QDot-565. α1A-GFP signal (green), QDot-565 signal (yellow) and colocalization determined in post-processing (white). Scale bar = 10 μm. **D.** S*pecificity of α1-QDot-565 in WT AMVM.* To demonstrate the specificity of the α1-QDot-565, WT AMVM were pretreated with an

excess prazosin (5 μM, 30 min, 37°C) then incubated with α1-AR-QDot-565 (25 nM, 30 min, 37°C). Two representative myocytes are shown. Scale bar = 10 μm.

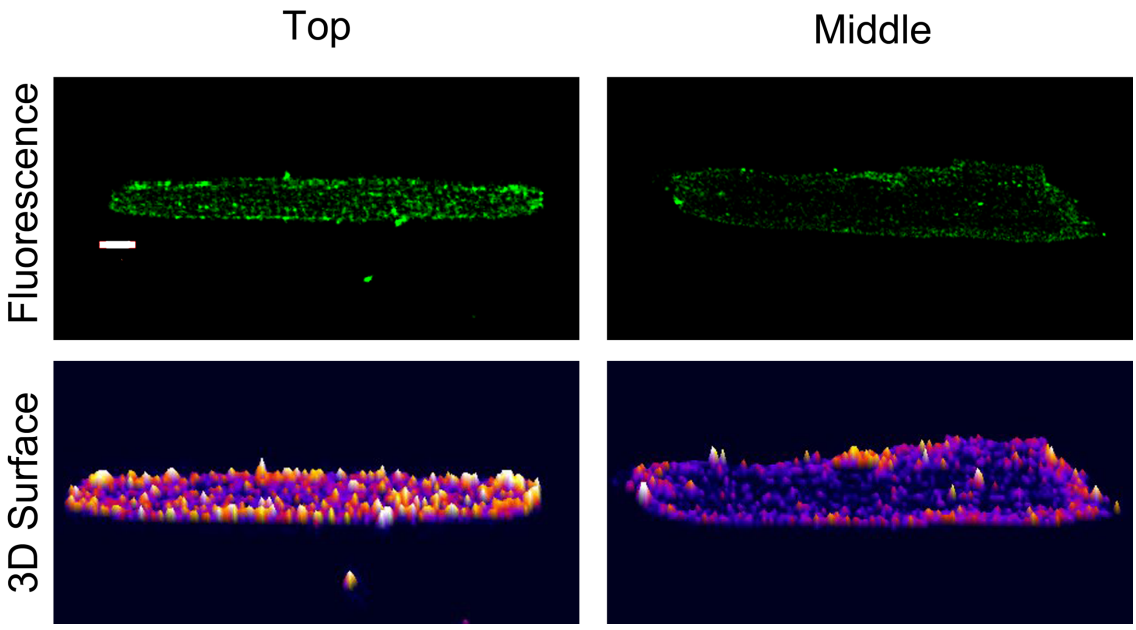

Figure 2.3. NCX1 localizes to the sarcolemma and not the center of adult cardiac myocytes.

A. *Endogenous NCX1 localizes to the sarcolemma in adult cardiac myocytes.* WT AMVM were isolated, cultured for 24 hours, fixed, permeabilized, and stained with the primary antibody against NCX1. Secondary antibody was conjugated to AlexaFluor488. Myocytes were imaged by confocal microscopy (60X oil immersion). A representative image from the surface and middle of the myocyte are shown. Scale bar = 20 pixels. **B**. *3D surface plot of fluorescent intensity of NCX1 signal.* 3D Surface images were created with FIJI to demonstrate NCX1 fluorescence intensity at the surface and at the middle of the cardiac myocyte.

2.5 Discussion

Here we validated a novel tool to study endogenous α1-AR localization and also are the first to report AT-R localization using a validated commercially available reagent in adult cardiac myocytes. These results are the first step in validating the overarching hypothesis of compartmentalization of Gq-receptor signaling in adult cardiac myocytes, with nuclear receptors (α1-ARs) being cardioprotective and sarcolemmal receptors (AT-Rs) being pathologic.

The concept of GPCR compartmentalization in cardiac myocytes is not without precedence. In co-cultures of sympathetic ganglionic neurons and neonatal rat cardiac myocytes, β1-ARs localize to regions of axonal contact rich in SAP97, AKAP97, catenins, and cadherins, whereas β2-ARs are excluded from these domains (164). In adult cardiac myocytes, β1-ARs are distributed over the entire sarcolemma, whereas β2-ARs are restricted deep within T-tubules (165). Finally, subpopulations of β1-ARs, β3-ARs, AT1-Rs, and AT2-Rs have been localized to the nuclear membranes in adult cardiac myocytes (166). These examples demonstrate that cardiac myocytes express GPCRs in different subcellular compartments, and our findings further support this model of GPCR expression in adult cardiac myocytes.

2.6 Acknowledgements

This work was funded by start-up funds from the University of Minnesota (TDO).

CHAPTER 3. Differential Activation of PLCβ1 by Gαq-Receptors in Adult Cardiac Myocytes

Erika F. Dahl[1], Steven C. Wu, PhD[2], Chastity L. Healy[2], Brian A. Harsch, MSc[3], Gregory C. Shearer, PhD[3], Timothy D. O'Connell, PhD[2]

[1] Department of Pharmacology, University of Minnesota, Minneapolis, MN 55455
[2] Department of Integrative Biology and Physiology, University of Minnesota, Minneapolis, MN 55455
[3] Department of Nutritional Sciences, Pennsylvania State Universty, University Park, PA 16802

3.1 Summary

Upon ligand binding, Gαq-receptors (Gq-receptors) activate phospholipase Cβ1 (PLCβ1), which cleaves phosphatidylinositol-4,5-bisphosphate (PIP_2) to produce inositol-1,4,5-trisphosphate (IP_3) and diacylglycerol (DAG). Conventional Gq-receptor signaling suggests that all Gq-receptors localize to and initiate this PLCβ1 signaling cascade at the sarcolemma in adult cardiac myocytes. Further, previous work has indicated that both PLCβ1 and PIP_2 localize solely to the sarcolemma. Yet, based on the finding that α1-ARs and AT-Rs localize to different subcellular compartments, we hypothesize that α1-ARs and AT-Rs activate proximal signaling in differential subcellular compartments as well. Our results indicate that PLCβ1 and PIP_2 localize to both the sarcolemma and nuclear membrane. We also show that α1-ARs and AT-Rs activate PLCβ1 in different subcellular compartments, with α1-ARs activating PLCβ1 at the nuclear membrane and AT-Rs activating PLCβ1 at the sarcolemma. Taken together, these results demonstrate that Gq-receptor mediated activation of signaling is able to occur at both the nuclear membrane and sarcolemma in adult cardiac myocytes.

3.2 Introduction

G-protein coupled receptors that signal through Gαq (Gq-receptors) share a common proximal signaling pathway through the activation of phospholipase Cβ1 (PLCβ1), which cleaves phosphatidylinositol-4,5-bisphosphate (PIP_2) to produce inositol-1,4,5-trisphosphate (IP_3) and diacylglycerol (DAG). In adult cardiac myocytes, PLCβ1 and its substrate PIP_2 have been localized solely to the sarcolemma where evidence suggests that PLCβ1 promotes cardiac contractile dysfunction further implicating Gq-

receptors in promotion of cardiac pathology (27). Yet, our previous results indicate that not all Gq-receptors localize to the sarcolemma with α1-ARs primarily localizing to the nuclear membrane in adult cardiac myocytes (14). How then do α1-ARs initiate signaling if both the enzyme and substrate downstream of Gq-receptor activation reside solely in the sarcolemma? Evidence in other cell types suggests that PIP_2 localizes to the nuclear membrane, but no such studies have been carried out in adult cardiac myocytes (167). Thus, we sought to identify the localization of PLCβ1 and PIP_2 in adult cardiac myocytes and to test the hypothesis that that α1-ARs and AT-Rs activate proximal signaling in differential subcellular compartments as well. If our experimental evidence supports this hypothesis, that would indicate that Gq-receptors can activate distinct subcellular pools of PLCβ1 further implying that adult cardiac myocytes are capable of compartmentalizing Gq-receptor mediated signaling events.

3.3 Methods

Mouse Lines

In this study, male and female C57BL/6J mice (10-15 weeks of age) were used as the source of primary adult cardiac myocytes. Male and female C57BL/6J mice were included due to no historical evidence indicating differences in receptor (α1-AR and AT-R) density. All animals were treatment naïve and housed under 12-hour light/dark cycle and fed standard chow. The use of all animals in this study conformed to the PHS Guide for Care and Use of Laboratory Animals and was approved by the University of Minnesota Institutional Animal Care and Use Committee. The University of Minnesota provides AAALAC-accredited services and resources for using animals in research, including animal ordering, care, facilities, housing, and training for researchers and lab personnel.

Cell Lines

Cell lines used in this study include, N38 embryonic mouse hypothalamus cells to validate the PLCβ1 antibody, and HEK293 cells used for adenoviral amplification. Both cell lines were cultured in Dulbecco's Modified Eagle's Medium (DMEM) supplemented with 10% fetal bovine serum and 1% penicillin/streptomycin. Cells were incubated at 5% CO_2 and 37°C. No information on sex or cell authentication information is available for either cell line.

Isolation and Culture of AMVM

As we have described previously (161), adult mouse ventricular myocytes were isolated from wild-type male and female C57BL/6J mice between 10 and 15 weeks of age. Briefly, mice were anesthetized with isoflurane (3% for induction, 1.5% for maintenance), injected with heparin (100 IU/mL), the pleural cavity was opened and the heart removed, cannulated on a retrograde perfusion apparatus, and perfused with collagenase type II to dissociate ventricular myocytes. Isolated cardiac myocytes were plated at a density of 50 rod-shaped myocytes per square millimeter on laminin-coated culture dishes. Myocytes were cultured in MEM with Hank's Balanced Salt Solution, 1 mg/ml bovine serum albumin, 10 mM 2,3-butanedione monoxime, and 100 U/ml Penicillin in a 2% CO_2 incubator at 37°C. All reagents were purchased from Sigma Aldrich unless otherwise specified. Full details of the buffers, enzymes, cell culture medium, all procedures for isolation and culturing of AMVM and a detailed diagram of the perfusion apparatus were described in detail previously (161). Following plating, myocytes were counted at a magnification of 20X to determine cell viability. Adenovirus was added based on previously determined multiplicity of infections. Infected myocytes were incubated in a 2% CO_2 incubator at 37°C for 40 hours. If myocytes were left uninfected (PLCβ1 immunocytochemistry experiments), myocytes were incubated in a 2% CO_2 incubator at 37°C for 24 hours before beginning experiments.

Isolation of Nuclei from AMVM

Immediately following isolation, myocytes were allowed to settle by gravity before aspiration of supernatant. Myocytes were washed in Buffer A (10 mM K-HEPES, 1.5 mM $MgCl_2$, 10 mM KCl, 0.2 mM activated Na_3VO_4, 1 mM DTT, 50 U/mL DNase, 10 μL/mL protease inhibitor cocktail) and centrifuged at 25 x *g* for 2 minutes. Supernatant was aspirated and the myocytes were resuspended in Buffer A. Myocytes were incubated on ice for 15 minutes to allow for swelling, and subsequently homogenized for 20 strokes using a dounce homogenizer. The homogenate was centrifuged for 2 minutes at 25 x *g*. The supernatant was collected and the pellet was resuspended in Buffer A. The homogenization and centrifugation steps were repeated, and the pellet was

resuspended in Buffer A. The resuspended pellet was then sonicated and the homogenate was centrifuged at 2,000 x *g* for 15 minutes to collect nuclei. 1.95M sucrose was added to the pellet and layered on top of 1.95M sucrose in an Ultra-Clear Beckman Coulter 14 x 89 mm centrifuge tube. The supernatant containing the myocyte sarcolemmal fraction and cytosolic fractions was added to a separate Ultra-Clear Beckman Coulter 14 x 89 mm centrifuge tube. The nuclei (tube 1) and myocyte sarcolemmal/cytosolic fractions (tube 2) were centrifuged at 100,000 x *g* for 90 minutes at 4°C. The nuclear pellet from tube 1 was resuspended in Buffer C (20 mM Na-HEPES, 1.5 mM $MgCl_2$, 0.2 mM EDTA, 0.2 mM EGTA, 25% Glycerol, 0.5 mM DTT, 0.5 mM PMSF, 10 μL/mL protease inhibitor cocktail). The supernatant from tube 2 was collected as the cytosolic fraction and the pellet from the tube 2 was resuspended in Buffer C for the myocyte sarcolemmal membrane fraction.

Localization of Phospholipase Cβ1 in AMVM

The PLCβ1 antibody was validated by measuring PLCβ1 mRNA levels and PLCβ1 protein levels by immunocytochemistry following siRNA-mediated knockdown of PLCβ1 in N38 mouse embryonic hypothalamus cells (generous gift from the lab of Dr. Alessandro Bartolomucci). N38 cells were plated on glass coverslips at a density of 0.5 x 10^6 in 35 mm dishes. 24 hours after plating, cells were transfected with 80 pmol of either PLCβ1 Gene Solution siRNA or Silencer Negative Control siRNA using Lipofectamine RNAiMAX reagent, following manufacturer's instructions. Cells were incubated at 37°C for 72 hours. A portion of cells from each treatment (PLCβ1 siRNA and negative control siRNA) were harvested for quantitative reverse transcriptase PCR analysis using the RNeasy Fibrous Tissue Mini Kit, following manufacturer's instructions. cDNA was synthesized from 2 μg of total RNA using SuperScript III First-Strand Synthesis System for RT-PCR. PCR primer sequences are as follows: PLCβ1 forward GCC CCT GGA GAT TCT GGA GT and PLCβ1 reverse GGG AGA CTT GAG GTT CAC CTT T. The second portion of cells were fixed and stained with anti PLCβ1-C terminal (1:100 dilution) followed by the appropriate AlexaFluor488 secondary antibody (1:500 dilution). Cells were imaged by confocal microscopy. Adult cardiac myocytes were fixed and stained using the exact dilution of primary antibody as N38 cells. AF488 (1:500 dilution) was used as the secondary antibody.

Identification of Nuclear PIP_2

PIP_2 extraction was carried out as described by (168) with some modifications. Briefly, 20 μL of the nuclear fraction was pipetted into 1.7 mL Eppendorf tubes with 225 μL of cold methanol added to the samples. After briefly vortexing the samples, 750 μL of cold methyl-tert-butyl ether was added to the samples followed by brief vortex and shaking for 6 minutes at 4°C. 250 μL of HPLC grade water was then added to the samples and briefly vortexed and the phases were separated by centrifugation at 14,000 rpm for 2 minutes. 350 μL of the upper organic phase was collected and placed in 1.5 mL Eppendorf tubes and dried in a speed vac. The samples were resuspended with 100 μL of methanol/toluene (9:1 v/v), vortexed briefly, and centrifuged at 14,000 rpm for 2 minutes to remove any debris. 50 μL of the samples was transferred to 250 μL autosampler vials. The samples' electrospray mass spectra were analyzed on a hybrid quadrupole triple ion trap mass spectrometer (Triple TOF 5600, AB Sciex Instrument). All scans were performed in negative ionization mode and a mass-to-charge (m/z) range from 50 to 1200 at an infusion rate of 5 μl/min. PIP2[4',5'](18:1(9Z)/18:1(9Z)) was obtained from Avanti Polar Lipids.

Adenoviral Production

GFP-PHD and NLS-GFP PHD: The GFP-C1-PLCdelta-PH (GFP-PHD) plasmid was obtained from Addgene. To construct NLS-GFP-PHD, the nuclear localization sequence (NLS) from the classical monopartite NLS of the SV40 large T-antigen (169) was added to the C-terminus of GFP-PHD using mini-gene technology. The sequence of the monopartite NLS is: GCA TGT GTC CAA AGA AAA AGC GCA AGG TAA. Integrated DNA Technologies synthesized the mini gene that included monopartite NLS flanked by an Age I and Xho I restriction sites. pShuttle CMV GFP-PHD was digested with Age I and Xho I and the resulting fragment was replaced with the AgeI-monopartite NLS-Xho I mini-gene using ligation.

Viral amplification and purification: All viruses were produced using the AdEasy Adenoviral Vector System (Agilent). Briefly, chosen fusion proteins were cloned into the pShuttle-CMV vector. Positive clones were recombined into bacterial cell line BJ5183 using electroporation. DNA was isolated from positive clones and transfected into HEK293 cells using Effectene transfection reagent. Virus was amplified for three rounds of replication. Viruses were purified using OptiPrep gradients and ultracentrifugation

(35,000 x *g* for 18 hours). Viruses were titered using Adeno-X Rapid Titer Kit per manufacturer's instructions. All constructs were sequence verified in the University of Minnesota sequencing core. For experiments, cultured AMVM were counted at 20X and infected with adenoviruses at the following multiplicity of infection: GFP-PHD 100 (titer: 2.4×10^8) and NLS-GFP-PHD 500 (titer: 1.4×10^{10}).

Analysis of Phospholipase Cβ1 Activity

To measure PLCβ1 activity in adult cardiac myocytes, cultured AMVM plated on coverslips were infected with either 100 MOI GFP-PHD or 500 MOI NLS-GFP-PHD for 40 hours at 37°C. Myocytes were treated with either vehicle, PE (20 μM) in the absence and presence of prazosin (1 mM), or AngII (100 nM) in the absence or presence of losartan (5 μM) for 5 minutes at 37°C. Pretreatment with antagonists (prazosin or losartan) was carried out for 30 minutes at 37°C before agonist (PE or AngII) treatment. Myocytes were fixed and mounted exactly as described for α1-QDot 565. Confocal images were captured on an Olympus FluoView FV1000 IX2 Inverted Confocal Microscope at 60X magnification (oil immersion). 3D surface plots were created in FIJI using the 3D surface plot plugin.

Statistical Analysis

All data plotting and statistical analysis was performed using Prism 6 software. All information on statistical parameters can be found in figure legends. PLCβ1 immunofluorescent intensity was quantified on whole images using FIJI. Data were analyzed by student's t-test and $P<0.05$ was considered significant. PLCβ1 mRNA levels were quantified by densitometry using ImageLab (Bio-Rad). Data were analyzed by student's t-test and $P<0.05$ was considered significant. To quantify activation of PLCβ1, AMVM expressing GFP-PHD or NLS-GFP-PHD were exposed to agonist or vehicle, and classified as responders (movement of probe off the membrane) and non-responders (no apparent movement of probe) by another investigator blinded to treatment group. Data were analyzed by Chi-Square and $P<0.05$ was considered significant.

3.4 Results

Phospholipase Cβ1 (PLCβ1) and its substrate phosphatidylinositol-4,5-bisphosphate (PIP_2) localize to the nuclei in adult cardiac myocytes.

Proximal Gq-receptor signaling involves activation of PLCβ1 and cleavage of PIP_2 into IP_3 and DAG. While it is generally accepted that Gq-receptors activate PLCβ1 to hydrolyze PIP_2 at the sarcolemma (157), it is not clear if this occurs at the nucleus in AMVM. Although Gq-receptors localize to the nucleus in AMVM, including α1-ARs (**Figure 2.1**, (28, 81, 154)), as well as small populations of AT-Rs (69) and ET-Rs (71), it is not certain that either PLCβ1 or PIP_2 localize to the nucleus (32). In other cells, PIP_2 hydrolysis is observed in the nuclear matrix, but is reported to be independent of Gq-receptor signaling (170). However, nuclear α1-ARs activate intranuclear PKCδ in nuclei isolated from AMVM (154), suggesting production of DAG from a yet to be defined nuclear phosphatidylinositol species. Further, both AT-Rs and ET-Rs induce intranuclear signaling dependent on the production of inositol phosphates in AMVM (69, 171).

Based on prior demonstrations of Gq-receptor localization and signaling at the nucleus, we sought to clarify whether PLCβ1 is localized to the nucleus in adult cardiac myocytes. First, we sought to validate potential PLCβ1 antibodies. Preferably, we would employ AMVM from PLCβ1 knockout-mice, but these mice exhibit spontaneous seizures and high mortality around 3 weeks of age (172). Alternatively, we attempted to use siRNA technology to knock down PLCβ1 in AMVM, but were unable to achieve significant PLCβ1 mRNA knockdown by 40 hours, likely due to low turnover of PLCβ1 in cultured AMVM. Subsequently, we attempted to validate potential PLCβ1 antibodies using siRNA technology in the N38 embryonic mouse hypothalamic cell line due to PLCβ1 enrichment in the brain (REFS). To assess PLCβ1 knockdown, N38 cells were transfected with either PLCβ1 siRNA or scramble siRNA for 72 hours. We observed knockdown of PLCβ1 mRNA (**Figure 3.1C**, quantified in **Figure 3.1D**) and knockdown of PLCβ protein was visualized by decrease in staining of the PLCβ1 antibody (**Figure 3.1A** quantified in **Figure 3.1B**). Finally, we stained wild type AMVM with the PLCβ1 antibody and our results indicate that PLCβ1 localizes to the sarcolemma, t-tubules and nuclear envelope (**Figure 3.2A**, nuclei indicated with white arrows).

PIP_2, the substrate for PLCβ1, localizes to the sarcolemma in AMVM (32, 173, 174). Yet, identifying a population of nuclear PIP_2 has been elusive because either 1) PIP_2 is not present at the nucleus or 2) the methods used to detect PIP_2 have been insufficient. To address this conundrum, we isolated AMVM nuclei using differential centrifugation, and analyzed samples by mass spectrometry to determine if PIP_2 is present in nuclear membranes in AMVM. To detect the presence of PIP_2 species, we ran two blanks and two AMVM nuclear samples spiking one of each with commercially available 36:2 PIP_2, PIP_2[4',5'](18:1(9Z)/18:1(9Z)). Using ESI-MS scan with precursor ion *m/z* 281 (carboxylated anion of oleic acid – C18:1), we were able identify PIP_2 36:2 species in all the samples except the non-spiked blank (**Figure 3.2B**, left panel). Spectra of the peak showing a parent ion *m/z* 1021 (**Figure 3.2B**, right panel) confirming the identity of the commercially available 36:2 PI(4,5)P2 in the PIP_2 spiked blank sample with ion fragments at *m/z* 259, 281, 339, and 419 corresponding to the inositol phosphate (IP), the oleic acid backbone, inositol diphosphate (IP_2), and inositol triphosphate (IP_3) components of the fragmented 36:2 PIP_2.

Similar to previous PIP_2 analyses (175), we used negative ion MS/MS to analyze the product ions of *m/z* 1045 (38:4 PIP_2), the most abundant PIP_2 species in the nuclear fraction sample without the PIP_2 spike (**Figure 3.2C**). Ions at *m/z* 259, 283, 303, 339, and 419 correspond to IP, carboxylate anion fatty acyl chains of stearic acid, the arachidonic acid backbone, IP_2, and IP_3, all portions of the fragmented 38:4 PIP_2 spectrum. Our results indicate that PIP_2 localizes to membranes within the nuclei of AMVM, which to our knowledge is the first such demonstration. In total, our findings reveal that PLCβ1 and its substrate, PIP_2, are found in the same subcellular compartments as both the α1-AR (nuclear) and AT-R (sarcolemma), suggesting the potential for compartmentalized Gq-receptor signaling in adult cardiac myocytes.

AT-Rs, but not α1-ARs, activate PLCβ1 at the sarcolemma in adult cardiac myocytes.

Based on the observed distinct subcellular compartmentalization of α1-ARs and AT-Rs (**Figure 2.1**), we reasoned that AT-Rs would activate proximal signaling at the sarcolemma and α1-ARs at the nuclei. To test this, we measured the compartmentalization of Gq-receptor activation of PLCβ1 with the PLCβ1 activity sensor GFP-C1-PLCδ-PH (GFP-PHD, **Figure 3.3A**). GFP-PHD is comprised of GFP fused to

the N-terminus of the pleckstrin homology domain of PLCδ1, which preferentially binds PIP_2 over other membrane phosphatidylinositols *in vitro* (31). In general, GFP-PHD associates with PIP_2 in membranes in the basal state, and upon Gq-receptor stimulation, PLCβ1 hydrolyzes PIP_2, and as PIP_2 is depleted, GFP-PHD dissociates from the membrane. In AMVM expressing GFP-PHD, the probe localized to the sarcolemma and t-tubules in the basal state, in agreement with previous reports (32). More importantly, the α1-agonist phenylephrine (PE), in the absence or presence of prazosin produced no change in the localization of GFP-PHD compared to vehicle (**Figure 3.3B**, quantified in **3.3C**). Conversely, AngII induced a marked dissociation of GFP-PHD from the membrane compared to vehicle, which was blocked by the non-selective AT-R antagonist losartan indicating a receptor-specific effect (**Figure 3.3D**, quantified in **3.3E**). These results demonstrate that AT-Rs, but not α1-ARs, activate PLCβ1 at the sarcolemma in adult cardiac myocytes consistent with the subcellular compartmentalization of each receptor.

α1-ARs, but not AT-Rs, activate PLCβ1 at the nuclear envelope in adult cardiac myocytes.

Interestingly, GFP-PHD was not detected at the nuclear membrane in the basal state (**Figure 3.3**). We suggest there are two explanations for this observation: 1) PIP_2 is not present in the nuclear membrane, despite our identification of PIP_2 in nuclear membranes (**Figure 3.2**) or 2) GFP-PHD, which lacks a NLS, is unable to target the nucleus to bind nuclear PIP_2. To clarify this and additionally determine if Gq-receptor mediated activation of PLCβ1 possibly occurs at the nucleus, we inserted a NLS sequence at the N-terminus of GFP-PHD to create NLS-GFP-PHD (**Figure 3.4A**). Insertion of a NLS promoted nuclear localization of GFP-PHD (**Figure 3.4B** and **3.4C**) suggesting PIP_2 is found in the nucleus, in agreement with detection of nuclear PIP_2 by mass spectrometry (**Figure 3.2**). Additionally, using the same experimental conditions as our experiments with GPF-PHD, the α1-agonist PE induced a marked dissociation of NLS-GFP-PHD from the nuclear membrane, which was blocked by prazosin (**Figure 3.4B**, quantified in **3.4C**). Conversely, AngII, in the absence or presence of losartan, produced little change in the localization of NLS-GFP-PHD (**Figure 3.4 D**, quantified in **3.4E**). These results demonstrate that α1-ARs, but not AT-Rs, primarily activate PLCβ1 at the nuclear membrane in AMVM. The combined results from experiments using GFP-

PHD and NLS-GFP-PHD indicate that α1-AR- and AT-R-mediated proximal signaling is confined to distinct subcellular compartments consistent with receptor localization.

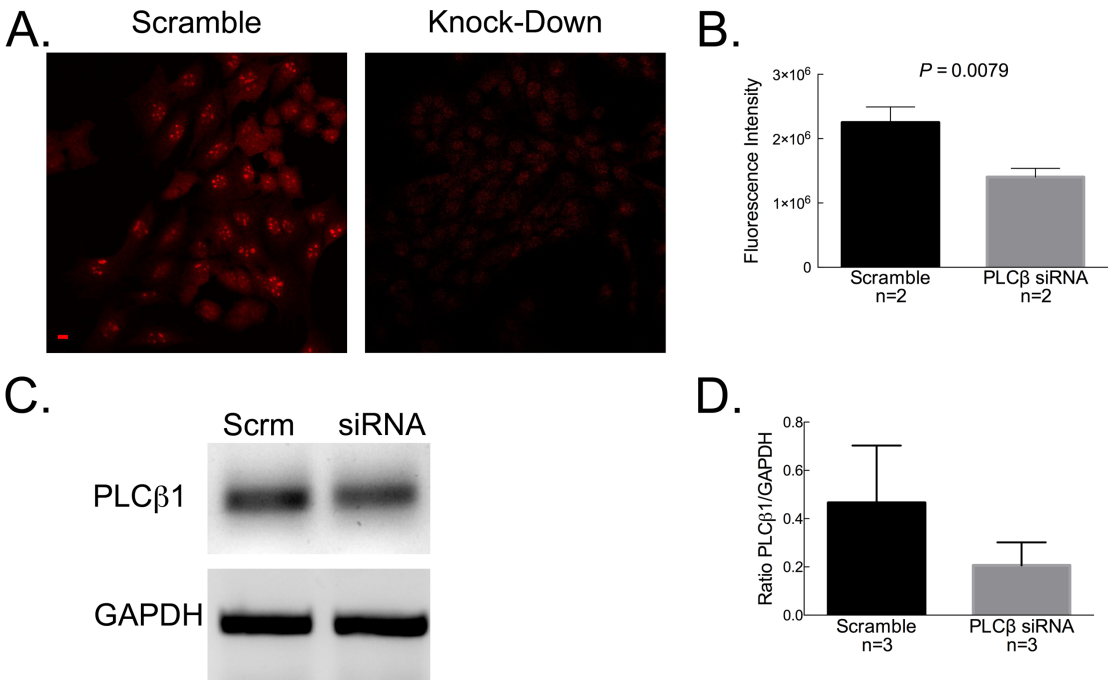

Figure 3.1. Validation of PLCβ1 antibody in N38 cells.

A. *Visualization of siRNA-mediated PLCβ1 protein knockdown.* N38 cells (embryonic mouse hypothalamic cells) were transfected with either 80 pmol PLCβ1 siRNA or scrambled siRNA using Lipofectamine RNAiMAX for 72 hours at 37°C. Cells were fixed and stained with a primary antibody against PLCβ1. Secondary antibody was conjugated to AlexaFluor594. Cells were imaged using confocal microscopy (20X). Scale bar = 10 μm. **B.** *Quantification of siRNA-mediated PLCβ1 protein knockdown.* Fluorescence intensity was measured using FIJI (n=2). Data are represented as mean ± SEM. Data were analyzed by paired student's t-test, and $P<0.05$ was considered significant. **C.** *siRNA-mediated PLCβ1 mRNA knockdown.* N38 cells were transfected as in **A**. After 72 hours, RNA was harvested using RNAEasy kit, and PLCβ1 mRNA levels were measured by RT-PCR. Results of densitometry analysis of PLCβ1 mRNA levels are shown in **D**. **D**. *Quantification of siRNA-mediated PLCβ1 mRNA knockdown*. Ratio of GAPDH to PLCβ1 was quantified using densitometry (n=3). Data are represented as mean ± SEM.

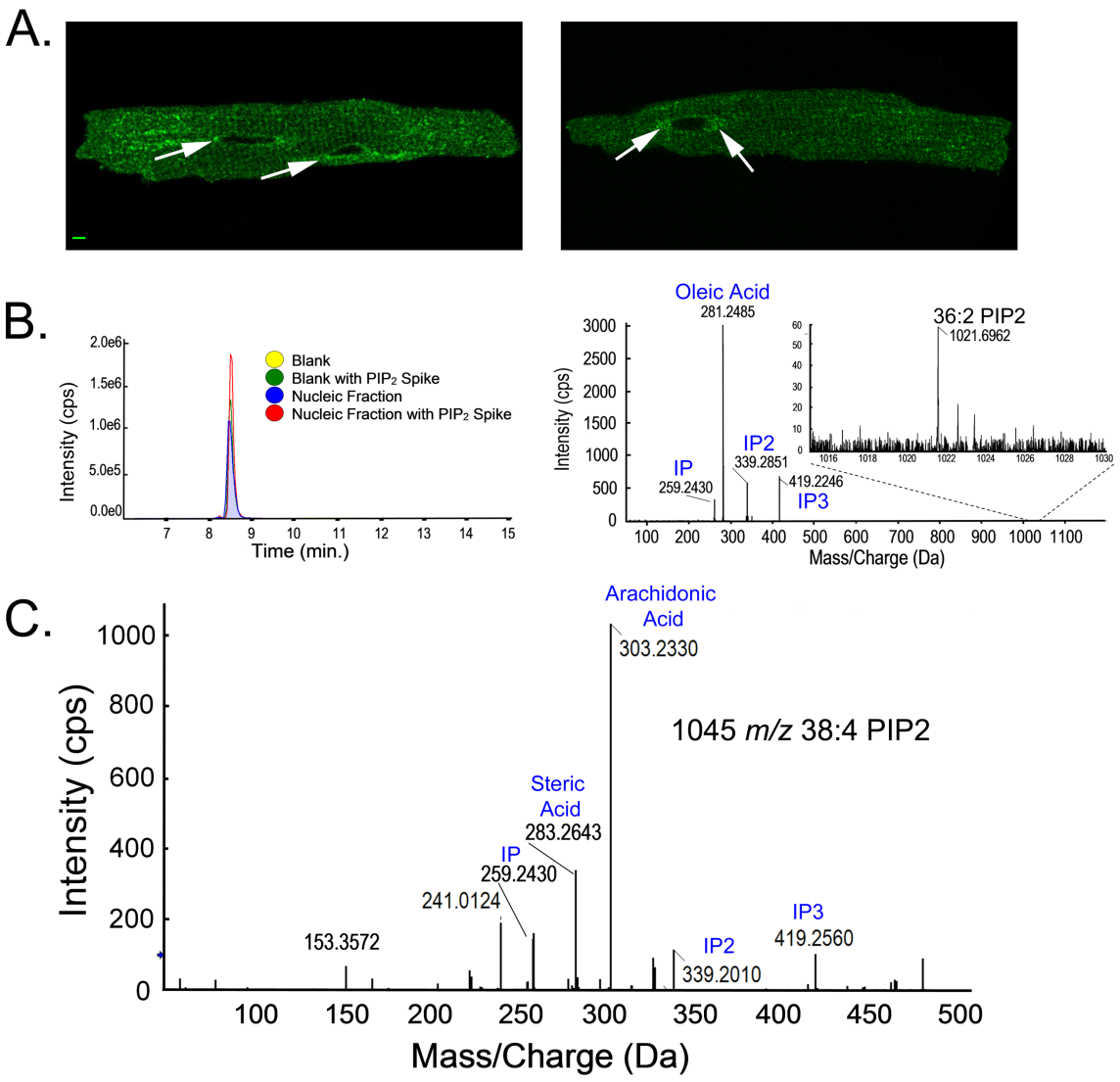

Figure 3.2. PLCβ1 and PIP_2 localize to the nuclear membrane in adult cardiac myocytes

A. *Endogenous PLCβ1 localizes to the sarcolemma and nuclear membrane in AMVM.* WT AMVM were isolated, cultured for 24 hours, fixed, permeabilized, and stained with the primary antibody against PLCβ1. Secondary antibody was conjugated to AlexaFluor488. Myocytes were imaged by confocal microscopy (60X oil immersion). Arrows indicate nuclear membrane. Two representative images are shown. Scale bar = 10 µm. **B.** *Detection and identification of PIP_2[4',5'](18:1(9Z)/18:1(9Z)) in AMVM nuclear fractions.* Blank and nuclear extracts were analyzed with and without PIP_2[4',5'](18:1(9Z)/18:1(9Z)). The yellow peak (not detected) represents blank sample

with no PIP_2 spike, the green peak represents the blank sample with PIP_2 spike, the blue peak represents the nuclear fraction with no PIP_2 spike and the red peak represents the nuclear fraction with PIP_2 spike (left panel). ESI-MS scans of the PIP_2 spiked blank sample with precursor ion m/z 281 showing m/z 1021 identifying the compound as 36:2 PIP2 (right panel). **C.** *Identification of PIP_2 species in AMVM nuclear fractions.* Product ions of m/z 1045 (38:4 PIP2) of the non-spiked nuclear fraction sample.

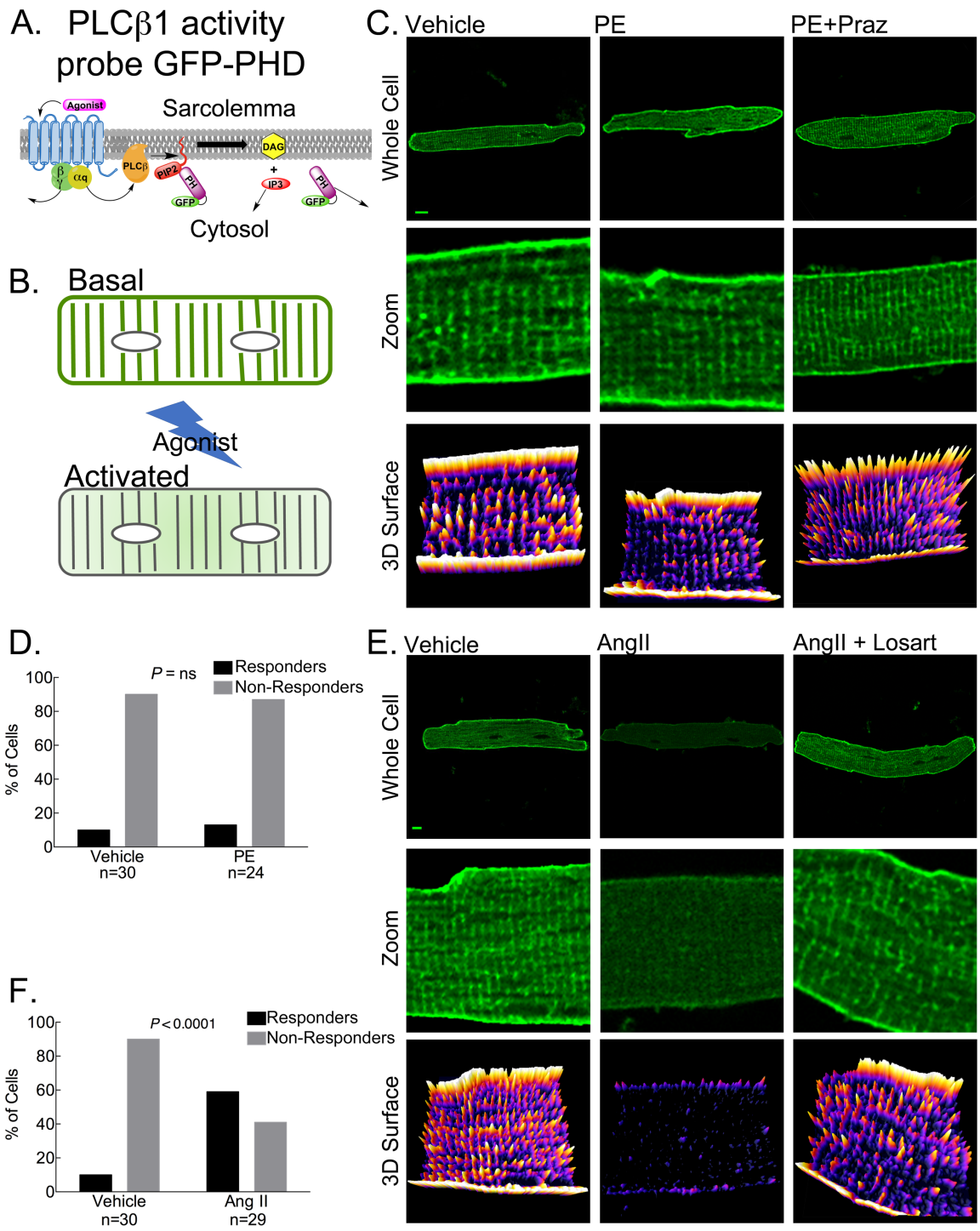

Figure 3.3. AT-Rs, but not α1-ARS, activate PLCβ1 at the sarcolemma in adult cardiac myocytes

A. *Schematic representation of GFP-PHD*. GFP-PHD consists of the pleckstrin homology domain of phospholipase Cδ attached to the carboxyl terminus of GFP. The PH domain of PLCδ has high affinity for PIP_2, and in the basal state, GFP-PHD binds to

membrane PIP_2, and cleavage of PIP_2 by PLCβ1 releases the probe from the membrane, decreasing membrane GFP fluorescence (33). **B.** *GFP-PHD function*. In the basal state (Basal), GFP-PHD localizes to the sarcolemma bound to PIP_2, and upon activation of PLCβ1 (Activated), PIP_2 is cleaved and the probe moves into the cytoplasm. **C and E.** *α1-ARs (**C**) do not activate PLCβ1 at the sarcolemma, but AT-Rs do (**E**).* WT AMVM expressing GFP-PHD were treated with vehicle (left panels) or PE (20 μM, 5 min, 37°C) in the absence and presence of prazosin (1 mM, 30 min pretreatment, 37°C, middle panels and right panels respectively)), or AngII (100 nM, 5 min, 37°C) in the absence and presence of losartan (5 μM, 30 min pretreatment, 37°C, middle and right panels respectively). 3D Surface images were created with FIJI to demonstrate GFP-PHD fluorescence intensity. Scale bar = 10 µm. **D and F.** *Quantification of sarcolemmal PLCβ1 activity downstream of α1-ARs (**D**) and AT-Rs (**F**).* Myocytes were classified by another investigator blinded to treatment group as responders defined by GFP-PHD movement off the sarcolemma or non-responders defined by no movement of GFP-PHD either at baseline or following agonist treatment. Data were analyzed by Chi Square and $P<0.05$ was considered significant. Data are represented as mean ± SEM. Vehicle (n=30 myocytes from 7 hearts); PE (n=24 myocytes from 4 hearts); AngII (n=29 myocytes from 4 hearts).

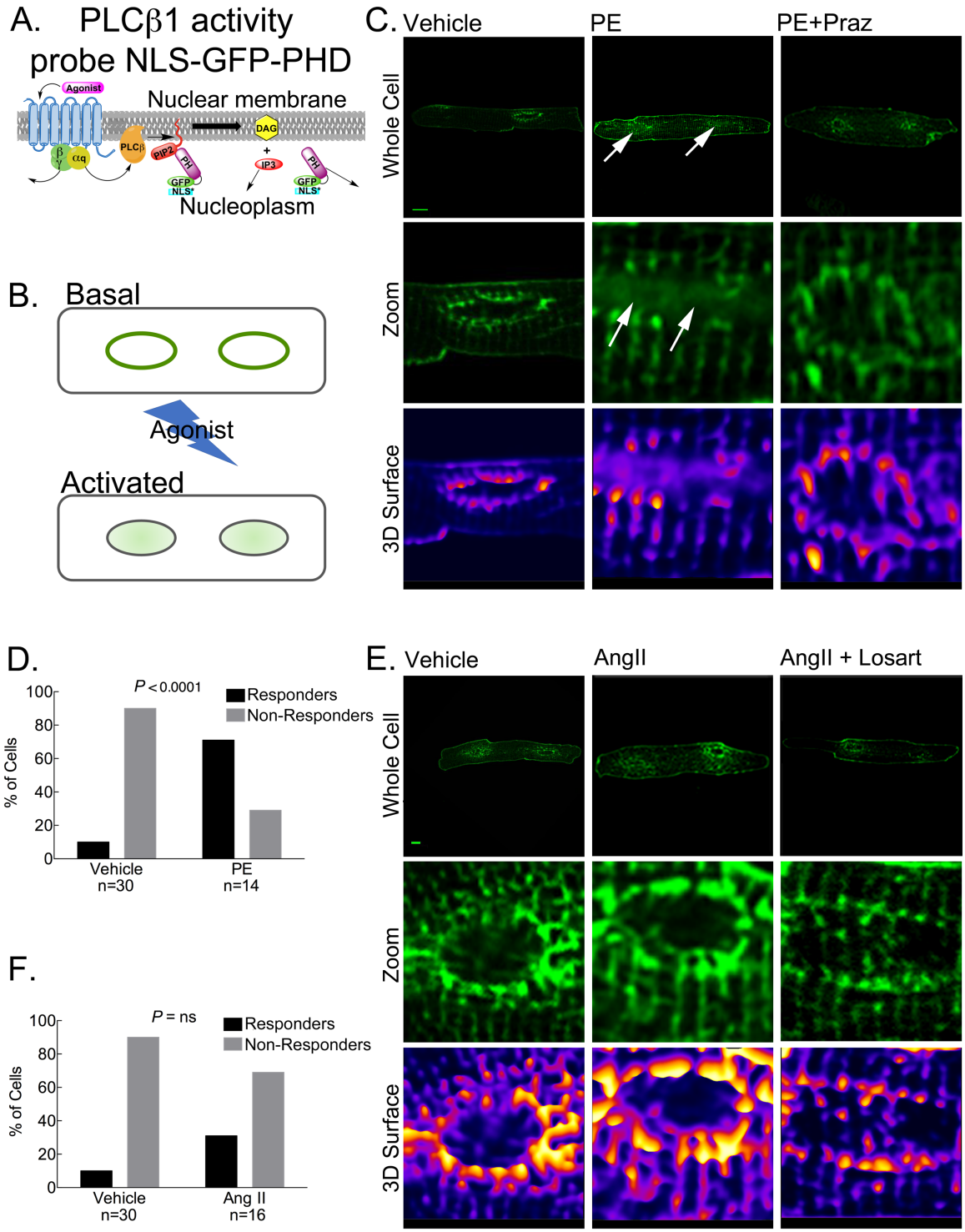

Figure 3.4. α1-ARs and, to a lesser extent, AT-Rs activate PLCβ1 at the nuclear membrane in adult cardiac myocytes.

A. *Schematic representation of NLS-GFP-PHD.* NLS-GFP-PHD consists of GFP-PHD tagged with an amino-terminal nuclear localization sequence (NLS) from the SV40 large T-antigen to promote localization of the probe to the nucleus. NLS-GFP-PHD is thought to operate the same as GFP-PHD (**Figure 3.3**), but at the nuclear membrane(33). **B.** *GFP-PHD function*. In the basal state (Basal), GFP-PHD-NLS localizes primarily to the nuclear membrane bound to PIP_2, and upon activation of PLCβ1 (Activated), PIP_2 is cleaved and the probe moves into the nucleoplasm. **C and E.** *α1-ARs (**C**) activate PLCβ1 at the nuclear membrane, but AT-Rs do not (**E**).* WT AMVM expressing NLS-GFP-PHD were treated with either vehicle (left panels) or PE (20 μM, 5 min, 37°C) in the absence or presence of prazosin (1 mM, 30 min pretreatment, 37°C, middle and right panels respectively) or AngII (100 nM, 5 min, 37°C) in the absence and presence of losartan (5 μM, 30 min pretreatment, 37°C, middle and right panels respectively).). Arrows indicate nuclear membrane activation of PLCβ1 by α1-ARs. 3D Surface images were created with FIJI to demonstrate NLS-GFP-PHD fluorescence intensity. Scale bar = 10 μm. **D and F.** *Quantification of nuclear PLCβ1 activity downstream of α1-ARs (**D**) and AT-Rs (**F**).* Myocytes were classified by another investigator blinded to treatment group as responders defined by NLS-GFP-PHD movement off the nuclear membrane or non-responders defined by no movement of NLS-GFP-PHD either at baseline or following agonist treatment. Data were analyzed by Chi Square and $P<0.05$ was considered significant. Data are represented as mean ± SEM. Vehicle (n=30 myocytes from 7 hearts); PE (n=14 myocytes from 4 hearts); AngII (n=16 myocytes from 4 hearts).

3.5 Discussion

Here, we identified a potential mechanistic explanation for unique Gq-receptor function in adult cardiac myocytes predicated upon subcellular compartmentalization of proximal Gq-receptor signaling. We found that both PLCβ1 and its substrate PIP_2 localize to the nuclear membrane in adult cardiac myocytes. Further, we found that nuclear α1-ARs induce intranuclear activation of PLCβ1, whereas sarcolemmal AT-Rs induce sarcolemmal activation of PLCβ1. This is the first such demonstration of differential PLCβ1 activation downstream of Gq-receptors in adult cardiac myocytes. Previous reports relied upon the GFP-PHD probe as a tool to localize PIP_2, but never has GFP-PHD or our newly constructed NLS-GFP-PHD probe been used to study the activity of PLCβ1.

The results of this study give further support to the idea that adult cardiac myocytes have both the presence of the signaling molecules (Gαq, PIP_2, PLCβ1) and the ability to activate signaling at both the nuclear membrane and the sarcolemma. Further, these results support the novel paradigm that not all Gq-signaling is detrimental in the setting of heart failure, and that nuclear (α1-AR) signaling is protective whereas sarcolemmal (AT-R) signaling is pathologic. Of note, reconstitution of a sarcolemmal PLCβ1 inhibitory peptide prevents the loss of contractile function in a murine model of heart failure (176). This finding indicates that sarcolemmal activation of PLCβ1 promotes contractile dysfunction which agrees with our model of AT-R sarcolemmal activation of PLCβ1 inducing contractile dysfunction in adult cardiac myocytes. In addition, activation of nuclear PLCβ1 downstream of α1-ARs promotes sustained cardiac function and a cardioprotective phenotype. These results advance the understanding of compartmentalized signaling in adult cardiac myocytes downstream of Gq-receptors.

3.6 Acknowledgements

The authors would like to acknowledge Dr. Alessandro Bartolomucci, University of Minnesota, for his generous gift of N38 cells and Christy Long for her effort in making the

GFP-PHD virus. This work was funded by start-up funds from the University of Minnesota (TDO) and start-up funds from Pennsylvania State University (GCS).

CHAPTER 4. Differential Activation of ERK by Gαq-Receptors in Adult Cardiac Myocytes

Erika F. Dahl[1], Steven C. Wu, PhD[2], Chastity L. Healy[2], Jocelyn Perry[2], Timothy D. O'Connell, PhD[2]

[1]Department of Pharmacology, University of Minnesota, MN 55455, U.S.
[2]Department of Integrative Biology and Physiology, University of Minnesota, MN 55455, U.S.

4.1 Summary

In cardiac myocytes, α1-adrenergic receptors (α1-ARs) promote myocyte survival, whereas angiotension receptors (AT-R) promote myocyte death. Because both receptors share common proximal Gαq-signaling pathways, we have previously suggested that compartmentalization of receptor signaling could contribute to the differential phenotype. Here, we used fluorescence lifetime imaging in adult cardiac myocytes expressing the ERK activity biosensor EKAR to compare individual myocyte-specific α1-AR and AT-R mediated activation of ERK. Our results indicate that α1-AR signaling induced ERK activity in a higher percentage of myocytes, but the degree of activation per myocyte was similar. Furthermore, we found that the localization of ERK activity was different, with both receptors activating cytosolic ERK, but only α1-ARs activating perinuclear ERK. Further, we found that α1-ARs, but not AT-Rs, promote mitochondrial membrane stability. The reduced extent (number of myocytes) and differential localization of AT-R mediated ERK activation relative to α1-ARs, and the reduction in mitochondrial stability and myocyte survival downstream of AT-Rs relative to α1-ARs suggests a possible association with cardiac myocyte survival.

4.2 Introduction

In cardiac myocytes, convention indicates that Gαq-signaling promotes cell death (155). While true for angiotensin receptors (AT-Rs) (177), we previously identified an α1A-adrenergic receptor (α1A-AR) ERK survival signaling pathway (56). Mechanistically, we have suggested that differential subcellular compartmentalization of Gq-coupled receptors could explain this difference (14). We previously demonstrated that α1-ARs localize to and induce intranuclear signaling in adult cardiac myocytes (14),

whereas AT-Rs primarily localize to and signal at the sarcolemma (69). Therefore, we hypothesized that both degree and intracellular location of ERK activation might explain the differences between α1-ARs and AT-Rs on myocyte survival. To test this hypothesis, we used an ERK activity biosensor to investigate α1-AR and AT-R mediated ERK activation with fluorescence lifetime imaging microscopy (FLIM) in adult cardiac myocytes. Briefly, our results indicate α1-ARs activate ERK more efficaciously with a different subcellular localization than AT-Rs. Further we employed a live-cell mitochondrial membrane potential assay using the dye JC-1 which accumulates in intact mitochondria. Our results demonstrated that α1-ARs, but not AT-Rs, improve mitochondrial membrane potential and cardiac myocyte cell survival. These results provide mechanistic insight into the differential effects on cell survival of these receptors.

4.3 Methods

Adult Mouse Ventricular Myocytes (AMVM)
AMVM were isolated and cultured as previously described from male and female 10-15 week old C57BL/6J mice (161).

Extracellular Signal-Regulated Kinase Activity Reporter (EKAR)
The cytoplasmic EKAR plasmid was a gift from Karel Svoboda (Addgene, #18679). EKAR consists of the Cerulean and Venus FRET pair, a substrate phosphorylation peptide, and a phospho-binding domain. ERK activation induces phosphorylation of EKAR leading to increased FRET (FRET-on) (178) (**Figure 4.1C**). A cytoplasmic EKAR adenovirus was made with the AdEasy System (Agilent).

Fluorescent Lifetime Imaging Microscopy (FLIM) and Analysis of EKAR activity
Cardiac myocytes were plated on laminin-coated glass coverslips in a 14mm microwell within 35mm petri dishes (MatTek), infected with EKAR adenovirus, and cultured for 40 hours at 37°C. Myocytes were treated with either 20 μM phenylephrine (PE) or 100 nM angiotensin II (AngII) (Sigma Aldrich), at 25°C for 5 minutes. All data was collected on an Olympus FluoView FV1000 IX2 Inverted Confocal Microscope with PicoQuant 405 pulsed laser (80 MHz) at 60X magnification (oil immersion). On average, 1 x 10^7 photons were collected per cell on SPCM software (Becker & Hickl). Data was analyzed using FLIMFit software (Imperial College London) using the time-domain fluorescence lifetime algorithm for production of intensity images (179). Data was calculated by setting the

instrumental response function (IRF) to time zero which was assumed to be the peak of the IRF by manipulating the time minimum under the IRF tab (179). Images were fit using the following settings: pixel-wise global fitting, global binning, 2-exponential decay components, global fitting, and variable projection.

Due to technical limitations caused by myocyte death from phototoxicity due to prolonged laser stimulation during live-cell FLIM and the tendency of contracting myocytes to move out of focus, myocyte pairs consisting of untreated (vehicle) and treated (PE or AngII) from the same dish were used rather than a single myocyte stimulated for 5 minutes. Raw intensities were determined, and were standardized to the number of photons collected. Then the level of ERK activation was calculated by the fold-change of treated vs. control for paired myocytes from each dish. “Responders” were defined as cell pairs which had an intensity ratio of vehicle to drug-treated greater than 1 and non-responders were defined as cell pairs which had an intensity ratio of vehicle to drug-treated less than or equal to 1. Values are expressed as mean ±SEM. Data were analyzed by a paired, two-tailed student’s t-test (treated vs control) and presented as fold-change using Prism 6.0 (Graphpad Software, Inc.) and $P<0.05$ was considered significant.

Western Blotting and Analysis

Cardiac myocytes were plated on 35mm laminin coated dishes, cultured for 24 hours, and treated for 5 minutes at 37°C with either PE (20 μM,) or AngII (100 nM), and harvested in 2x laemmli sample buffer. Densitometry was performed using Image Lab software (Bio-Rad). Data are presented as a ratio of the phosphorylated to total ERK signal. Values are expressed as mean ±SEM. Data were analyzed by one-way ANOVA, and $P<0.05$ was considered significant.

JC-1 Mitochondrial Membrane Potential Assay

Cardiac myocytes were plated on 35mm laminin coated dishes, cultured for 24 hours, and treated for 2 hours at 37°C with either Vehicle, Doxorubicin (2 μM), PE (20 μM,) or AngII (100 nM). After 2 hours, myocytes were loaded with 5 μM JC-1 (ThermoFisher) for 30 minutes at 37°C, and after 30 minutes the medium containing JC-1 was aspirated and replaced with fresh, dye-free medium. All data was collected on an Olympus FluoView FV1000 IX2 Inverted Confocal Microscope using a 10X objective (air) and the

AF594 filter set. 3 images per treatment dish were collected, and fluorescence intensity and rod-round count were determined using FIJI.

4.4 Results

Based on the differential effects of α1-ARs and AT-Rs on cardiac myocyte survival, we sought to determine if Gq-receptor activation of ERK correlated with cardiac myocyte survival. To address this, we treated AMVM with either the α1-AR agonist PE or the AT-R agonist AngII and measured ERK phosphorylation at Thr202/Tyr204 as a marker of ERK activation. As expected, PE produced a more robust activation of ERK than AngII (**Figure 4.1A** and **4.1B**).

Western blots provide a one-dimensional readout of ERK activation in a population of cells or tissue, but provide no insight into degree or localization of cell-specific kinase activity. To address this, we used FLIM in AMVM expressing the ERK activity biosensor EKAR to compare α1-AR and AT-R mediated activation of ERK. PE induced ERK activity in 14/21 myocytes (**Figure 4.1C, 4.1D,** and **Figure 4.3**). Previously, we have demonstrated that the α1A-subtype activates ERK in adult cardiac myocytes (56), and therefore, observing PE induced ERK activity in two-thirds of myocytes is consistent with prior findings that the α1A-subtype is expressed in only 60% of adult cardiac myocytes (180). Importantly, in responding myocytes, PE increased activity by 17% (**Figure 4.1E**) and ERK activity was localized to the cytosol and perinuclear space (**Figure 4.1F**). This pattern of α1-induced ERK activity is consistent with our prior demonstration that α1-ARs localize to and induce intranuclear signaling in adult cardiac myocytes (28, 81, 154). Conversely, AngII induced ERK activity in only 9/22 myocytes (**Figure 4.2A, 4.2B** and **Figure 4.3**), but in responding myocytes, AngII increased ERK activity by 14%, similar in degree to α1-ARs (**Figure 4.2C**), but only in the cytosol with no apparent perinuclear component.

In summary, we found that despite sharing common proximal signaling pathways, α1-ARs and AT-Rs differentially activate ERK in adult cardiac myocytes. Using FLIM, we found that α1-ARs activated ERK in a greater percentage of cardiac myocytes than AT-Rs (α1-AR: 14/21; AT-R: 7/22, $P<0.05$, ChiSquare). While the degree

of activation in each responding myocyte was similar (27% vs 20%), we also observed that the localization of ERK activity was different, with both receptors activating cytosolic ERK, but only α1-ARs activating perinuclear ERK.

The anti-apoptotic mechanism of ERK activation in adult cardiac myocytes is thought to be due to mitochondrial membrane stabilization (181). Thus, we sought to understand the effects of α1-ARs and AT-Rs on mitochondrial membrane potential. To address this, we employed JC-1, a dye that is sensitive to mitochondrial membrane potential. When the mitochondrial membrane potential is intact, JC-1 accumulates in the mitochondria as a multimer and fluoresces in the red spectra. When the mitochondrial membrane potential has been lost, JC-1 accumulates in the cytosol as a monomer and fluoresces in the green spectra. We treated myocytes with vehicle, doxorubicin which is a known pro-apoptotic stimuli (182), PE, or AngII and studied the mitochondrial membrane potential using JC-1. Our results indicate that only PE was able to prevent the loss of mitochondrial membrane potential and actually improve mitochondrial membrane potential in live adult cardiac myocytes (**Figure 4.4A** and **4.4B**). Also, in further support of our previous work, α1-ARs, but not AT-Rs, prevented cardiac myocyte cell death (**Figure 4.4C**). In summary, we found that α1-ARs, but not AT-Rs, prevent mitochondrial membrane destabilization and promote cardiac myocyte cell survival.

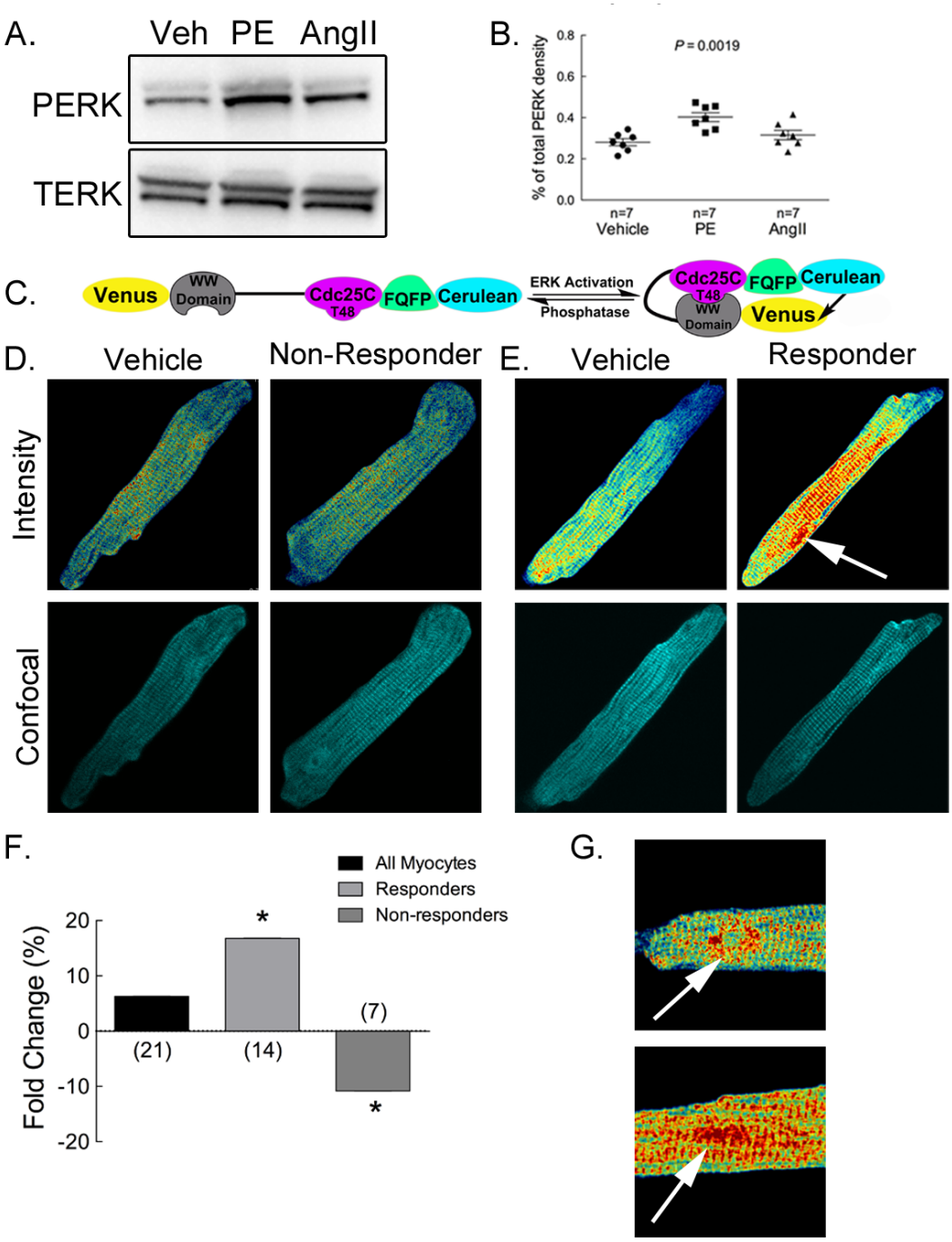

Figure 4.1. α1-ARs activate ERK in the cytosol and at the nucleus in two-thirds of adult cardiac myocytes.

A. *ERK Western blot.* WT AMVM were treated with vehicle, 20 μM PE, or 100 nM AngII for 5 min. Western blots were performed with primary antibodies to phosphorylated ERK (PERK (Thr202/Tyr204), top) or total ERK (TERK, bottom). **B.** *Quantification of ERK phosphorylation.* Densitometry presented as a ratio of PERK to TERK signal for n=7 different cultures. Data were analyzed as described in Methods. **C.** *Schematic of EKAR.*

D, E. *α1-induced EKAR activity.* Intensity images are shown (top), with red indicating increased EKAR activity, for non-responder (**D**) and responder myocytes (**E**) (vehicle, left or 20 μM PE, right). Cerulean fluorescent confocal images are shown for each myocyte (bottom). **F.** *Quantification of α1-induced EKAR activity.* Fold-change in intensity is shown for each group (all myocytes (n=21 from 6 hearts), responders (n=14), or non-responders (n=7), calculation described in methods. **G.** *Magnification of nuclei from responding myocytes*. Arrows indicate nuclei.

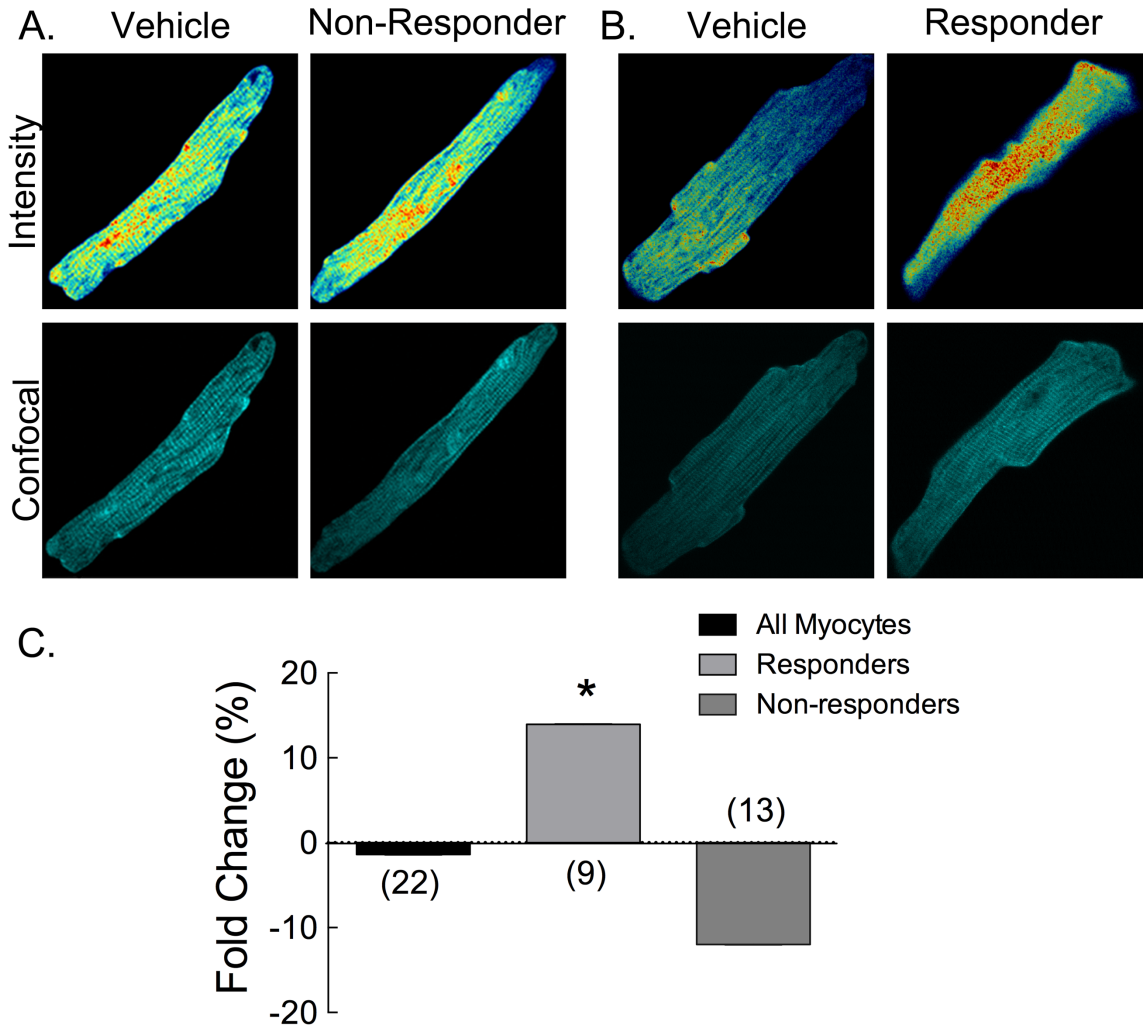

Figure 4.2. AT-Rs activate ERK in the cytosol in one-third of adult cardiac myocytes.

A,B. *AT-R induced EKAR activity.* Intensity images are shown (top) for non-responder (**A**) and responder myocytes (**B**) (vehicle, left or 100 nM AngII, right). Cerulean fluorescent confocal images are shown for each myocyte (bottom). **C.** *Quantification of AT-R induced EKAR activity.* Fold-change in intensity is shown for each group (all myocytes (n=22 from 7 hearts), responders (n=9), or non-responders (n=13), calculation described in methods.

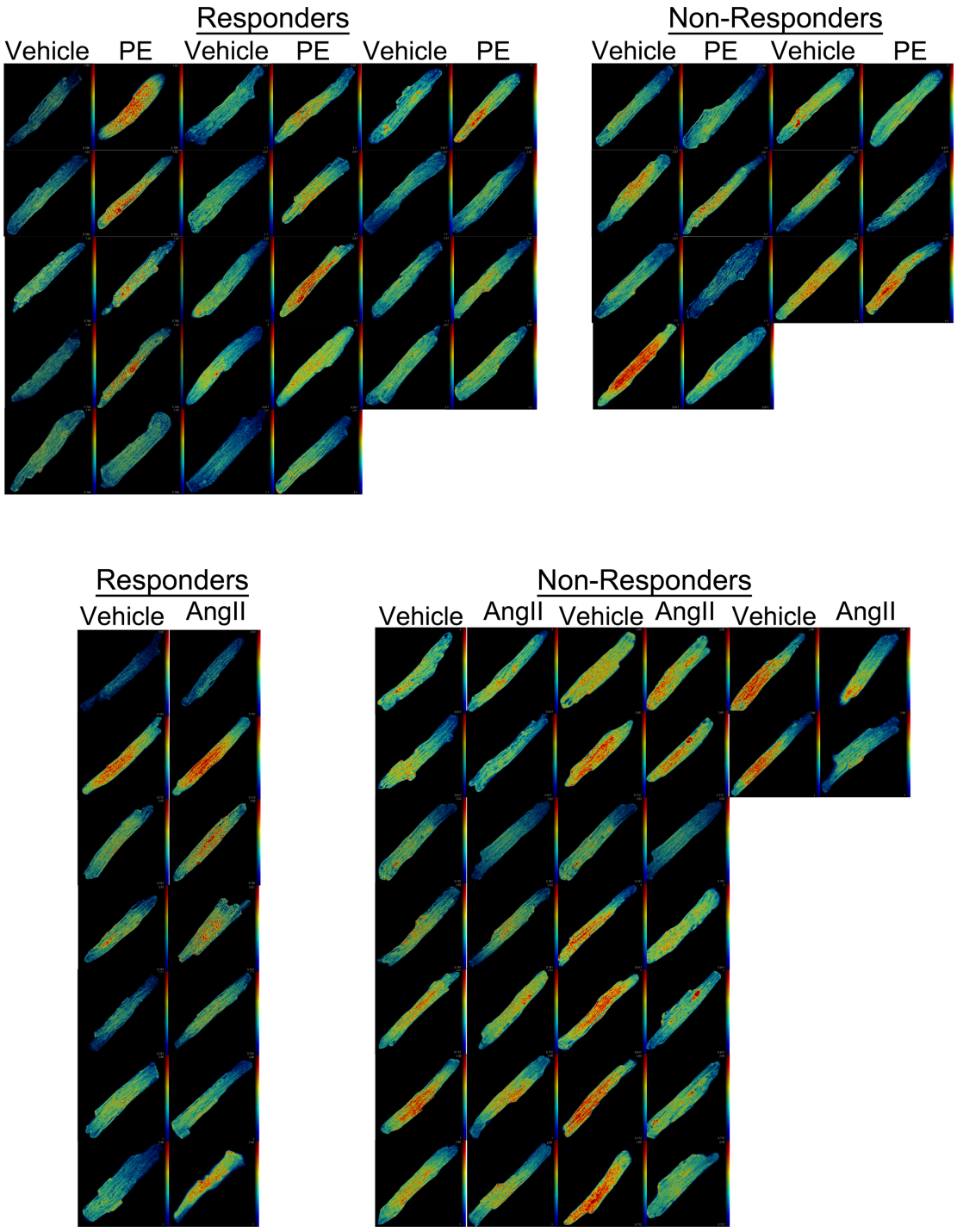

Figure 4.3. Compilation of ERK1/2 activation downstream of α1-ARs and AT-Rs in cardiac myocytes.

Compilation of all myocytes treated with PE (top) or AngII (bottom) used in **Figures 4.1** and **4.2**.

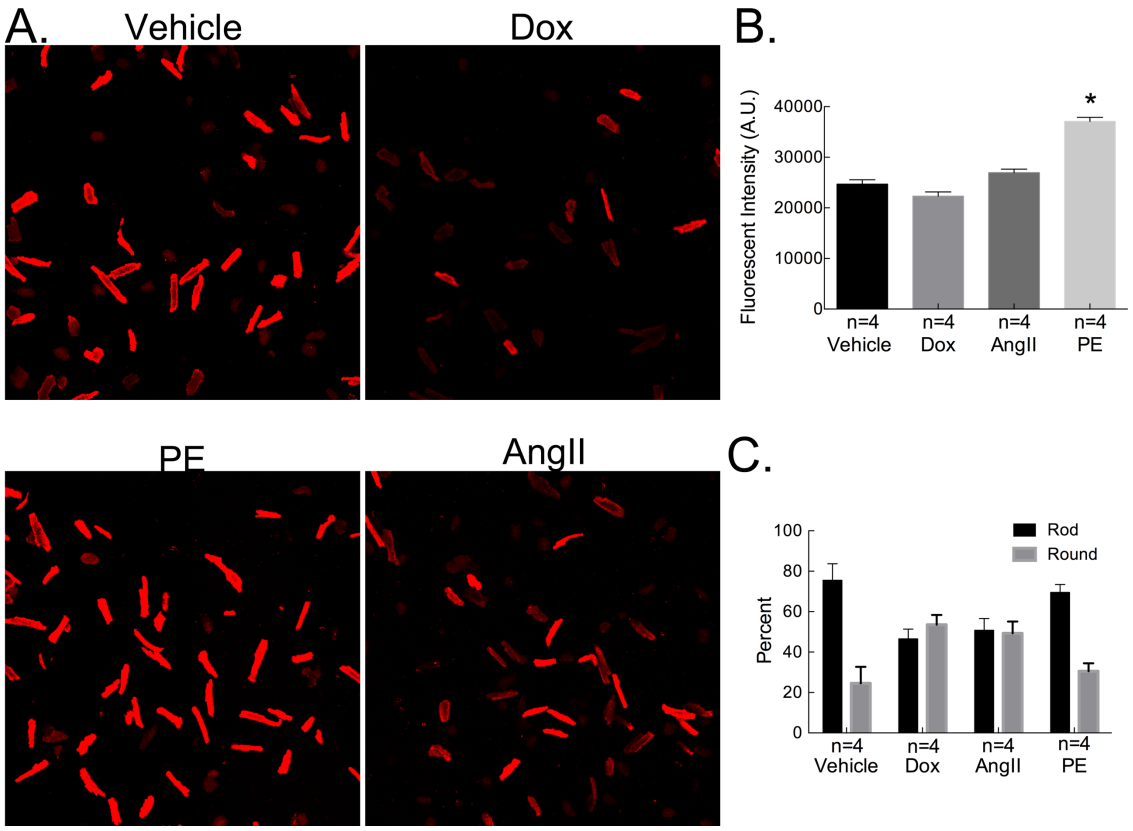

Figure 4.4. α1-ARs, but not AT-Rs, promote mitochondrial membrane stabilization and cardiac myocyte cell survival.

A. *Mitochondrial membrane potential assay*. Images of myocytes treated with vehicle (top left), 2 μM doxorubicin (top right), 20 μM PE (bottom left), or 100 nM AngII (bottom right) for 2 hours and subsequently loaded with JC-1. Images were collected at 10X using confocal microscopy. **B.** *Quantification of mitochondrial membrane potential.* Fluorescent intensity of cells were determined using FIJI. Raw fluorescent intensity counts were plotted using FIJI. One-way ANOVA, *P* >0.05 was considered significant (denoted by *) n=4 hearts. Vehicle=449 cells, Dox=457 cells, AngII=718 cells, PE=682 cells. C. *Quantification of myocyte morphology.* Cell counts for number of rod shaped and number of round shaped myocyte were carried out using FIJI. n=4 hearts. Vehicle=449 cells, Dox=457 cells, AngII=718 cells, PE=682 cells. One-way ANOVA, *P* >0.05 was considered significant (denoted by *)

4.5 Discussion

While α1A-ERK signaling prevents cardiac myocyte death (56), the reduced extent (%myocytes) of AT-R mediated ERK activation relative to α1-ARs measured by Western blot suggests a possible association between the extent of Gq-coupled receptor ERK activation and survival. However, using FLIM, we found that the degree of AT-R mediated ERK activation was similar on a per myocyte basis. The mechanistic basis for the reduced extent of AT-R mediated ERK activation, and whether failure to activate ERK in an individual myocyte contributes to AT-R pro-cell death signaling is unclear. Multiple possibilities exist to explain this finding, including that the nuclear α1-AR signalosome is more efficacious in activating ERK than the sarcolemmal AT-R signalosome, or that analogous to α1-ARs (180), AT-Rs may only be expressed in a small number of myocytes.

In conclusion, using FLIM in adult cardiac myocytes, we identified novel differences in α1-AR and AT-R mediated activation of ERK, both degree and localization. Also, using JC-1 we found that α1-ARs, but not AT-Rs, promote stability of the mitochondrial membrane, and that α1-ARs, but not AT-Rs, promote cardiac myocyte cell survival. Taken together, these results provide new insights into ERK mediated survival signaling.

4.6 Acknowledgements

This work was supported by funds from the University of Minnesota (TDO).

CHAPTER 5. Differential Activation of Hypertrophic Transcriptomes by Gαq-Receptors in Adult Cardiac Myocytes

Erika F. Dahl[1], Chastity L. Healy[2], Timothy D. O'Connell, PhD[2]

[1] Department of Pharmacology, University of Minnesota, Minneapolis, MN 55455
[2] Department of Integrative Biology and Physiology, University of Minnesota, Minneapolis, MN 55455

5.1 Summary

In adult cardiac myocytes, Gq-receptor mediated excitation-transcription coupling, the mechanism whereby myocytes compartmentalize calcium signals to induce hypertrophic transcription, has been thought to occur only at the sarcolemma. Yet, based on differential Gq-receptor localization and activation of proximal signaling pathways, we sought to test the hypothesis that nuclear α1-ARs will promote will promote a unique transcriptional response versus AT-Rs based on their differential localization. We hypothesized that this transcriptional response would mirror the physiologic response downstream of both receptors. Our results indicate that α1-ARs, but not AT-Rs, induce IP_3 sensitive HDAC5 export and that α1-ARs more robustly activate transcription in adult cardiac myocytes with AT-R induced transcriptional responses largely being a subset of α1-ARs'. These results identify distinct difference in the transcriptomes induced by α1-ARs and AT-Rs that align with their distinct subcellular localization and activation of proximal signaling to produce differential activation of hypertrophic signaling pathways.

5.2 Introduction

The current model of Gq-receptor hypertrophic signaling is largely based on ET-R signaling and suggests that sarcolemmal Gq-receptors produce IP_3-dependent intranuclear calcium release, activation of calmodulin kinase, phosphorylation and

nuclear export of histone deacetylases (HDACs), and de-repression of transcription. This model is notable for explaining how cytosolic calcium transients required for contraction are segregated from IP_3-dependent nuclear calcium signals required for hypertrophic signaling. However, it is not entirely clear how this model might reconcile the data suggesting Gq-receptors induce unique physiology or our model of nuclear α1-cardioprotective signaling. Here, we report for the first time that in adult cardiac myocytes, α1-ARs and AT-Rs localize to and activate PLCβ1 in unique subcellular compartments. Further, we demonstrate that these compartmentalized proximal signals induce differential activation of nuclear hypertrophic signaling pathways to produce unique hypertrophic transcriptomes. Finally, these data provide a potential mechanistic explanation for distinct Gq-receptor function in adult cardiac myocytes and suggest a revision of the classic model of excitation-transcription coupling.

5.3 Methods

Mouse Lines

In this study, male and female C57BL/6J mice (10-15 weeks of age) were used as the source of primary adult cardiac myocytes. Male and female C57BL/6J mice were included due to no historical evidence indicating differences in receptor (α1-AR and AT-R) density or signaling cascades. Male FVB/NJ (10-11 weeks of age) mice were used for infusion of agonist to measure Gq-receptor induced hypertrophic transcriptional responses. Only male FVB/NJ mice were used for the Gq-receptor induced hypertrophic transcriptional responses due to historical evidence indicating a more robust hypertrophic response by male mice. All FVB/NJ mice were randomized to treatment groups (vehicle (n=6), AngII (n=4), or PE (n=4)). For implantation of mini-osmotic pumps, mice were anesthetized under isoflurane (3% for induction, 1.5% for maintenance) and animals were treated with buprenorphrine (1 mg/kg) for post-surgical analgesia. After implantation of osmotic pumps, animals were housed singly for the duration of the study to ensure safety of the incision site. All animals were treatment naïve and housed under 12-hour light/dark cycle and fed standard chow. The use of all animals in this study conformed to the PHS Guide for Care and Use of Laboratory Animals and was approved by the University of Minnesota Institutional Animal Care and Use Committee. The University of Minnesota provides AAALAC-accredited services and resources for using

animals in research, including animal ordering, care, facilities, housing, and training for researchers and lab personnel.

Cell Lines

The cell line used in this study are HEK293 cells used for adenoviral amplification. HEK293 cells were cultured in Dulbecco's Modified Eagle's Medium (DMEM) supplemented with 10% fetal bovine serum and 1% penicillin/streptomycin. Cells were incubated at 5% CO_2 and 37°C. No information on sex or cell authentication information is available for this cell line.

Isolation and Culture of AMVM

As we have described previously (161), adult mouse ventricular myocytes were isolated from wild-type male and female C57BL/6J mice between 10 and 15 weeks of age. Briefly, mice were anesthetized with isoflurane (3% for induction, 1.5% for maintenance), injected with heparin (100 IU/mL), the pleural cavity was opened and the heart removed, cannulated on a retrograde perfusion apparatus, and perfused with collagenase type II to dissociate ventricular myocytes. Isolated cardiac myocytes were plated at a density of 50 rod-shaped myocytes per square millimeter on laminin-coated culture dishes. Myocytes were cultured in MEM with Hank's Balanced Salt Solution, 1 mg/ml bovine serum albumin, 10 mM 2,3-butanedione monoxime, and 100 U/ml Penicillin in a 2% CO_2 incubator at 37°C. All reagents were purchased from Sigma Aldrich unless otherwise specified. Full details of the buffers, enzymes, cell culture medium, all procedures for isolation and culturing of AMVM and a detailed diagram of the perfusion apparatus were described in detail previously (161).

Following plating, myocytes were counted at a magnification of 20X to determine cell viability. Adenovirus was added based on previously determined multiplicity of infections. Infected myocytes were incubated in a 2% CO_2 incubator at 37°C for 40 hours.

Adenoviral Production

The HDAC5-GFP adenovirus was a gift from Timothy McKinsey, Ph.D. (183).

Viral amplification and purification: The HDAC5 virus was amplified for three rounds of replication. The HDAC5 virus was purified using OptiPrep gradients and ultracentrifugation (35,000 x *g* for 18 hours). The HDAC5 virus was titered using Adeno-X Rapid Titer Kit per manufacturer's instructions. For experiments, cultured AMVM were

counted at 20X and infected with adenoviruses at the following multiplicity of infection 500 HDAC5-GFP (titer: 6.1 x 10^{15}).

Quantification and Statistical Analysis

Analysis of HDAC5 Nuclear Export

To measure Gq-receptor induced HDAC5 nuclear export, cultured AMVM plated on coverslips were infected with 5,000 MOI HDAC5-GFP for 40 hours at 37°C. Myocytes were treated with either vehicle, PE (20 μM), or AngII (100 nM) for either 30 minutes or 1 hour at 37°C. Pretreatment with 2-APB (2 μM) was carried out for 30 minutes at 37°C prior to PE treatment. Myocytes were fixed and mounted exactly as described for α1-QDot 565. Confocal images were captured on an Olympus FluoView FV1000 IX2 Inverted Confocal Microscope at 60X magnification (oil immersion).

Analysis of Hypertrophic Transcriptional Profiles

To analyze Gq-receptor hypertrophic transcriptional profiles, 10 to 11 week old FVB/NJ mice were dosed at 30 mg/kg/day for PE (n=4), 0.5 mg/kg/day for AngII (n=4), or vehicle (n=6) using implanted micro-osmotic pumps for 72 hours. Total RNA was harvested from isolated myocytes using RNeasy Fibrous Tissue Mini Kit, following manufacturer's instructions. Using total RNA as input, rRNA was removed via oligo-dT purification to enrich for mRNA, followed by random-primed reverse-transcription, second-strand cDNA synthesis, ligation of indexed adaptors for Illumina sequencing, and subsequent library creation from the resulting double-stranded DNA. 125 base pair paired end stranded RNA Sequencing was performed by the University of Minnesota Genomics Core using the Illumina HiSeq 2500 resulting in 10-20 million reads per sample.

Statistical Analysis

All data plotting and statistical analysis was performed using Prism 6 software. All information on statistical parameters can be found in figure legends. HDAC5-GFP fluorescent intensity was measured for whole myocytes and nuclei using FIJI. Nuclear fluorescence was subtracted from whole cell fluorescence to calculate cytosolic fluorescence. Ratio of cytosolic to nuclear fluorescence was plotted. Data were analyzed by One-Way ANOVA and $P<0.05$ was considered significant.

For RNAseq analysis, 126bp FastQ paired-end reads (n=11.6 Million per sample) were trimmed using Trimmomatic (v 0.33) enabled with the optional "-q" option; 3bp sliding-window trimming from 3' end requiring minimum Q30. Quality control checks on raw sequence data for each sample were performed with FastQC. Read mapping was performed via Bowtie (v2.2.4.0) using the UCSC mouse genome (mm10) as reference. Gene quantification was done via Cuffquant for FPKM values and Feature Counts for raw read counts. Differentially expressed genes were identified using the edgeR (negative binomial) feature in CLCGWB (Qiagen) using raw read counts. We filtered the generated list based on a minimum 1.7X Absolute Fold Change and FDR corrected $p < 0.05$. The filtered gene list was then used for further analysis of hypertrophic, survival-signaling, inotropic, and fibrotic gene ontologies. Search criterion were defined by commonly associated terms used in concordance with hypertrophy, survival-signaling, inotropy, and fibrosis, respectively. Search terms for hypertrophy were NF-kappa B, GATA4, MEF2, NFAT, ANF, TGF, hypertrophy, myosin heavy chain, MHC, c-myc, c-fos, cell growth, and natriuretic. Search terms for survival-signaling were ERK, MAPK, apoptotic, apoptosis, survival, and cell death. Search terms for inotropy were calcium, contraction, sarcoplasmic reticulum, troponin, myosin, actin, ryanodine, protein kinase C, and sarcomere. Search terms for fibrosis were collagen, matrix metalloprotease, fibrosis, fibroblast, extracellular matrix, matrix. All genes are represented with Entrez gene names (https://www.ncbi.nlm.nih.gov/gene). Prcomp was used to perform principal component analysis on a file containing normalized FPKM values across 14 samples with 24,345 genes across 3 groups. Ggplot was used to draw the PCA graph and stat_ellipse was used to delineate the 95% confidence intervals.

Data Availability
RNA-Seq Data Set is available at http://dx.doi.org/10.17632/pbw8ww4k55.1.

5.4 Results

α1-ARs, but not AT-Rs, induce IP_3-dependent nuclear export of HDAC5 in adult cardiac myocytes.

Gq-receptors induce hypertrophy through a mechanism known as excitation-transcription coupling (43). Conventionally, sarcolemmal Gq-receptor-mediated production of IP_3 elicits intranuclear calcium release from the nuclear envelope,

activation of calmodulin kinase type II, and phosphorylation and nuclear export of HDAC5 (43). Nuclear compartmentalization of IP_3-dependent calcium release allows myocytes to distinguish calcium required for contraction from calcium required for transcriptional signaling. Here, we examined whether differentially localized Gq-receptors would have the same effect on HDAC5 export. In AMVM expressing HDAC5-GFP, PE but not AngII induced a moderate, but significant, export of HDAC5 at 30 minutes (**Figure 5.1A** top panels, quantified in **5.1B**). By 1 hour, PE significantly induced HDAC5 nuclear export, whereas AngII did not (**Figure 5.1A** bottom panels, quantified in **5.1C**), consistent with previous reports for PE (184). To determine if PE-induced HDAC5 nuclear export was IP_3-dependent, AMVM expressing HDAC5-GFP were pretreated with the IP_3R inhibitor 2-aminoethoxydiphenyl borate (2-APB). Pretreatment with 2-APB abolished the PE-mediated HDAC5 nuclear export (**Figure 5.1D**, quantified in **5.1E**). Taken together, these results indicate that α1-ARs, but not AT-Rs, activate IP_3-dependent HDAC5 nuclear export in AMVM.

α1-ARs and AT-Rs induce unique transcriptomes in adult cardiac myocytes

Physiologically, α1-ARs and AT-Rs have diametrically opposed effects on the heart. α1-ARs induce physiologic hypertrophy, survival signaling, positive inotropy, and are not associated with fibrosis (14). AT-Rs induce pathologic hypertrophy, myocyte cell death, negative inotropy, and are pro-fibrotic (185, 186). We hypothesized that these differences in the physiologic function of cardiac α1-ARs and AT-Rs would be revealed in their transcriptomes and reflective of their distinct subcellular localization. To evaluate α1-AR and AT-R transcriptomes, we treated mice with vehicle, PE (30 mg/kg/day), or AngII (0.5 mg/kg/day) continually for 3 days using osmotic mini-pumps, at which point, we isolated cardiac myocytes and performed RNASeq. Consistent with our HDAC5 results and that HDAC5 activation relieves transcriptional repression, α1-ARs induced a larger transcriptional response, with a total of 806 genes changed (increased or decreased) 1.7-fold versus vehicle, whereas AT-Rs induced a much smaller response with only 173 genes changed 1.7- fold versus vehicle. 1.7 fold expression over vehicle was used as the threshold since adult cardiac myocytes are post-mitotic and generally do not induce large transcriptional responses. Interestingly, between α1-ARs and AT-Rs, 155 genes were changed by both agonists, indicating α1-ARs induced 651 unique

genes, whereas AT-Rs induced only 18 unique genes (**Figure 5.2A**). These results suggest that the AT-R transcriptome is largely a subset of the α1-AR transcriptome in cardiac myocytes.

To parse the RNASeq results further, we initially attempted to utilize the Ingenuity Pathway Analysis (IPA) software, but the majority of the database is derived from oncogenic studies and lacks cardiac myocyte specific pathways. Thus, we derived our own analysis and sorted genes that were regulated by α1-ARs alone, AT-Rs alone, or were in common between the two into gene ontologies corresponding to Gq-receptor biology: hypertrophy, survival signaling, inotropy, and fibrosis (**Figure 5.2B, Tables 5.1-5.4**). α1-ARs most robustly altered genes in all categories as compared to common genes and AT-R only genes. While surprising that α1-ARs altered more fibrotic genes than AT-Rs, these genes are not classically associated with alterations in the extracellular matrix leading to fibrosis (**Table 5.4**). Finally, principle component analysis (PCA) was performed to determine the degree of difference between vehicle, AngII, and PE treated samples (**Figure 5.2C**). Principle component 1 (PC1) accounted for 66% of the variance and aligned with the α1-AR transcriptomes, whereas PC2 accounted for 22% of the variance and aligned with the AT-R transcriptome. The AngII treated samples also closely grouped with the vehicle treated samples indicating that AT-Rs do not induce a highly distinct transcriptome from control, consistent with our gene ontology results (**Figure 5.2A** and **5.2B**) The top 25 genes determining PC1 and PC2 are presented in **Figure 5.2D**. Taken together, α1-ARs robustly activate transcription in adult cardiac myocytes whereas AT-Rs minimally activate transcription. These results identify distinct differences in the transcriptomes induced by α1-ARs and AT-Rs that align with their distinct subcellular localization and activation of proximal signaling to produce differential activation of nuclear hypertrophic signaling pathways.

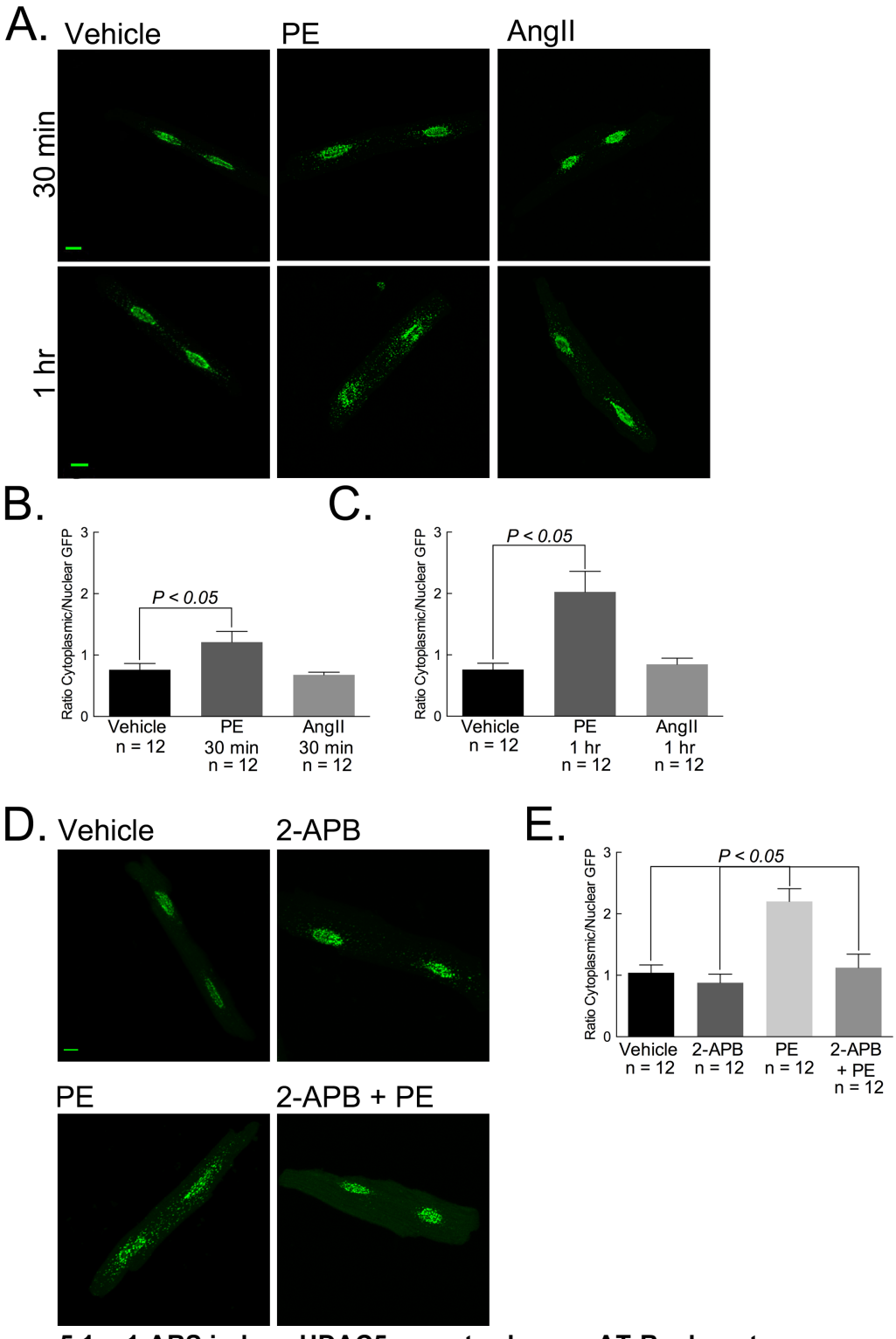

Figure 5.1. α1-ARS induce HDAC5 export, whereas AT-Rs do not.

A. *α1-ARs activate HDAC5 nuclear export, whereas AT-Rs do not.* WT AMVM expressing HDAC5-GFP were treated with either vehicle (left panels), 20 μM PE (middle

panels), or 100 nM AngII (right panels) for either 30 minutes (top panels) or 1 hour (bottom panels) at 37°C. Scale bar = 10 μm. **B** and **C.** *Quantification of HDAC5 export induced by α1-ARs and AT-Rs.* Cytoplasmic and nuclear GFP fluorescence was quantified using FIJI, and the ratio of cytoplasmic to nuclear GFP was plotted as an indication of HDAC5 nuclear export at 30 minutes (**B**) and 1 hour (**C**). Data are represented as mean ± SEM. Data were analyzed by one-way ANOVA, and $P<0.05$ was considered significant. Vehicle (n=12 myocytes from 6 hearts); PE (n=12 myocytes from 6 hearts); AngII (n=12 myocytes from 6 hearts) **D.** *HDAC5 export is inhibited in the presence of IP_3R inhibitor, 2-APB.* WT AMVM expressing HDAC5-GFP were treated with 2-APB (2 μM, 30 minutes at 37°C) prior to treatment with PE (1 hour at 37°C, middle panel). Scale bar = 10 μm. **D.** *Quantification of HDAC5 export in the presence of IP_3R inhibitor, 2-APB.* The ratio of cytoplasmic to nuclear GFP was calculated and plotted. Data are represented as mean ± SEM. Data were analyzed by one-way ANOVA, and $P<0.05$ was considered significant. Vehicle (n=12 myocytes from 6 hearts); 2-APB (n=12 myocytes from 6 hearts); PE (n=12 myocytes from 6 hearts); PE+2-ABP (n=12 myocytes from 6 hearts).

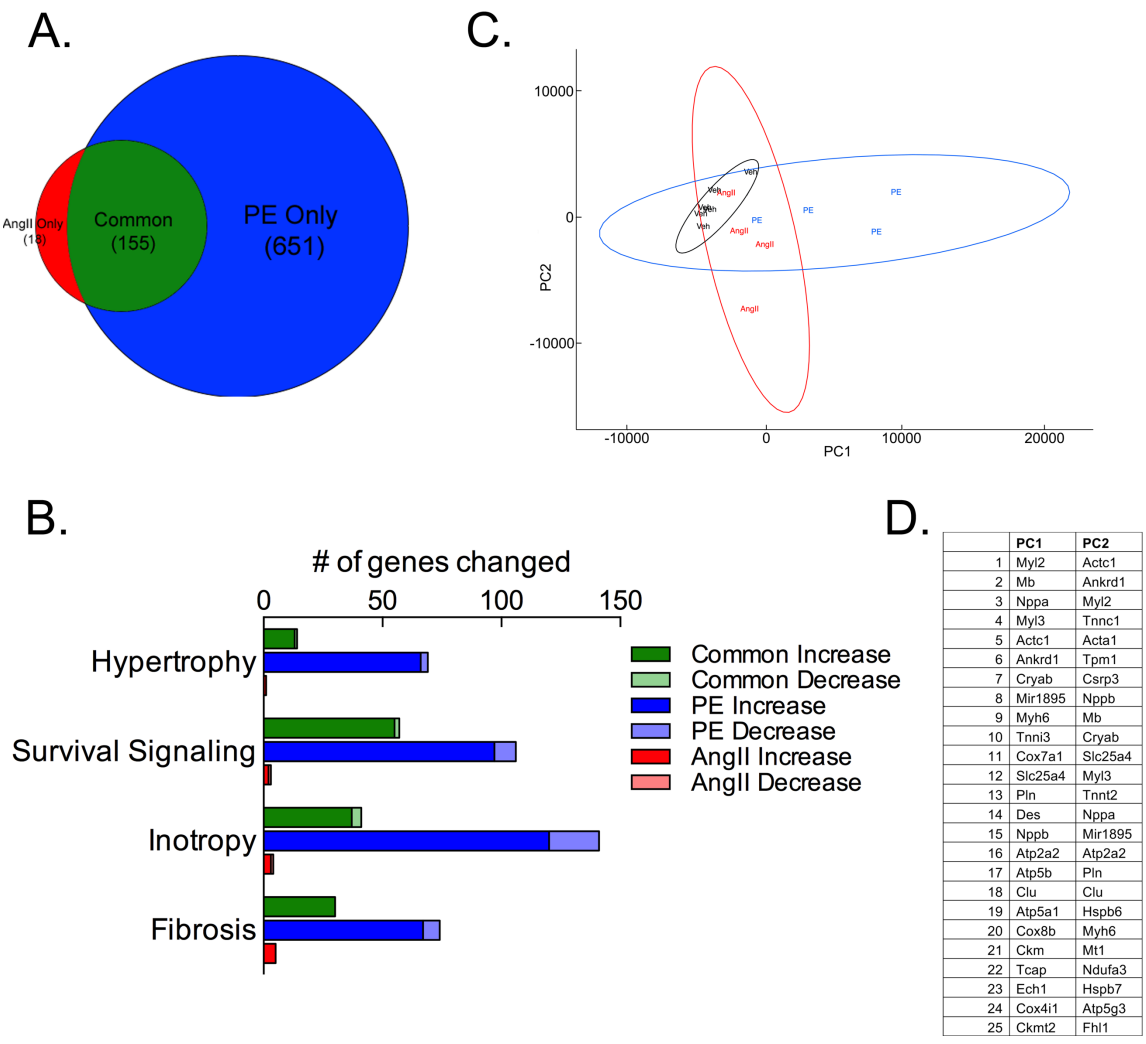

	PC1	PC2
1	Myl2	Actc1
2	Mb	Ankrd1
3	Nppa	Myl2
4	Myl3	Tnnc1
5	Actc1	Acta1
6	Ankrd1	Tpm1
7	Cryab	Csrp3
8	Mir1895	Nppb
9	Myh6	Mb
10	Tnni3	Cryab
11	Cox7a1	Slc25a4
12	Slc25a4	Myl3
13	Pln	Tnnt2
14	Des	Nppa
15	Nppb	Mir1895
16	Atp2a2	Atp2a2
17	Atp5b	Pln
18	Clu	Clu
19	Atp5a1	Hspb6
20	Cox8b	Myh6
21	Ckm	Mt1
22	Tcap	Ndufa3
23	Ech1	Hspb7
24	Cox4i1	Atp5g3
25	Ckmt2	Fhl1

Figure 5.2. α1-ARs robustly activate transcriptional responses in adult cardiac myocytes whereas AT-ARs do not.

A. *Venn diagram of α1-AR- and AT-R-induced transcriptomes.* The gene list generated by RNAseq was filtered based on a minimum 1.7X absolute fold change and FDR corrected $P<0.05$. PE treatment altered 801 transcripts (655 unique) by at least 1.7 fold, whereas AngII only altered 173 (18 unique), with 155 common between the two treatments. **B.** *Gene ontology analysis α1AR- and AT-R-induced transcriptomes.* Gq-receptors regulate hypertrophy, survival signaling, inotropy, and fibrosis. Therefore, using non-overlapping search terms unique to these different biologic functions, genes were sorted into subclasses of hypertrophy, survival signaling, inotropy, and fibrosis. The total number of genes altered (increased and decreased) in common or by PE or AngII alone are plotted in the graph. Search terms used to sort genes associated with hypertrophy: NF-kappa B, GATA4, MEF2, NFAT, ANF, TGF, hypertrophy, myosin heavy

chain, MHC, c-myc, c-fos, cell growth, natriuretic; Search terms for survival signaling: ERK, MAPK, apoptotic, apoptosis, survival, cell death; Search terms for inotropy: calcium, contraction, sarcoplasmic reticulum, troponin, myosin, actin, ryanodine, protein kinase C, and sarcomere; Search terms for fibrosis: collagen, matrix metalloprotease, fibrosis, fibroblast, extracellular matrix, matrix. **C.** *Principle Component Analysis of α1-AR and AT-R induced transcriptomes*. Principle component analysis of fragments per kilobase of exon per million reads mapped (FPKM). PC1 determined 66% of all variance between samples. PC2 determined 22% of all variance between samples. **D.** *Top 25 genes determining PC1 and PC2*. Top 25 genes for PC1 and PC2 were determined using FPKM loadings.

Gene Ontology Category	AngII	PE	Common
Immune Response	**0**	**19**	**5**
Increase	0	19	5
	-	*Cd14, Cd44, Cd84, Clec4n, Fcer1g, Fcgr1, Fcgr3, H2-DMb1, H2-DMb2, Havcr2, Il1b, Ncf4,Slc11a1, Tgfb3, Tlr1, Tnfrsf11a, Tnfsf11, Tnfsf14, Trem2*	*Fcgr2b, Il6, Inhba, Lgals3, Tgfb2*
Decrease	0	0	0
	-	-	-
Kinase & Phosphatase Activity	**0**	**6**	**4**
Increase	0	6	3
	-	*Btk, Ikbke, Pak1, Pi16, Pik3ap1, Rcan1*	*Cdkn1a, Nckap1l, Ptk2b*
Decrease	0	0	1
	-	-	Akap5
Transcription Regulation	**0**	**7**	**1**
Increase	0	6	1
	-	*Bcl3, Col14a1, Igfbp2, Il7r, Nupr1, Zc3h12d*	*Spi1*
Decrease	0	1	0
	-	Nlrc5	-
G-protein Coupled Receptors & Activity	**0**	**6**	**0**
Increase	0	5	0
	-	*Frzb, Htr2b, Rasgrp4, Rrad, Sfrp1*	-
Decrease	0	1	0
	-	*Adra1a*	-
Growth Factor	**0**	**4**	**2**
Increase	0	4	2
	-	*Cgref1, Ctgf, Hbegf, Igf1*	*Csf2rb, Fhl1*
Decrease	0	0	0
	-	-	-

Table 5.1. Molecular function of Hypertrophic Genes induced by α1ARs, ATRs, or in common.

As described in **Figure 5.2**, genes were sorted into Gq-receptor functional subclasses of hypertrophy, survival signaling, inotropy, and fibrosis using non-overlapping search terms unique to Gq-receptor biologic functions. Search terms for hypertrophy were: NF-kappa B, GATA4, MEF2, NFAT, ANF, TGF, hypertrophy, myosin heavy chain, MHC, c-myc, c-fos, cell growth, natriuretic. Hypertrophic genes were further sorted by molecular

function and listed in the table, with the number of genes increased or decreased indicated along with the specific genes in each category.

Gene Ontology Category	AngII Only	PE Only	Common
Immune Response	**0**	**18**	**12**
Increase	0	18	12
	-	*Ccl12, Ccl4, Ccl6, Ccr1, Cd44, Cd84, Gdf15, Gdf6, Il1b, Il33, Lgals1, Lif, Tgfb3, Tnfrsf11a, Tnfrsf11b, Tnfrsf23, Tnfsf11, Tnfsf14*	*Ccl2, Ccl9, Ccl22, Ccr2, Cd24a, Crlf1, Il6, Il11, Il1rn, Inhba, Socs3, Tgfb2*
Decrease	0	0	0
	-	-	-
Kinase & Phosphatase Activity	**0**	**20**	**7**
Increase	0	15	6
	-	*Dram1, Dusp26, Havcr2, Hck, Hk3, Ikbke, Pak1, Pak3, Pak6, Peg10, Pik3ap1, Ptn, Ptpn6Ptprc, Sphk1*	*Cdkn1a, Hsb1, Mylk2, Nckap1l, Ptk2b, Snai1*
Decrease	0	5	1
	-	*Dusp4, Ephb1, Map4k2, Ptprr, Prkcg*	*Kit*
G-protein Coupled Receptors & Activity	**0**	**16**	**0**
Increase	0	14	0
	-	*Ccl7, Ccl8, Ccr5, Cdh1, Cx3cr1, Frzb, Gpnmb, Htr2b, Lpar3, Mpz, Ncf2, Ntsr2, Rgs14, Sfrp1*	-
Decrease	0	2	0
	-	*Adra1a, Brinp1*	-
Transcription Regulation	**2**	**6**	**4**
Increase	1	5	3
	Atf3	*Creb3l1, Irf5, Isl1, Myc, Twist1*	*Ankrd2, Plac8, Spi1*
Decrease	1	1	1
	Sox4	*Sox7*	*Mycn*
Enzyme	**0**	**11**	**0**
Increase	0	10	0

Table 5.2. Molecular function of Survival Signaling Genes induced by α1ARs, ATRs, or in common.

As described in **Figure 5.2**, genes were sorted into Gq-receptor functional subclasses of hypertrophy, survival signaling, inotropy, and fibrosis using non-overlapping search terms unique to Gq-receptor biologic functions. Search terms for survival signaling were: ERK, MAPK, apoptotic, apoptosis, survival, cell death. Survival signaling genes were further sorted by molecular function and listed in the table, with the number of genes increased or decreased indicated along with the specific genes in each category.

Gene Ontology Category	AngII	PE	Common
Kinase & Phosphatase Activity	**0**	**23**	**7**
Increase	0	20	5
	-	*Bmp1, Camk2n2, Ccl4, Ccr1, Cnn1, Coro1a, Dbn1, Dpysl3, Fbn1, Fkbp10, Hck, Myo1g, Pacsin1, Pak1, Pak3, Pak6, Plek, Ptpn6, Ptprc, Sphk1*	*Acp5, Fgr, Mylk2, Nckap1l, Ptk2b*
Decrease	0	3	2
	-	*Dgkh, Mylk4, Prkcg*	*Akap5, Kit*
G-protein Coupled Receptors & Activity	**0**	**19**	**3**
Increase	0	15	2
	-	*Ackr1, Adgre1, Cdh1, Dock2, Fpr2, Fstl1Htr2b, Lpar3, Rab27b, Rac2, Rhou, Sfrp1, Tgm2, Tnfsf11, Was*	*Lrp8, Ptafr*
Decrease	0	4	1
	-	*Adra1a, Celsr3, Gpr17, Tbxa2r*	*Apln*
Immune Response	**0**	**12**	**6**
Increase	0	12	6
	-	*Alox5ap, C3ar1, C5ar1, Ccl12, Ccr5, Cd84,Cxcl13, Gpr35, Il1b, Ncf1, Panx1, Runx1*	*Ccl2, Cd24a, Crlf1, Sele, Selp, Tgfb2*
Decrease	0	0	0
	-	-	-
Ion Channel	**0**	**13**	**4**
Increase	0	9	4
	-	*Atp1a3, Clca3a, Fzd2, Itih4, Kcnab2, Kcnn4, Slc8a2, Trem2, Trpm2*	*Hcn1, Ltbp2, Sypl2, Syt12*
Decrease	0	4	0
	-	*Ano10, Cacna1s, Clcn1, Cracr2a*	-

Table 5.3. Molecular function of Inotropy Genes induced by α1ARs, AT-Rs, or in common.

Search terms for inotropy were: calcium, contraction, sarcoplasmic reticulum, troponin, myosin, actin, ryanodine, protein kinase C, and sarcomere. Inotropy genes were further

sorted by molecular function and listed in the table, with the number of genes increased or decreased indicated along with the specific genes in each category.

Gene Ontology Category	AngII	PE	Common
Extracellular Matrix Modulation	**1**	**27**	**11**
Increase	1	27	11
	Mmp9	*Acan, Adamts2, Col11a1, Col12a1, Col14a1, Col16a1, Col18a1, Col6a1, Col6a2, Eln, Emilin1, Fbln2, Fbn1, Fbn2, Frem1, Itga11, Itgb3, Mmp12, Mmp14, Mmp19, Mmp8, Mrc2, P4ha3, Pcolce, Postn, Serpinh1, Vacn*	*Adam8, Adamts4, Col1a1, Col1a2, Col3a1, Col5a1, Col5a2, Mmp3, Spp1, Thbs1, Thbs4*
Decrease	0	0	0
	-	-	-
Immune Response	**0**	**6**	**7**
Increase	0	6	7
	-	*Bgn, Ccdc80, Cd44, Tgfb3, Tnfsf11b*	*Ccl2, Cxcl5, Il17ra, Il6, Itgb2, Lgals3, Tgfb2*
Decrease	0	0	0
	-	-	-
Kinase & Phosphatase Activity	**0**	**7**	**2**
Increase	0	6	2
	-	*Ccnb1, Cnn1, Dusp26, Fam20c, Pak1, Pak3*	*Cdkn1a, Ptk2b*
Decrease	0	1	0
	-	*Ptprz1*	-
Transcription Regulation	**0**	**7**	**0**
Increase	0	5	0
	-	*Bcl3, Creb3l1, Myc, Nupr1, Sh3pxd2b*	-
Decrease	0	2	0
	-	*Dach1, Tcf15*	-
Peptidase	**0**	**4**	**3**
Increase	0	4	3

Table 5.4. Molecular function of Fibrosis Genes induced by α1ARs, AT-Rs, or in common.

As described in **Figure 5.2**, genes were sorted into Gq-receptor functional subclasses of hypertrophy, survival signaling, inotropy, and fibrosis using non-overlapping search terms unique to Gq-receptor biologic functions. Search terms for fibrosis were: collagen,

matrix metalloprotease, fibrosis, fibroblast, extracellular matrix, matrix. Fibrosis genes were further sorted by molecular function and listed in the table, with the number of genes increased or decreased indicated along with the specific genes in each category.

5.5 Discussion

Here we report our findings that α1-ARs and AT-Rs differentially activate transcriptional machinery and transcriptional responses in adult cardiac myocytes. Gq-receptors differentially activate transcriptional machinery, with α1-ARs, but not AT-Rs, promoting IP_3 sensitive HDAC5 export. We also found that Gq-receptors differentially activate transcriptional responses with α1-ARs inducing robust transcriptional responses in genes that correspond to α1-AR physiologic function, whereas AT-Rs activate genes that are largely a subset of α1-AR regulated genes. These results are the first indicating that α1-ARs and AT-Rs differentially regulate transcription in adult cardiac myocytes and support the idea that this is due to their localization and compartmentalization of proximal signaling cascades.

The first report of IP_3 sensitive transcriptional regulation in adult cardiac myocytes was based on ET-Rs (43). In that report, sarcolemmal ET-Rs activate sarcolemmal PLCβ1 to produce IP_3 which traverses the cardiac myocyte and activates IP_3Rs in the inner nuclear membrane to induce HDAC5 export (43). Our results indicate a more nuanced view of this signaling cascade with nuclear α1-ARs inducing IP_3 sensitive HDAC5 export, but sarcolemmal AT-Rs failing to induce HDAC5 export. This seemingly conflicting result can be explained by the localization of these receptors in adult cardiac myocytes: α1-ARs at the nuclear membrane, AT-Rs at the sarcolemma, and ET-Rs at the bottom of the t-tubules which are in close proximity to the nuclear membrane (187). Our results indicate that IP_3 must be produced in close apposition to the nuclear membrane in order to induce transcriptional activation indicating that α1-ARs and ET-Rs, but not AT-Rs, are capable of inducing this signaling cascade.

5.6 Acknowledgements

The authors would like to acknowledge Dr. Timothy McKinsey, University of Colorado, for his generous gift of the HDAC5-GFP virus and Dr. Jop van Berlo, University of Minnesota, for his help in conceptualizing the project. The authors would also like to thank the University of Minnesota Genomics Center for their assistance in RNASeq data analysis. This work was supported by funds from the University of Minnesota (TDO).

CHAPTER 6. CONCLUSIONS AND FUTURE DIRECTIONS

6.1 Conclusions

Here, we identified a potential mechanistic explanation for unique Gq-receptor function in adult cardiac myocytes predicated upon subcellular compartmentalization of proximal Gq-receptor signaling. We found that α1-ARs localize to the nucleus and induce intranuclear activation of PLCβ1, activate perinuclear and cytosolic ERK, stimulate IP_3-dependent nuclear export of HDAC5, and activate a robust and unique transcriptome associated with hypertrophic, survival, inotropic, and (anti)-fibrotic gene programs. Conversely, we observed that AT-Rs primarily localize to, activate PLCβ1 at the sarcolemma, activate ERK only in the cytoplasm, but have little effect on nuclear export of HDAC5, and induce a small transcriptome that is a subset of the α1-transcriptome. More importantly, these findings are consistent with our hypothesis that Gq-receptor localization dictates function by showing compartmentalization of proximal Gq-signaling events is correlated with phenotypic outcome in adult cardiac myocytes.

The excitation-transcription model of Gq-receptor mediated hypertrophic signaling in adult cardiac myocytes proposes that sarcolemmal Gq-receptors induce IP_3 production and IP_3-sensitive intranuclear calcium release from perinuclear calcium stores to activate calmodulin kinase, phosphorylate and induce nuclear export of HDAC5, and thereby activate transcription (**Figure 6.1A)**. Both ET-Rs and insulin-like growth factor receptors conform to this model (43, 171, 188). Our data indicate that α1-ARs support this model as well, but interestingly, AT-Rs do not. Although we observed AT-R mediated activation of PLCβ1 and further downstream activation of ERK, we failed to detect AT-R mediated nuclear export of HDAC5, and found a much smaller transcriptional response. One interpretation of this result is that close proximity to the nucleus is required for Gq-receptor mediated activation of IP_3-dependent hypertrophic signaling. In support of this interpretation, α1-ARs localize to the inner nuclear membrane (154), and ET-Rs and insulin-like growth factor receptors localize to the bottom of t-tubules in close apposition to the nucleus in adult cardiac myocytes (187, 188). Further, the failure of AT-Rs to induce nuclear export of HDAC5 suggest that AT-R-mediated activation of PLCβ1 at the sarcolemma either fails to generate enough IP_3 to reach the nucleus or that IP_3 is degraded before it reaches the nucleus. The potential degradation of IP_3 prior to reaching the nucleus might be analogous to the compartmentalization of cAMP signaling in cardiac myocytes (189). While the current

model of excitation-transcription coupling suggests that Gq-receptors induce IP_3 production at the sarcolemma leading to activation of IP_3-dependent calcium release at the nucleus to induce HDAC5-export and promote gene transcription, our new model is more nuanced. Our model suggests Gq-receptor induced IP_3 production is compartmentalized and that IP_3 produced inside the nucleus (or possibly in close proximity to the nucleus) induces HDAC5 export to promote gene transcription, whereas IP_3 produced at a distance from the nucleus (at the sarcolemma) has a different, and smaller effect on transcriptional regulation (**Figure 6.1B**). This would suggest that Gq-receptor compartmentalization has a large influence on the transcriptomes induced by differentially localized Gq-receptors, illustrating the fundamental physiologic importance of Gq-receptor compartmentalization.

The consensus view of cardiac Gq-receptor function has been that Gq-receptors mediate pathologic remodeling, promoting maladaptive hypertrophy, myocyte cell death, and negative inotropic responses (155). However, in clinical trials of hypertension (Antihypertensive and Lipid-Lowering Treatment to Prevent Heart Attack Trial, ALLHAT) and HF (Vasodilator Heart Failure Trial, V-HeFT), α1-AR antagonists worsened outcomes (190, 191). Further, our studies indicate that α1-ARs are cardioprotective, promoting adaptive or physiologic hypertrophy, prevention of cell death, and positive inotropic effects identifying a mechanistic basis for the negative results of α1-AR antagonists in clinical trials (14). In short, the cardioprotective nature of α1-ARs stands in stark contrast to the consensus view of maladaptive Gq-receptor function. Here, our data suggests that compartmentalization of Gq-receptors could explain differences in Gq-receptor function. We demonstrated that although both α1-ARs and AT-Rs activate PLCβ1, they do so in different subcellular compartments which has a profound effect on activation of intranuclear hypertrophic signaling and transcriptional activation. Therefore, we suggest that nuclear Gq-receptor signaling, typified byα1-ARs, is cardioprotective. Aside from α1-ARs, a small population of functional ET-Rs and AT-Rs localize to the nucleus as well (69, 71), although their physiologic significance is unclear. Conversely, we observed AT-Rs primarily at the sarcolemma, but not in close proximity to the nucleus, which might suggest that Gq-receptor signaling at the sarcolemma is pathologic, which is supported by studies with AT-Rs (185, 186). In support of this concept, adenoviral mediated expression of the PLCβ1b at the sarcolemma induces

contractile dysfunction (27). In summary, our hypothetical model of compartmentalized Gq-receptor signaling, where nuclear Gq-receptor signaling is cardioprotective, suggests a more nuanced view of Gq-receptor function in cardiac myocytes.

The concept of GPCR compartmentalization in cardiac myocytes is not without precedence. In co-cultures of sympathetic ganglionic neurons and neonatal rat cardiac myocytes, β1-ARs localize to regions of axonal contact rich in SAP97, AKAP97, catenins, and cadherins, whereas β2-ARs are excluded from these domains (164). In adult cardiac myocytes, β1-ARs are distributed over the entire sarcolemma, whereas β2-ARs are restricted deep within T-tubules (165). Finally, platelet-derived growth factor receptors, which also signal through Gs, localize to caveolae in cardiac myocytes and do not induce an inotropic response (166). These examples demonstrate that cardiac myocytes compartmentalize Gs-mediated GPCR signaling, analogous to our findings with Gq-receptors.

Aside from the potential of targeting α1-ARs in HF (14) our identification of cardioprotective nuclear α1-AR signaling also has implications outside of heart. In the peripheral vasculature, α1-ARs mediate contraction of smooth muscle, and α1-AR antagonists were one of the first treatments for hypertension (HTN). For the same reason, α1-AR antagonists are used to treat lower urinary tract symptoms (LUTS) and benign prostatic hyperplasia (BPH) (192). Estimates suggest that 9.5 million men over 65 will develop BPH (193), and of these, 87% will have concomitant HTN and 40% will have a previous admission for HF (194). However, α1-AR antagonists increased mortality and increased the risk of HF in ALLHAT (190), and are no longer a first-line treatment for HTN, but α1-AR antagonists still used in BPH. Interestingly, nuclear localization of α1-ARs in cardiac myocytes does not extend to smooth muscle cells, where α1-ARs localize to the cell surface with some fraction internal but not at the nucleus (195). Development of a next-generation membrane impermeable α1-blocker could reduce cardiotoxic side effects of current α1-blockers, restoring their use in HTN and improving their safety in BPH. Therefore, compartmentalization of GPCRs can have an important biological impact in multiple systems.

In conclusion, our findings support a model of compartmentalized Gq-receptor signaling in adult cardiac myocytes. This model, largely based on our identification of cardioprotective nuclear α1-AR signaling, provides a plausible mechanistic basis to

explain the unique function of cardiac Gq-receptors. Additionally, this model suggests a re-examination of the classic paradigm of maladaptive Gq signaling in cardiac myocytes in favor of a more nuanced view of compartmentalized Gq-receptor signaling.

A. Conventional model

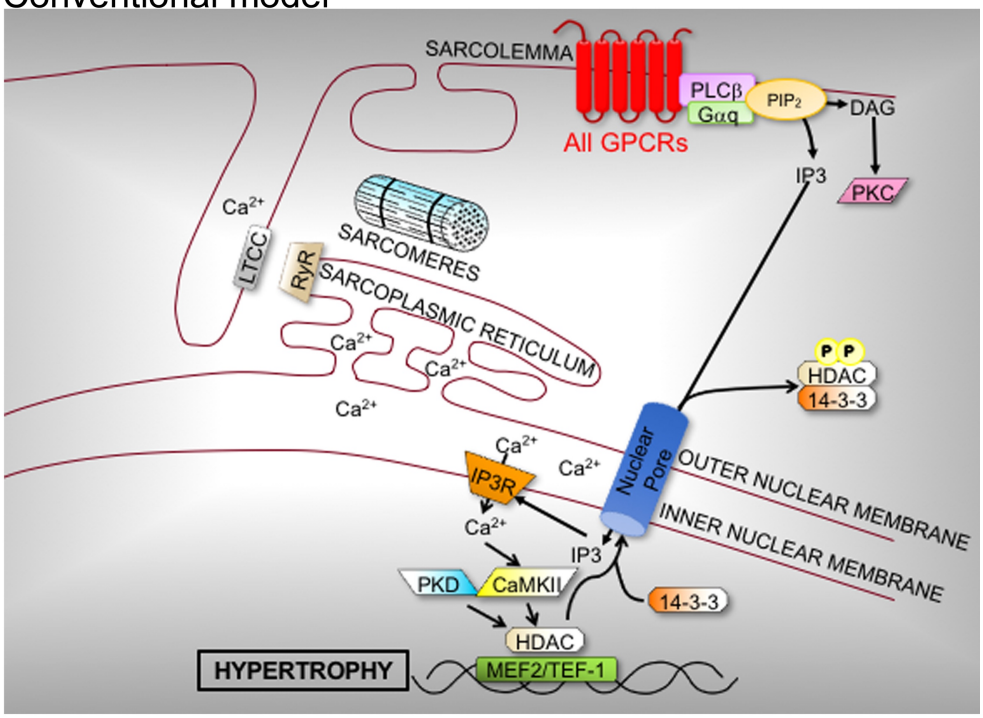

B. Updated model

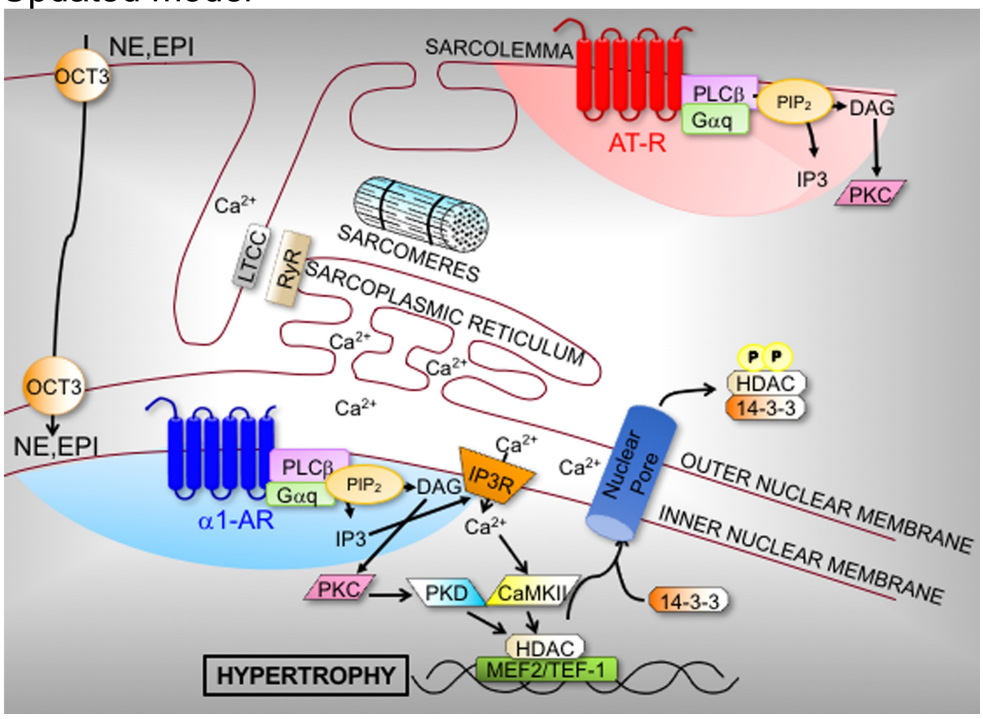

Figure 6.1. Novel model of excitation-transcription coupling in adult cardiac myocytes.

A. *Conventional model of excitation-transcription coupling in adult cardiac myocytes***.** All Gαq-receptors localize to the sarcolemma in adult cardiac myocytes. Upon ligand binding, sarcolemmal PLCβ1 is activated and cleaves PIP_2 into DAG and IP_3. DAG goes on to activate protein kinase C isoforms (PKCs) and induce contraction. IP_3 traverses the myocyte and binds to the IP_3R on the inner nuclear membrane inducing intranuclear calcium release. Calcium activates calmodulin (CaM) and calcium-calmodulin dependent protein kinase II (CaMKII), which phosphorylates HDAC5. HDAC5 phosphorylation triggers HDAC5 nuclear export and de-repression of transcription. **B.** *Updated model of excitation-transcription coupling in adult cardiac myocytes.* α1-ARs (nuclear) and AT-Rs (sarcolemmal) are differentially localized in adult cardiac myocytes (**Figure 2.1**). Upon ligand binding to either α1-ARs or AT-Rs, PLCβ1 is activated either at the nucleus (α1AR, **Figure 3.4**) or at the sarcolemma (AT-R, **Figures 3.3**). AT-R induced PLCβ1 activation at the sarcolemma fails to induce HDAC5 nuclear export, whereas α1AR induced PLCβ1 activation at the nucleus induces HDAC5 nuclear export. Furthermore, α1-AR induced HDAC5 nuclear export is IP_3-dependent (blocked by 2-APB) (**Figure 5.1**). Consistent with α1-induced, IP_3-dependent HDAC5 nuclear export, α1-ARs induce a robust transcriptional response, whereas AT-Rs, which fail to induce HDAC5 export, produce a transcriptional response that is largely a subset of α1-AR induced transcriptional responses (potentially suggesting a different non-HDAC dependent mechanism of transcription) (**Figure 5.2**).

6.2 Future Directions

Receptor Localization Dictates Function

The work presented in this thesis concludes that Gq-receptor localization plays a central role in Gq-receptor function with sarcolemmal Gq-receptors (AT-Rs) being pathologic and nuclear Gq-receptors (α1-ARs) being cardioprotective. Yet, whether nuclear localization of Gq-receptors is required for cardioprotective signaling has not been tested. We hypothesize that adult cardiac myocyte nuclear Gq-receptors are cardioprotective. To test this hypothesis we propose two different strategies: 1) nuclear localization of AT-Rs and 2) nuclear localized DREADD-Gq.

To test the hypothesis that subcellular localization defines Gq-receptor function and that nuclear localization Gq-receptors is cardioprotective, we would drive localization of AT-Rs to the nuclear membrane. To accomplish this, we would create a construct with the AT1R as a backbone and add a 2x-NLS sequence in order to drive nuclear localization, a strategy that we have previously validated. We would focus on the AT1R due to previous work indicating that AT1Rs are the main driver of pathologic remodeling in the heart (196). We would create an adenoviral construct of the nuclear AT1R, express it in AT1R knockout adult cardiac myocytes, activate the receptor using an intracellularly applied AT-R ligand, and study PLCβ1 activation, ERK activation, and hypertrophic transcriptional induction. If our hypothesis is supported, we would expect to see that the nuclear AT1R construct would induce nuclear PLCβ1 activation, perinuclear and cytosolic ERK activation, and induce an HDAC-dependent hypertrophic transcriptome more closely resembling that of α1-ARs. If the hypothesis is not supported and nuclear expression of AT1Rs does not alter their phenotype, then we could conclude that the nuclear localization of Gq-receptors is not sufficient to induce a cardioprotective phenotype in adult cardiac myocytes.

The second strategy to address the hypothesis that nuclear localization of Gq-receptors is cardioprotective is to separate receptor specific effects from the G-protein effects. Experimentally, we would express a nuclear construct of just the Gαq protein called DREADD-Gq in adult cardiac myocytes. DREADDs are designer receptors exclusively activated by designer drugs, whereby the DREADD-Gq receptor is only activated by clozapine-N-oxide (CNO). We would activate the nuclear DREADD-Gq

using CNO and study PLCβ1 activation, ERK activation, and hypertrophic transcriptional induction. If our hypothesis is supported, we would expect to see that the nuclear DREADD-Gq construct would induce nuclear PLCβ1 activation, perinuclear and cytosolic ERK activation, and induce a hypertrophic transcriptome similar to what we see with α1-ARs. If the hypothesis is not supported and nuclear expression of DREADD-Gq does not recapitulate the α1-AR phenotype, then we could conclude that the receptor and not the G-protein is necessary and sufficient to induce a cardioprotective phenotype in adult cardiac myocytes.

Transcriptomics

The current work presented in this thesis included an RNA-Sequencing study that looked at the cardiac myocyte specific effects of either α1-AR or AT-R activation on the hypertrophic transcriptome. This study allowed us to look at the total population of cardiac myocytes and how activation of either the α1-AR or AT-R affected the transcriptional outcome. While useful, recent work in the lab of Dr. Paul Simpson indicated that not all adult cardiac myocytes express the α1A-AR, with only about 60% of myocytes expressing the receptor. This result was further supported by our work with EKAR where we saw ERK activation downstream of α1-ARs in about two-thirds of the myocytes. Thus, future work to understand receptor expression in individual cardiac myocytes may begin to explain the physiologic responses we see including ERK activation and transcriptional responses. In order to begin to uncover these potential differences in cardiac myocyte expression of AT-Rs, we would undertake single cell transcriptomics. We would isolate adult cardiac myocytes and sort them using flow cytometry into single cell suspensions, we would then isolate the RNA on a single cell basis, and perform transcriptomics. We expect to see similar results as the α1-AR study with not all cardiac myocytes expressing AT-Rs or not all cardiac myocytes expressing AT-Rs in similar amounts. This result would allow us to then correlate AT-R expression with ERK activation and transcriptional activation and further our understanding of how receptor expression effects signal transduction in adult cardiac myocytes.

ET-Rs: The other Gq-Receptor

The work presented in this thesis focused solely on two prototypical Gq-receptors: AT-Rs and α1-ARs. Yet in adult cardiac myocytes, there is another Gq-receptor that is

expressed: the endothelin receptor (ET-R). While AT-Rs and α1-ARs have seemingly opposed effects in adult cardiac myocytes with AT-Rs being pathologic and α1-ARs being cardioprotective, ET-Rs fall somewhere in the middle. Previous work with ET-Rs using radioligand-binding on fractionated adult cardiac myocytes indicates that ETR levels are half that of α1-ARs, and identifies 95% of endogenous ETRs at the plasma membrane, with 5% of endogenous ETRs in the nuclear fraction (71, 81{Boivin, 2003 #2613). Further work using a fluorescent endothelin (ET), the ligand for ET-Rs, localized ET-Rs to the bottom of the t-tubules in adult cardiac myocytes, and blocking ET access to t-tubules prevented ET-R signaling (187). These lines of evidence indicate that ET-Rs do not localize to the surface of the sarcolemma like AT-Rs, and that ET-Rs also do not primarily localize to the nuclear membrane like α1-ARs but localize in a separate compartment in adult cardiac myocytes. ET-R effects on the adult cardiac myocyte are mixed, in cultured cardiac myocytes, ETRs promote survival and positive inotropy (85). In mice, ET overexpression induces HF (197), but ETR KO mice show less consistent results, with global KO inducing embryonic lethality (148-150), and cardiac-specific KO suggesting direct and indirect effects to induce HF (198). In humans, ETR antagonists show no benefit in acute or chronic HF (199). Thus, further work needs to be completed to understand how ET-Rs compartmentalized signaling in adult cardiac myocytes.

In context of the signaling paradigm presented in this thesis, we hypothesize that ET-Rs will share some aspects of AT-Rs (localization, PLCβ1 activation) and will also share some aspects of α1-ARs (ERK activation, hypertrophic transcriptome). To address this hypothesis, we will activate endogenous ET-Rs in adult cardiac myocytes with ET and study their localized activation of PLCβ1, ERK, and hypertrophic transcriptome. If our hypothesis is supported, we would expect to see that endogenous ET-Rs would induce sarcolemmal and nuclear PLCβ1 activation due to their close proximity to the nuclear membrane, perinuclear and cytosolic ERK activation, and induce a hypertrophic transcriptome that overlaps both AT-Rs and α1-ARs. This experiment will allow us to further define the compartmentalization of Gq-signaling in adult cardiac myocytes.

Bibliography

1. Kobilka BK, and Deupi X. Conformational complexity of G-protein-coupled receptors. *Trends Pharmacol Sci.* 2007;28(8):397-406.
2. Rosenbaum DM, Rasmussen SG, and Kobilka BK. The structure and function of G-protein-coupled receptors. *Nature.* 2009;459(7245):356-63.
3. Fredriksson R, Lagerstrom MC, Lundin LG, and Schioth HB. The G-protein-coupled receptors in the human genome form five main families. Phylogenetic analysis, paralogon groups, and fingerprints. *Mol Pharmacol.* 2003;63(6):1256-72.
4. Boivin B, Vaniotis G, Allen BG, and Hebert TE. G protein-coupled receptors in and on the cell nucleus: a new signaling paradigm? *J Recept Signal Transduct Res.* 2008;28(1-2):15-28.
5. Ussher JR, Baggio LL, Campbell JE, Mulvihill EE, Kim M, Kabir MG, et al. Inactivation of the cardiomyocyte glucagon-like peptide-1 receptor (GLP-1R) unmasks cardiomyocyte-independent GLP-1R-mediated cardioprotection. *Mol Metab.* 2014;3(5):507-17.
6. Ali S, Ussher JR, Baggio LL, Kabir MG, Charron MJ, Ilkayeva O, et al. Cardiomyocyte glucagon receptor signaling modulates outcomes in mice with experimental myocardial infarction. *Mol Metab.* 2015;4(2):132-43.
7. Lorente P, Lacampagne A, Pouzeratte Y, Richards S, Malitschek B, Kuhn R, et al. gamma-aminobutyric acid type B receptors are expressed and functional in mammalian cardiomyocytes. *Proc Natl Acad Sci U S A.* 2000;97(15):8664-9.
8. Nechiporuk T, Urness LD, and Keating MT. ETL, a novel seven-transmembrane receptor that is developmentally regulated in the heart. ETL is a member of the secretin family and belongs to the epidermal growth factor-seven-transmembrane subfamily. *J Biol Chem.* 2001;276(6):4150-7.
9. Shiratsuchi T, Nishimori H, Ichise H, Nakamura Y, and Tokino T. Cloning and characterization of BAI2 and BAI3, novel genes homologous to brain-specific angiogenesis inhibitor 1 (BAI1). *Cytogenet Cell Genet.* 1997;79(1-2):103-8.
10. Foster SR, Blank K, See Hoe LE, Behrens M, Meyerhof W, Peart JN, et al. Bitter taste receptor agonists elicit G-protein-dependent negative inotropy in the murine heart. *FASEB J.* 2014;28(10):4497-508.
11. Neves SR, Ram PT, and Iyengar R. G protein pathways. *Science.* 2002;296(5573):1636-9.
12. Madamanchi A. Beta-adrenergic receptor signaling in cardiac function and heart failure. *Mcgill J Med.* 2007;10(2):99-104.
13. Mustafa SJ, Morrison RR, Teng B, and Pelleg A. Adenosine receptors and the heart: role in regulation of coronary blood flow and cardiac electrophysiology. *Handb Exp Pharmacol.* 2009(193):161-88.
14. O'Connell TD, Jensen BC, Baker AJ, and Simpson PC. Cardiac alpha1-adrenergic receptors: novel aspects of expression, signaling mechanisms, physiologic function, and clinical importance. *Pharmacol Rev.* 2014;66(1):308-33.
15. Siehler S. Regulation of RhoGEF proteins by G12/13-coupled receptors. *Br J Pharmacol.* 2009;158(1):41-9.
16. Singh RM, Cummings E, Pantos C, and Singh J. Protein kinase C and cardiac dysfunction: a review. *Heart Fail Rev.* 2017;22(6):843-59.
17. Rhee SG. Regulation of phosphoinositide-specific phospholipase C. *Annu Rev Biochem.* 2001;70:281-312.

18. Saunders CM, Larman MG, Parrington J, Cox LJ, Royse J, Blayney LM, et al. PLC zeta: a sperm-specific trigger of Ca(2+) oscillations in eggs and embryo development. *Development.* 2002;129(15):3533-44.
19. Hwang JI, Oh YS, Shin KJ, Kim H, Ryu SH, and Suh PG. Molecular cloning and characterization of a novel phospholipase C, PLC-eta. *Biochem J.* 2005;389(Pt 1):181-6.
20. Tappia PS, Liu SY, Shatadal S, Takeda N, Dhalla NS, and Panagia V. Changes in sarcolemmal PLC isoenzymes in postinfarct congestive heart failure: partial correction by imidapril. *Am J Physiol.* 1999;277(1 Pt 2):H40-9.
21. Wolf RA. Association of phospholipase C-delta with a highly enriched preparation of canine sarcolemma. *Am J Physiol.* 1992;263(5 Pt 1):C1021-8.
22. Wang H, Oestreich EA, Maekawa N, Bullard TA, Vikstrom KL, Dirksen RT, et al. Phospholipase C epsilon modulates beta-adrenergic receptor-dependent cardiac contraction and inhibits cardiac hypertrophy. *Circ Res.* 2005;97(12):1305-13.
23. Arthur JF, Matkovich SJ, Mitchell CJ, Biden TJ, and Woodcock EA. Evidence for selective coupling of alpha 1-adrenergic receptors to phospholipase C-beta 1 in rat neonatal cardiomyocytes. *J Biol Chem.* 2001;276(40):37341-6.
24. Meij JT. Regulation of G protein function: implications for heart disease. *Mol Cell Biochem.* 1996;157(1-2):31-8.
25. Bahk YY, Lee YH, Lee TG, Seo J, Ryu SH, and Suh PG. Two forms of phospholipase C-beta 1 generated by alternative splicing. *J Biol Chem.* 1994;269(11):8240-5.
26. Grubb DR, Iliades P, Cooley N, Yu YL, Luo J, Filtz TM, et al. Phospholipase Cbeta1b associates with a Shank3 complex at the cardiac sarcolemma. *FASEB J.* 2011;25(3):1040-7.
27. Grubb DR, Crook B, Ma Y, Luo J, Qian HW, Gao XM, et al. The atypical 'b' splice variant of phospholipase Cbeta1 promotes cardiac contractile dysfunction. *J Mol Cell Cardiol.* 2015;84:95-103.
28. Wright CD, Chen Q, Baye NL, Huang Y, Healy CL, Kasinathan S, et al. Nuclear alpha1-adrenergic receptors signal activated ERK localization to caveolae in adult cardiac myocytes. *Circ Res.* 2008;103(9):992-1000.
29. Woodcock EA, Du XJ, Reichelt ME, and Graham RM. Cardiac alpha 1-adrenergic drive in pathological remodelling. *Cardiovasc Res.* 2008;77(3):452-62.
30. Czech MP. PIP2 and PIP3: complex roles at the cell surface. *Cell.* 2000;100(6):603-6.
31. Stauffer TP, Ahn S, and Meyer T. Receptor-induced transient reduction in plasma membrane PtdIns(4,5)P2 concentration monitored in living cells. *Curr Biol.* 1998;8(6):343-6.
32. Zhang L, Malik S, Pang J, Wang H, Park KM, Yule DI, et al. Phospholipase cepsilon hydrolyzes perinuclear phosphatidylinositol 4-phosphate to regulate cardiac hypertrophy. *Cell.* 2013;153(1):216-27.
33. Cho H, Kim YA, Yoon JY, Lee D, Kim JH, Lee SH, et al. Low mobility of phosphatidylinositol 4,5-bisphosphate underlies receptor specificity of Gq-mediated ion channel regulation in atrial myocytes. *Proc Natl Acad Sci U S A.* 2005;102(42):15241-6.
34. Carrasco S, and Merida I. Diacylglycerol, when simplicity becomes complex. *Trends Biochem Sci.* 2007;32(1):27-36.

35. Takeishi Y, Goto K, and Kubota I. Role of diacylglycerol kinase in cellular regulatory processes: a new regulator for cardiomyocyte hypertrophy. *Pharmacol Ther.* 2007;115(3):352-9.
36. Yang C, and Kazanietz MG. Divergence and complexities in DAG signaling: looking beyond PKC. *Trends Pharmacol Sci.* 2003;24(11):602-8.
37. Puceat M, Hilal-Dandan R, Strulovici B, Brunton LL, and Brown JH. Differential regulation of protein kinase C isoforms in isolated neonatal and adult rat cardiomyocytes. *J Biol Chem.* 1994;269(24):16938-44.
38. Steinberg SF. Cardiac actions of protein kinase C isoforms. *Physiology (Bethesda).* 2012;27(3):130-9.
39. Leung E, Johnston CI, and Woodcock EA. Stimulation of phosphatidylinositol metabolism in atrial and ventricular myocytes. *Life Sci.* 1986;39(23):2215-20.
40. Hund TJ, Ziman AP, Lederer WJ, and Mohler PJ. The cardiac IP3 receptor: uncovering the role of "the other" calcium-release channel. *J Mol Cell Cardiol.* 2008;45(2):159-61.
41. Zima AV, and Blatter LA. Inositol-1,4,5-trisphosphate-dependent Ca(2+) signalling in cat atrial excitation-contraction coupling and arrhythmias. *J Physiol.* 2004;555(Pt 3):607-15.
42. Bare DJ, Kettlun CS, Liang M, Bers DM, and Mignery GA. Cardiac type 2 inositol 1,4,5-trisphosphate receptor: interaction and modulation by calcium/calmodulin-dependent protein kinase II. *J Biol Chem.* 2005;280(16):15912-20.
43. Wu X, Zhang T, Bossuyt J, Li X, McKinsey TA, Dedman JR, et al. Local InsP3-dependent perinuclear Ca2+ signaling in cardiac myocyte excitation-transcription coupling. *J Clin Invest.* 2006;116(3):675-82.
44. Dewenter M, von der Lieth A, Katus HA, and Backs J. Calcium Signaling and Transcriptional Regulation in Cardiomyocytes. *Circ Res.* 2017;121(8):1000-20.
45. Bogoyevitch MA, Glennon PE, Andersson MB, Clerk A, Lazou A, Marshall CJ, et al. Endothelin-1 and fibroblast growth factors stimulate the mitogen-activated protein kinase signaling cascade in cardiac myocytes. The potential role of the cascade in the integration of two signaling pathways leading to myocyte hypertrophy. *J Biol Chem.* 1994;269(2):1110-9.
46. Bogoyevitch MA, Glennon PE, and Sugden PH. Endothelin-1, phorbol esters and phenylephrine stimulate MAP kinase activities in ventricular cardiomyocytes. *FEBS Lett.* 1993;317(3):271-5.
47. Bogoyevitch MA, Ketterman AJ, and Sugden PH. Cellular stresses differentially activate c-Jun N-terminal protein kinases and extracellular signal-regulated protein kinases in cultured ventricular myocytes. *J Biol Chem.* 1995;270(50):29710-7.
48. Clerk A, Bogoyevitch MA, Anderson MB, and Sugden PH. Differential activation of protein kinase C isoforms by endothelin-1 and phenylephrine and subsequent stimulation of p42 and p44 mitogen-activated protein kinases in ventricular myocytes cultured from neonatal rat hearts. *J Biol Chem.* 1994;269(52):32848-57.
49. Sugden PH, and Clerk A. "Stress-responsive" mitogen-activated protein kinases (c-Jun N-terminal kinases and p38 mitogen-activated protein kinases) in the myocardium. *Circ Res.* 1998;83(4):345-52.
50. Cohen P. The search for physiological substrates of MAP and SAP kinases in mammalian cells. *Trends Cell Biol.* 1997;7(9):353-61.

51. Garrington TP, and Johnson GL. Organization and regulation of mitogen-activated protein kinase signaling pathways. *Curr Opin Cell Biol.* 1999;11(2):211-8.
52. Braz JC, Bueno OF, De Windt LJ, and Molkentin JD. PKC alpha regulates the hypertrophic growth of cardiomyocytes through extracellular signal-regulated kinase1/2 (ERK1/2). *J Cell Biol.* 2002;156(5):905-19.
53. Bueno OF, De Windt LJ, Tymitz KM, Witt SA, Kimball TR, Klevitsky R, et al. The MEK1-ERK1/2 signaling pathway promotes compensated cardiac hypertrophy in transgenic mice. *Embo J.* 2000;19(23):6341-50.
54. Sanna B, Bueno OF, Dai YS, Wilkins BJ, and Molkentin JD. Direct and indirect interactions between calcineurin-NFAT and MEK1-extracellular signal-regulated kinase 1/2 signaling pathways regulate cardiac gene expression and cellular growth. *Mol Cell Biol.* 2005;25(3):865-78.
55. Liang Q, Wiese RJ, Bueno OF, Dai YS, Markham BE, and Molkentin JD. The transcription factor GATA4 is activated by extracellular signal-regulated kinase 1- and 2-mediated phosphorylation of serine 105 in cardiomyocytes. *Mol Cell Biol.* 2001;21(21):7460-9.
56. Huang Y, Wright CD, Merkwan CL, Baye NL, Liang Q, Simpson PC, et al. An alpha1A-adrenergic-extracellular signal-regulated kinase survival signaling pathway in cardiac myocytes. *Circulation.* 2007;115(6):763-72.
57. Lefkowitz RJ. G protein-coupled receptors. III. New roles for receptor kinases and beta-arrestins in receptor signaling and desensitization. *J Biol Chem.* 1998;273(30):18677-80.
58. Magalhaes AC, Dunn H, and Ferguson SS. Regulation of GPCR activity, trafficking and localization by GPCR-interacting proteins. *Br J Pharmacol.* 2012;165(6):1717-36.
59. Touhara K, Inglese J, Pitcher JA, Shaw G, and Lefkowitz RJ. Binding of G protein beta gamma-subunits to pleckstrin homology domains. *J Biol Chem.* 1994;269(14):10217-20.
60. Pitcher JA, Touhara K, Payne ES, and Lefkowitz RJ. Pleckstrin homology domain-mediated membrane association and activation of the beta-adrenergic receptor kinase requires coordinate interaction with G beta gamma subunits and lipid. *J Biol Chem.* 1995;270(20):11707-10.
61. Sato PY, Chuprun JK, Schwartz M, and Koch WJ. The evolving impact of g protein-coupled receptor kinases in cardiac health and disease. *Physiol Rev.* 2015;95(2):377-404.
62. Diviani D, Lattion AL, Larbi N, Kunapuli P, Pronin A, Benovic JL, et al. Effect of different G protein-coupled receptor kinases on phosphorylation and desensitization of the alpha1B-adrenergic receptor. *J Biol Chem.* 1996;271(9):5049-58.
63. Stanasila L, Abuin L, Dey J, and Cotecchia S. Different internalization properties of the alpha1a- and alpha1b-adrenergic receptor subtypes: the potential role of receptor interaction with beta-arrestins and AP50. *Mol Pharmacol.* 2008;74(3):562-73.
64. Gartner F, Seidel T, Schulz U, Gummert J, and Milting H. Desensitization and internalization of endothelin receptor A: impact of G protein-coupled receptor kinase 2 (GRK2)-mediated phosphorylation. *J Biol Chem.* 2013;288(45):32138-48.

65. Rockman HA, Choi DJ, Rahman NU, Akhter SA, Lefkowitz RJ, and Koch WJ. Receptor-specific in vivo desensitization by the G protein-coupled receptor kinase-5 in transgenic mice. *Proc Natl Acad Sci U S A.* 1996;93(18):9954-9.
66. Poupart ME, Fessart D, Cotton M, Laporte SA, and Claing A. ARF6 regulates angiotensin II type 1 receptor endocytosis by controlling the recruitment of AP-2 and clathrin. *Cell Signal.* 2007;19(11):2370-8.
67. Tarigopula M, Davis RT, 3rd, Mungai PT, Ryba DM, Wieczorek DF, Cowan CL, et al. Cardiac myosin light chain phosphorylation and inotropic effects of a biased ligand, TRV120023, in a dilated cardiomyopathy model. *Cardiovasc Res.* 2015;107(2):226-34.
68. Branco AF, and Allen BG. G protein-coupled receptor signaling in cardiac nuclear membranes. *J Cardiovasc Pharmacol.* 2015;65(2):101-9.
69. Tadevosyan A, Maguy A, Villeneuve LR, Babin J, Bonnefoy A, Allen BG, et al. Nuclear-delimited angiotensin receptor-mediated signaling regulates cardiomyocyte gene expression. *J Biol Chem.* 2010;285(29):22338-49.
70. Fu ML, Schulze W, Wallukat G, Elies R, Eftekhari P, Hjalmarson A, et al. Immunohistochemical localization of angiotensin II receptors (AT1) in the heart with anti-peptide antibodies showing a positive chronotropic effect. *Receptors Channels.* 1998;6(2):99-111.
71. Boivin B, Chevalier D, Villeneuve LR, Rousseau E, and Allen BG. Functional endothelin receptors are present on nuclei in cardiac ventricular myocytes. *J Biol Chem.* 2003;278(31):29153-63.
72. Boivin B, Lavoie C, Vaniotis G, Baragli A, Villeneuve LR, Ethier N, et al. Functional beta-adrenergic receptor signalling on nuclear membranes in adult rat and mouse ventricular cardiomyocytes. *Cardiovasc Res.* 2006;71(1):69-78.
73. Wu SC, and O'Connell TD. Nuclear compartmentalization of alpha1-adrenergic receptor signaling in adult cardiac myocytes. *J Cardiovasc Pharmacol.* 2015;65(2):91-100.
74. Lange A, Mills RE, Lange CJ, Stewart M, Devine SE, and Corbett AH. Classical nuclear localization signals: definition, function, and interaction with importin alpha. *J Biol Chem.* 2007;282(8):5101-5.
75. Radu A, Blobel G, and Moore MS. Identification of a protein complex that is required for nuclear protein import and mediates docking of import substrate to distinct nucleoporins. *Proc Natl Acad Sci U S A.* 1995;92(5):1769-73.
76. Kalderon D, Richardson WD, Markham AF, and Smith AE. Sequence requirements for nuclear location of simian virus 40 large-T antigen. *Nature.* 1984;311(5981):33-8.
77. Robbins J, Dilworth SM, Laskey RA, and Dingwall C. Two interdependent basic domains in nucleoplasmin nuclear targeting sequence: identification of a class of bipartite nuclear targeting sequence. *Cell.* 1991;64(3):615-23.
78. Gilchrist D, and Rexach M. Molecular basis for the rapid dissociation of nuclear localization signals from karyopherin alpha in the nucleoplasm. *J Biol Chem.* 2003;278(51):51937-49.
79. Wickner WT, and Lodish HF. Multiple mechanisms of protein insertion into and across membranes. *Science.* 1985;230(4724):400-7.
80. Zuleger N, Kerr AR, and Schirmer EC. Many mechanisms, one entrance: membrane protein translocation into the nucleus. *Cellular and molecular life sciences : CMLS.* 2012;69(13):2205-16.

81. Wright CD, Wu SC, Dahl EF, Sazama AJ, and O'Connell TD. Nuclear localization drives alpha1-adrenergic receptor oligomerization and signaling in cardiac myocytes. *Cell Signal.* 2012;24:794-802.
82. Morinelli TA, Raymond JR, Baldys A, Yang Q, Lee MH, Luttrell L, et al. Identification of a putative nuclear localization sequence within ANG II AT(1A) receptor associated with nuclear activation. *Am J Physiol Cell Physiol.* 2007;292(4):C1398-408.
83. Kosugi S, Hasebe M, Tomita M, and Yanagawa H. Systematic identification of cell cycle-dependent yeast nucleocytoplasmic shuttling proteins by prediction of composite motifs. *Proc Natl Acad Sci U S A.* 2009;106(25):10171-6.
84. Singh VP, Le B, Bhat VB, Baker KM, and Kumar R. High-glucose-induced regulation of intracellular ANG II synthesis and nuclear redistribution in cardiac myocytes. *Am J Physiol Heart Circ Physiol.* 2007;293(2):H939-48.
85. Sugden PH. An overview of endothelin signaling in the cardiac myocyte. *J Mol Cell Cardiol.* 2003;35(8):871-86.
86. Yanagisawa M, Kurihara H, Kimura S, Tomobe Y, Kobayashi M, Mitsui Y, et al. A novel potent vasoconstrictor peptide produced by vascular endothelial cells. *Nature.* 1988;332(6163):411-5.
87. Fabbrini MS, Valsasina B, Nitti G, Benatti L, and Vitale A. The signal peptide of human preproendothelin-1. *FEBS Lett.* 1991;286(1-2):91-4.
88. Blais V, Fugere M, Denault JB, Klarskov K, Day R, and Leduc R. Processing of proendothelin-1 by members of the subtilisin-like pro-protein convertase family. *FEBS Lett.* 2002;524(1-3):43-8.
89. Shimada K, Matsushita Y, Wakabayashi K, Takahashi M, Matsubara A, Iijima Y, et al. Cloning and functional expression of human endothelin-converting enzyme cDNA. *Biochem Biophys Res Commun.* 1995;207(2):807-12.
90. Stow LR, Jacobs ME, Wingo CS, and Cain BD. Endothelin-1 gene regulation. *FASEB J.* 2011;25(1):16-28.
91. Thomas PB, Liu EC, Webb ML, Mukherjee R, Hebbar L, and Spinale FG. Exogenous effects and endogenous production of endothelin in cardiac myocytes: potential significance in heart failure. *Am J Physiol.* 1996;271(6 Pt 2):H2629-37.
92. Campden R, Audet N, and Hebert TE. Nuclear G protein signaling: new tricks for old dogs. *J Cardiovasc Pharmacol.* 2015;65(2):110-22.
93. Martelli AM, Gilmour RS, Bertagnolo V, Neri LM, Manzoli L, and Cocco L. Nuclear localization and signalling activity of phosphoinositidase C beta in Swiss 3T3 cells. *Nature.* 1992;358(6383):242-5.
94. Divecha N, Rhee SG, Letcher AJ, and Irvine RF. Phosphoinositide signalling enzymes in rat liver nuclei: phosphoinositidase C isoform beta 1 is specifically, but not predominantly, located in the nucleus. *Biochem J.* 1993;289 (Pt 3):617-20.
95. Mazzoni M, Bertagnolo V, Neri LM, Carini C, Marchisio M, Milani D, et al. Discrete subcellular localization of phosphoinositidase C beta, gamma and delta in PC12 rat pheochromocytoma cells. *Biochem Biophys Res Commun.* 1992;187(1):114-20.
96. Arantes LA, Aguiar CJ, Amaya MJ, Figueiro NC, Andrade LM, Rocha-Resende C, et al. Nuclear inositol 1,4,5-trisphosphate is a necessary and conserved signal for the induction of both pathological and physiological cardiomyocyte hypertrophy. *J Mol Cell Cardiol.* 2012;53(4):475-86.

97. Luo D, Yang D, Lan X, Li K, Li X, Chen J, et al. Nuclear Ca2+ sparks and waves mediated by inositol 1,4,5-trisphosphate receptors in neonatal rat cardiomyocytes. *Cell Calcium.* 2008;43(2):165-74.
98. Zima AV, Bare DJ, Mignery GA, and Blatter LA. IP3-dependent nuclear Ca2+ signalling in the mammalian heart. *J Physiol.* 2007;584(Pt 2):601-11.
99. Vetter SW, and Leclerc E. Novel aspects of calmodulin target recognition and activation. *Eur J Biochem.* 2003;270(3):404-14.
100. Rosenberg OS, Deindl S, Sung RJ, Nairn AC, and Kuriyan J. Structure of the autoinhibited kinase domain of CaMKII and SAXS analysis of the holoenzyme. *Cell.* 2005;123(5):849-60.
101. Mollova MY, Katus HA, and Backs J. Regulation of CaMKII signaling in cardiovascular disease. *Front Pharmacol.* 2015;6:178.
102. Gray CB, and Heller Brown J. CaMKIIdelta subtypes: localization and function. *Front Pharmacol.* 2014;5:15.
103. Schworer CM, Rothblum LI, Thekkumkara TJ, and Singer HA. Identification of novel isoforms of the delta subunit of Ca2+/calmodulin-dependent protein kinase II. Differential expression in rat brain and aorta. *J Biol Chem.* 1993;268(19):14443-9.
104. Srinivasan M, and Begum N. Regulation of protein phosphatase 1 and 2A activities by insulin during myogenesis in rat skeletal muscle cells in culture. *J Biol Chem.* 1994;269(17):12514-20.
105. Zhang T, Kohlhaas M, Backs J, Mishra S, Phillips W, Dybkova N, et al. CaMKIIdelta isoforms differentially affect calcium handling but similarly regulate HDAC/MEF2 transcriptional responses. *J Biol Chem.* 2007;282(48):35078-87.
106. Zhu W, Zou Y, Shiojima I, Kudoh S, Aikawa R, Hayashi D, et al. Ca2+/calmodulin-dependent kinase II and calcineurin play critical roles in endothelin-1-induced cardiomyocyte hypertrophy. *J Biol Chem.* 2000;275(20):15239-45.
107. Sei CA, Irons CE, Sprenkle AB, McDonough PM, Brown JH, and Glembotski CC. The a-adrenergic stimulation of atrial natriuretic factor expression in cardiac myocytes requires calcium influx, protein kinase C, and calmodulin-regulated pathways. *J Biol Chem.* 1991;266(24):15910-6.
108. Sucharov CC, Mariner PD, Nunley KR, Long C, Leinwand L, and Bristow MR. A beta1-adrenergic receptor CaM kinase II-dependent pathway mediates cardiac myocyte fetal gene induction. *Am J Physiol Heart Circ Physiol.* 2006;291(3):H1299-308.
109. Valverde AM, Sinnett-Smith J, Van Lint J, and Rozengurt E. Molecular cloning and characterization of protein kinase D: a target for diacylglycerol and phorbol esters with a distinctive catalytic domain. *Proc Natl Acad Sci U S A.* 1994;91(18):8572-6.
110. Avkiran M, Rowland AJ, Cuello F, and Haworth RS. Protein kinase d in the cardiovascular system: emerging roles in health and disease. *Circ Res.* 2008;102(2):157-63.
111. Johannes FJ, Prestle J, Eis S, Oberhagemann P, and Pfizenmaier K. PKCu is a novel, atypical member of the protein kinase C family. *J Biol Chem.* 1994;269(8):6140-8.
112. Harrison BC, Kim MS, van Rooij E, Plato CF, Papst PJ, Vega RB, et al. Regulation of cardiac stress signaling by protein kinase d1. *Mol Cell Biol.* 2006;26(10):3875-88.

113. Roberts NA, Haworth RS, and Avkiran M. Effects of bisindolylmaleimide PKC inhibitors on p90RSK activity in vitro and in adult ventricular myocytes. *Br J Pharmacol.* 2005;145(4):477-89.
114. Haworth RS, Cuello F, Herron TJ, Franzen G, Kentish JC, Gautel M, et al. Protein kinase D is a novel mediator of cardiac troponin I phosphorylation and regulates myofilament function. *Circ Res.* 2004;95(11):1091-9.
115. Vega RB, Harrison BC, Meadows E, Roberts CR, Papst PJ, Olson EN, et al. Protein kinases C and D mediate agonist-dependent cardiac hypertrophy through nuclear export of histone deacetylase 5. *Mol Cell Biol.* 2004;24(19):8374-85.
116. Bers DM. Ca(2)(+)-calmodulin-dependent protein kinase II regulation of cardiac excitation-transcription coupling. *Heart Rhythm.* 2011;8(7):1101-4.
117. Hallhuber M, Burkard N, Wu R, Buch MH, Engelhardt S, Hein L, et al. Inhibition of nuclear import of calcineurin prevents myocardial hypertrophy. *Circ Res.* 2006;99(6):626-35.
118. Okamura H, Aramburu J, Garcia-Rodriguez C, Viola JP, Raghavan A, Tahiliani M, et al. Concerted dephosphorylation of the transcription factor NFAT1 induces a conformational switch that regulates transcriptional activity. *Mol Cell.* 2000;6(3):539-50.
119. Wilkins BJ, Dai YS, Bueno OF, Parsons SA, Xu J, Plank DM, et al. Calcineurin/NFAT coupling participates in pathological, but not physiological, cardiac hypertrophy. *Circ Res.* 2004;94(1):110-8.
120. Molkentin JD, Lu JR, Antos CL, Markham B, Richardson J, Robbins J, et al. A calcineurin-dependent transcriptional pathway for cardiac hypertrophy. *Cell.* 1998;93(2):215-28.
121. Belmonte SL, and Blaxall BC. G protein coupled receptor kinases as therapeutic targets in cardiovascular disease. *Circ Res.* 2011;109(3):309-19.
122. Dorn GW, 2nd. GRK mythology: G-protein receptor kinases in cardiovascular disease. *J Mol Med (Berl).* 2009;87(5):455-63.
123. Kunapuli P, and Benovic JL. Cloning and expression of GRK5: a member of the G protein-coupled receptor kinase family. *Proc Natl Acad Sci U S A.* 1993;90(12):5588-92.
124. Dzimiri N, Muiya P, Andres E, and Al-Halees Z. Differential functional expression of human myocardial G protein receptor kinases in left ventricular cardiac diseases. *Eur J Pharmacol.* 2004;489(3):167-77.
125. Vinge LE, Andressen KW, Attramadal T, Andersen GO, Ahmed MS, Peppel K, et al. Substrate specificities of g protein-coupled receptor kinase-2 and -3 at cardiac myocyte receptors provide basis for distinct roles in regulation of myocardial function. *Mol Pharmacol.* 2007;72(3):582-91.
126. Kim J, Ahn S, Ren XR, Whalen EJ, Reiter E, Wei H, et al. Functional antagonism of different G protein-coupled receptor kinases for beta-arrestin-mediated angiotensin II receptor signaling. *Proc Natl Acad Sci U S A.* 2005;102(5):1442-7.
127. Yi XP, Gerdes AM, and Li F. Myocyte redistribution of GRK2 and GRK5 in hypertensive, heart-failure-prone rats. *Hypertension.* 2002;39(6):1058-63.
128. Yi XP, Zhou J, Baker J, Wang X, Gerdes AM, and Li F. Myocardial expression and redistribution of GRKs in hypertensive hypertrophy and failure. *Anat Rec A Discov Mol Cell Evol Biol.* 2005;282(1):13-23.
129. Johnson LR, Scott MG, and Pitcher JA. G protein-coupled receptor kinase 5 contains a DNA-binding nuclear localization sequence. *Mol Cell Biol.* 2004;24(23):10169-79.

130. Martini JS, Raake P, Vinge LE, DeGeorge BR, Jr., Chuprun JK, Harris DM, et al. Uncovering G protein-coupled receptor kinase-5 as a histone deacetylase kinase in the nucleus of cardiomyocytes. *Proc Natl Acad Sci U S A.* 2008;105(34):12457-62.
131. Galasinski SC, Resing KA, Goodrich JA, and Ahn NG. Phosphatase inhibition leads to histone deacetylases 1 and 2 phosphorylation and disruption of corepressor interactions. *J Biol Chem.* 2002;277(22):19618-26.
132. Gold JI, Martini JS, Hullmann J, Gao E, Chuprun JK, Lee L, et al. Nuclear translocation of cardiac G protein-Coupled Receptor kinase 5 downstream of select Gq-activating hypertrophic ligands is a calmodulin-dependent process. *PLoS One.* 2013;8(3):e57324.
133. Lefkowitz RJ, and Shenoy SK. Transduction of receptor signals by beta-arrestins. *Science.* 2005;308(5721):512-7.
134. Patel PA, Tilley DG, and Rockman HA. Physiologic and cardiac roles of beta-arrestins. *J Mol Cell Cardiol.* 2009;46(3):300-8.
135. Nelson CD, Perry SJ, Regier DS, Prescott SM, Topham MK, and Lefkowitz RJ. Targeting of diacylglycerol degradation to M1 muscarinic receptors by beta-arrestins. *Science.* 2007;315(5812):663-6.
136. Perry SJ, Baillie GS, Kohout TA, McPhee I, Magiera MM, Ang KL, et al. Targeting of cyclic AMP degradation to beta 2-adrenergic receptors by beta-arrestins. *Science.* 2002;298(5594):834-6.
137. Wei H, Ahn S, Shenoy SK, Karnik SS, Hunyady L, Luttrell LM, et al. Independent beta-arrestin 2 and G protein-mediated pathways for angiotensin II activation of extracellular signal-regulated kinases 1 and 2. *Proc Natl Acad Sci U S A.* 2003;100(19):10782-7.
138. Ma L, and Pei G. Beta-arrestin signaling and regulation of transcription. *J Cell Sci.* 2007;120(Pt 2):213-8.
139. Kang J, Shi Y, Xiang B, Qu B, Su W, Zhu M, et al. A nuclear function of beta-arrestin1 in GPCR signaling: regulation of histone acetylation and gene transcription. *Cell.* 2005;123(5):833-47.
140. Berthouze-Duquesnes M, Lucas A, Sauliere A, Sin YY, Laurent AC, Gales C, et al. Specific interactions between Epac1, beta-arrestin2 and PDE4D5 regulate beta-adrenergic receptor subtype differential effects on cardiac hypertrophic signaling. *Cell Signal.* 2013;25(4):970-80.
141. Bkaily G, Avedanian L, and Jacques D. Nuclear membrane receptors and channels as targets for drug development in cardiovascular diseases. *Can J Physiol Pharmacol.* 2009;87(2):108-19.
142. Vaniotis G, Glazkova I, Merlen C, Smith C, Villeneuve LR, Chatenet D, et al. Regulation of cardiac nitric oxide signaling by nuclear beta-adrenergic and endothelin receptors. *J Mol Cell Cardiol.* 2013;62C:58-68.
143. Chrysant SG. Angiotensin II receptor blockers in the treatment of the cardiovascular disease continuum. *Clin Ther.* 2008;30 Pt 2:2181-90.
144. Harada K, Sugaya T, Murakami K, Yazaki Y, and Komuro I. Angiotensin II type 1A receptor knockout mice display less left ventricular remodeling and improved survival after myocardial infarction [see comments]. *Circulation.* 1999;100(20):2093-9.
145. Tadevosyan A, Vaniotis G, Allen BG, Hebert TE, and Nattel S. G protein-coupled receptor signalling in the cardiac nuclear membrane: evidence and possible roles

in physiological and pathophysiological function. *The Journal of physiology.* 2012;590(Pt 6):1313-30.
146. Baker KM, Chernin MI, Schreiber T, Sanghi S, Haiderzaidi S, Booz GW, et al. Evidence of a novel intracrine mechanism in angiotensin II-induced cardiac hypertrophy. *Regul Pept.* 2004;120(1-3):5-13.
147. van Kats JP, Methot D, Paradis P, Silversides DW, and Reudelhuber TL. Use of a biological peptide pump to study chronic peptide hormone action in transgenic mice. Direct and indirect effects of angiotensin II on the heart. *J Biol Chem.* 2001;276(47):44012-7.
148. Clouthier DE, Hosoda K, Richardson JA, Williams SC, Yanagisawa H, Kuwaki T, et al. Cranial and cardiac neural crest defects in endothelin-A receptor-deficient mice. *Development.* 1998;125(5):813-24.
149. Kurihara Y, Kurihara H, Suzuki H, Kodama T, Maemura K, Nagai R, et al. Elevated blood pressure and craniofacial abnormalities in mice deficient in endothelin-1. *Nature.* 1994;368(6473):703-10.
150. Yanagisawa H, Yanagisawa M, Kapur RP, Richardson JA, Williams SC, Clouthier DE, et al. Dual genetic pathways of endothelin-mediated intercellular signaling revealed by targeted disruption of endothelin converting enzyme-1 gene. *Development.* 1998;125(5):825-36.
151. Merlen C, Farhat N, Luo X, Chatenet D, Tadevosyan A, Villeneuve LR, et al. Intracrine endothelin signaling evokes IP3-dependent increases in nucleoplasmic Ca in adult cardiac myocytes. *J Mol Cell Cardiol.* 2013;62C:189-202.
152. Morris JB, Huynh H, Vasilevski O, and Woodcock EA. alpha(1)-Adrenergic receptor signaling is localized to caveolae in neonatal rat cardiomyocytes. *J Mol Cell Cardiol.* 2006;41(1):17-25.
153. Jensen BC, Swigart PM, and Simpson PC. Ten commercial antibodies for alpha-1-adrenergic receptor subtypes are nonspecific. *Naunyn Schmiedebergs Arch Pharmacol.* 2009;379(4):409-12.
154. Wu SC, Dahl EF, Wright CD, Cypher AL, Healy CL, and O'Connell TD. Nuclear localization of a1A-adrenergic receptors is required for signaling in cardiac myocytes: an "inside-out" a1-AR signaling pathway. *J Am Heart Assoc.* 2014;3(2):e000145.
155. Dorn GW, 2nd, and Brown JH. Gq signaling in cardiac adaptation and maladaptation. *Trends Cardiovasc Med.* 1999;9(1-2):26-34.
156. Michel MC, Wieland T, and Tsujimoto G. How reliable are G-protein-coupled receptor antibodies? *Naunyn Schmiedebergs Arch Pharmacol.* 2009;379(4):385-8.
157. Grubb DR, Vasilevski O, Huynh H, and Woodcock EA. The extreme C-terminal region of phospholipase Cbeta1 determines subcellular localization and function; the "b" splice variant mediates alpha1-adrenergic receptor responses in cardiomyocytes. *FASEB J.* 2008;22(8):2768-74.
158. Adams JW, Sakata Y, Davis MG, Sah VP, Wang Y, Liggett SB, et al. Enhanced Galphaq signaling: a common pathway mediates cardiac hypertrophy and apoptotic heart failure. *Proc Natl Acad Sci U S A.* 1998;95(17):10140-5.
159. D'Angelo DD, Sakata Y, Lorenz JN, Boivin GP, Walsh RA, Liggett SB, et al. Transgenic Galphaq overexpression induces cardiac contractile failure in mice. *Proc Natl Acad Sci U S A.* 1997;94(15):8121-6.

160. O'Connell TD, Swigart PM, Rodrigo MC, Ishizaka S, Joho S, Turnbull L, et al. Alpha1-adrenergic receptors prevent a maladaptive cardiac response to pressure overload. *J Clin Invest.* 2006;116(4):1005-15.
161. O'Connell TD, Rodrigo MC, and Simpson PC. Isolation and culture of adult mouse cardiac myocytes. *Methods Mol Biol.* 2007;357:271-96.
162. Zhou G, Wang L, Ma Y, Wang L, Zhang Y, and Jiang W. Synthesis of a quinazoline derivative: a new alpha(1)-adrenoceptor ligand for conjugation to quantum dots to study alpha(1)-adrenoceptors in living cells. *Bioorg Med Chem Lett.* 2011;21(19):5905-9.
163. Tang SS, Rogg H, Schumacher R, and Dzau VJ. Characterization of nuclear angiotensin-II-binding sites in rat liver and comparison with plasma membrane receptors. *Endocrinology.* 1992;131(1):374-80.
164. Shcherbakova OG, Hurt CM, Xiang Y, Dell'Acqua ML, Zhang Q, Tsien RW, et al. Organization of beta-adrenoceptor signaling compartments by sympathetic innervation of cardiac myocytes. *J Cell Biol.* 2007;176(4):521-33.
165. Nikolaev VO, Moshkov A, Lyon AR, Miragoli M, Novak P, Paur H, et al. Beta2-adrenergic receptor redistribution in heart failure changes cAMP compartmentation. *Science.* 2010;327(5973):1653-7.
166. Liu P, Ying Y, Ko YG, and Anderson RG. Localization of platelet-derived growth factor-stimulated phosphorylation cascade to caveolae. *J Biol Chem.* 1996;271(17):10299-303.
167. Shah ZH, Jones DR, Sommer L, Foulger R, Bultsma Y, D'Santos C, et al. Nuclear phosphoinositides and their impact on nuclear functions. *FEBS J.* 2013;280(24):6295-310.
168. Cajka T, and Fiehn O. Comprehensive analysis of lipids in biological systems by liquid chromatography-mass spectrometry. *Trends Analyt Chem.* 2014;61:192-206.
169. Dingwall C, and Laskey RA. Nuclear targeting sequences--a consensus? *Trends Biochem Sci.* 1991;16(12):478-81.
170. Ramazzotti G, Faenza I, Fiume R, Matteucci A, Piazzi M, Follo MY, et al. The physiology and pathology of inositide signaling in the nucleus. *J Cell Physiol.* 2011;226(1):14-20.
171. Higazi DR, Fearnley CJ, Drawnel FM, Talasila A, Corps EM, Ritter O, et al. Endothelin-1-stimulated InsP3-induced Ca2+ release is a nexus for hypertrophic signaling in cardiac myocytes. *Mol Cell.* 2009;33(4):472-82.
172. Kim D, Jun KS, Lee SB, Kang NG, Min DS, Kim YH, et al. Phospholipase C isozymes selectively couple to specific neurotransmitter receptors. *Nature.* 1997;389(6648):290-3.
173. Ziegelhoffer A, Tappia PS, Mesaeli N, Sahi N, Dhalla NS, and Panagia V. Low level of sarcolemmal phosphatidylinositol 4,5-bisphosphate in cardiomyopathic hamster (UM-X7.1) heart. *Cardiovasc Res.* 2001;49(1):118-26.
174. Mesaeli N, Tappia PS, Suzuki S, Dhalla NS, and Panagia V. Oxidants depress the synthesis of phosphatidylinositol 4,5-bisphosphate in heart sarcolemma. *Arch Biochem Biophys.* 2000;382(1):48-56.
175. Wenk MR, Lucast L, Di Paolo G, Romanelli AJ, Suchy SF, Nussbaum RL, et al. Phosphoinositide profiling in complex lipid mixtures using electrospray ionization mass spectrometry. *Nat Biotechnol.* 2003;21(7):813-7.

176. Filtz TM, Grubb DR, McLeod-Dryden TJ, Luo J, and Woodcock EA. Gq-initiated cardiomyocyte hypertrophy is mediated by phospholipase Cbeta1b. *FASEB J.* 2009;23(10):3564-70.
177. Tan L-B, Jalil JE, Pick R, Janicki JS, and Weber KT. Cardiac myocyte necrosis induced by angiotensin II. *Circ Res.* 1991;69:1185-95.
178. Harvey CD, Ehrhardt AG, Cellurale C, Zhong H, Yasuda R, Davis RJ, et al. A genetically encoded fluorescent sensor of ERK activity. *Proc Natl Acad Sci U S A.* 2008;105(49):19264-9.
179. Warren SC, Margineanu A, Alibhai D, Kelly DJ, Talbot C, Alexandrov Y, et al. Rapid global fitting of large fluorescence lifetime imaging microscopy datasets. *PLoS One.* 2013;8(8):e70687.
180. Myagmar BE, Flynn JM, Cowley PM, Swigart PM, Montgomery MD, Thai K, et al. Adrenergic Receptors in Individual Ventricular Myocytes: The Beta-1 and Alpha-1B Are in All Cells, the Alpha-1A Is in a Subpopulation, and the Beta-2 and Beta-3 Are Mostly Absent. *Circ Res.* 2017;120(7):1103-15.
181. Kwong JQ, and Molkentin JD. Physiological and pathological roles of the mitochondrial permeability transition pore in the heart. *Cell Metab.* 2015;21(2):206-14.
182. Ichikawa Y, Ghanefar M, Bayeva M, Wu R, Khechaduri A, Naga Prasad SV, et al. Cardiotoxicity of doxorubicin is mediated through mitochondrial iron accumulation. *J Clin Invest.* 2014;124(2):617-30.
183. McKinsey TA, Zhang CL, Lu J, and Olson EN. Signal-dependent nuclear export of a histone deacetylase regulates muscle differentiation. *Nature.* 2000;408(6808):106-11.
184. Chang CW, Lee L, Yu D, Dao K, Bossuyt J, and Bers DM. Acute beta-adrenergic activation triggers nuclear import of histone deacetylase 5 and delays G(q)-induced transcriptional activation. *J Biol Chem.* 2013;288(1):192-204.
185. Hein L, Stevens ME, Barsh GS, Pratt RE, Kobilka BK, and Dzau VJ. Overexpression of angiotensin AT1 receptor transgene in the mouse myocardium produces a lethal phenotype associated with myocyte hyperplasia and heart block. *Proc Natl Acad Sci U S A.* 1997;94(12):6391-6.
186. Paradis P, Dali-Youcef N, Paradis FW, Thibault G, and Nemer M. Overexpression of angiotensin II type I receptor in cardiomyocytes induces cardiac hypertrophy and remodeling. *Proc Natl Acad Sci U S A.* 2000;97(2):931-6.
187. Robu VG, Pfeiffer ES, Robia SL, Balijepalli RC, Pi Y, Kamp TJ, et al. Localization of functional endothelin receptor signaling complexes in cardiac transverse tubules. *J Biol Chem.* 2003;278(48):48154-61.
188. Ibarra C, Vicencio JM, Estrada M, Lin Y, Rocco P, Rebellato P, et al. Local control of nuclear calcium signaling in cardiac myocytes by perinuclear microdomains of sarcolemmal insulin-like growth factor 1 receptors. *Circ Res.* 2013;112(2):236-45.
189. Zaccolo M. cAMP signal transduction in the heart: understanding spatial control for the development of novel therapeutic strategies. *Br J Pharmacol.* 2009;158(1):50-60.
190. ALLHAT CRG. Major cardiovascular events in hypertensive patients randomized to doxazosin vs chlorthalidone: the antihypertensive and lipid-lowering treatment to prevent heart attack trial (ALLHAT). [see comments]. *Jama.* 2000;283(15):1967-75.

191. Cohn JN. The Vasodilator-Heart Failure Trials (V-HeFT). Mechanistic data from the VA Cooperative Studies. Introduction. *Circulation.* 1993;87(6 Suppl):VI1-4.
192. Roehrborn CG, and Schwinn DA. Alpha1-adrenergic receptors and their inhibitors in lower urinary tract symptoms and benign prostatic hyperplasia. *J Urol.* 2004;171(3):1029-35.
193. Vaughan ED, Jr. Medical management of benign prostatic hyperplasia--are two drugs better than one? *N Engl J Med.* 2003;349(25):2449-51.
194. Dhaliwal AS, Habib G, Deswal A, Verduzco M, Souchek J, Ramasubbu K, et al. Impact of alpha 1-adrenergic antagonist use for benign prostatic hypertrophy on outcomes in patients with heart failure. *Am J Cardiol.* 2009;104(2):270-5.
195. McGrath JC, Brown CM, and Wilson VG. Alpha-adrenoceptors: a critical review. *Med Res Rev.* 1989;9(4):407-533.
196. Ainscough JF, Drinkhill MJ, Sedo A, Turner NA, Brooke DA, Balmforth AJ, et al. Angiotensin II type-1 receptor activation in the adult heart causes blood pressure-independent hypertrophy and cardiac dysfunction. *Cardiovasc Res.* 2009;81(3):592-600.
197. Yang LL, Gros R, Kabir MG, Sadi A, Gotlieb AI, Husain M, et al. Conditional cardiac overexpression of endothelin-1 induces inflammation and dilated cardiomyopathy in mice. *Circulation.* 2004;109(2):255-61.
198. Zhao XS, Pan W, Bekeredjian R, and Shohet RV. Endogenous endothelin-1 is required for cardiomyocyte survival in vivo. *Circulation.* 2006;114(8):830-7.
199. Kohan DE, Cleland JG, Rubin LJ, Theodorescu D, and Barton M. Clinical trials with endothelin receptor antagonists: what went wrong and where can we improve? *Life Sci.* 2012;91(13-14):528-39.